

**THE PREFERRED ALTERNATIVE METHOD FOR MEASURING
PAVED ROAD DUST EMISSIONS FOR EMISSIONS
INVENTORIES:
“MOBILE TECHNOLOGIES vs. THE TRADITIONAL AP-42
METHODOLOGY”**

Rodney Langston, Russell S. Merle Jr., and Deborah Hart
Clark County Department of Air Quality and Environmental Management (DAQEM)
500 S Grand Central Parkway Ste 2001
P.O. Box 554000
Las Vegas, Nevada 89155-4000

Vic Etyemezian, Hampden Kuhns, and John Gillies
Desert Research Institute (DRI)
755 E Flamingo Road
Las Vegas, Nevada 89119-7363

Dennis Fitz and Kurt Bumiller
Center for Environmental Research and Technology
University of California, Riverside
1084 Columbia Avenue
Riverside, California 92507-0434

David E. James, Ph. D., P.E.
Department of Civil and Environmental Engineering
University of Nevada, Las Vegas
P.O. Box 45-4014
4505 Maryland Parkway
Las Vegas, Nevada 89154-4015

Abstract

This paper discusses Clark County Nevada’s experiment completed in September of 2006, which used two vehicle-based technologies to estimate paved road dust emissions, TRAKER (Testing Re-entrained Aerosol Kinetic Emissions from Roads), developed by the Desert Research Institute (DRI), and SCAMPER, (System of Continuous Aerosol Measurements of Particulate Emissions from Roadways) developed by the University of California in Riverside (CE-CERT).

Motor vehicles produce a significant fraction of the PM₁₀ emissions in the western United States. AP-42 (USEPA, 2006) measurements are time-consuming, require lane closure to collect samples, and don’t consider vehicle speed, frontal area, drag coefficient or silt reservoir depletion.

The experiment was designed to:

1. Examine and quantify relationships between vehicle-based technologies and AP-42 silt loading measurements.
2. Evaluate paved road dust emissions absent of replenishing sources.
3. Determine and quantify the relationships of emissions measured using PM₁₀ horizontal flux tower techniques, mobile measurement systems, and AP-42 methods.

Representative soil was evenly applied to an 800-meter section of road surface. SCAMPER and TRAKER made repeated test runs while an instrumented tower measured upwind-downwind horizontal PM₁₀ flux measurement. AP-42 methods were used to collect samples and calculate PM₁₀ emission factors. Both silt loadings and vehicle speeds were varied during the experiment.

Both TRAKER and SCAMPER measured rapid decay of the PM₁₀ emission rate. Both the tower flux and AP-42 silt loading measurements were consistent with the mobile methods. Decaying particle suspension rates suggest emission rates may be a function of vehicle speed and silt loading.

TABLE OF CONTENTS

1.0 INTRODUCTION

- 1.1 Phase IV Study Objectives
- 1.2 Phase IV Study Design Overview

2.0 BACKGROUND

- 2.1 EPA AP-42 Development and Limitations
- 2.2 Clark County Background with AP-42
- 2.3 Paved Road Phase I-Phase III

3.0 METHODOLOGY

- 3.1 Experimental Design
 - 3.1.1 Route Selection
- 3.2 Soil Selection and Application
 - 3.2.1 Soil Sampling Site Selection
 - 3.2.2 Soil Excavation and Packaging
 - 3.2.3 Soil Characterization
 - 3.2.4 Soil Application
- 3.3 Horizontal Flux Towers
- 3.4 EPA Method AP-42
 - 3.4.1 Plot Layout
 - 3.4.2 Vacuum Soil Recovery Method
 - 3.4.3 Field Soil Application History
- 3.5 Mobile Technologies
 - 3.5.1 SCAMPER
 - 3.5.2 TRAKER I
 - 3.5.3 TRAKER II

4.0 QA/QC

- 4.1 Horizontal Flux Towers
- 4.2 EPA Method AP-42
 - 4.2.1 Field Balance Mass Calibrations
 - 4.2.2 Road Plot Marking Uncertainty
 - 4.2.3 Sieve Analysis Calibration
- 4.3 Mobile Technologies
 - 4.3.1 SCAMPER
 - 4.3.2 TRAKER I
 - 4.3.3 TRAKER II

5.0 DATA HANDLING

- 5.1 Horizontal Flux Towers
- 5.2 EPA Method AP-42
 - 5.2.1 Organizing Bag Data
 - 5.2.2 Organizing AP-42 Emission Factor Data
 - 5.2.3 Unification of Data Sets

5.3 Mobile Technologies

5.3.1 SCAMPER

5.3.2 TRAKER I

5.3.3 TRAKER II

6.0 RESULTS

6.1 Short-Term Emission Factor Decay and Silt Loading Depletion

6.2 Comparison of Horizontal Flux Tower Emission Factors to EPA Method AP-42

6.3 Comparison of Horizontal Flux Tower Emission Factors to Mobile Technologies Emission Factors

6.4 Comparison of Calibrated Mobile Technologies Emission Factors to EPA Method AP-42 Emission Factors to measured PM₁₀ Horizontal Flux Tower Values

7.0 DISCUSSION

7.1 Real World Precision and Reproducibility

7.1.1 UCR Paved Road Phases II & III for DAQEM

7.1.2 DRI Studies- Clark County Phase II, Lake Tahoe and Idaho

7.2 Applying Phase IV Results in Real World Conditions- Explanation of Higher EF's in Phase IV

7.3 Advantages of Mobile Technologies

8.0 CONCLUSIONS

8.1 Conclusions

8.2 Recommendations

9.0 REFERENCES

10.0 KEY WORDS

11.0 ACKNOWLEDGEMENTS

LIST OF FIGURES

- 2-1 Map of Clark County 2/14/05-2/17/05 Sampling Route
- 3-1 Phase IV Route Map
- 3-2 Photograph of Master and Satellite Towers Showing Locations of DustTrak PM₁₀ Monitors.
- 3-3 Schematic of Field Sampling Layout
- 3-4 Phase IV Veterans Memorial Drive Plot Layouts
- 3-5 Isokinetic Inlet Schematic Diagram
- 3-6 Photographs of the Front and Rear of the SCAMPER
- 3-7 TRAKER Influence Monitors
- 3-8 TRAKER Vehicle and Instrumentation
- 3-9 TRAKER II Photographs
- 3-10 Schematics and Dimensions of TRAKER II
- 4-1 Scatter Plot of DustTrak PM₁₀ Average Concentrations and TEOM PM₁₀ Measurements
- 4-2 Scatter Plot of DustTrak Monitor Outfitted with PM_{2.5} inlet versus DustTrak with PM₁₀ Inlet
- 4-3 Comparison of Filter-Based PM₁₀ Measurements with DustTrak Outfitted with PM₁₀ Inlet
- 4-4 Comparison of Filter-Based PM_{2.5} Mass Measurement with DustTrak Outfitted with PM_{2.5} Inlet
- 4-5 TRAKER Coefficient of Variation Expressed as a Percentage for Left and Right PM₁₀ DustTrak signals as a Function of Speed
- 5-1 Illustration of Portions of Flux Plane Represented by DustTrak and Wind Instruments at Each Height
- 5-2 Schematic of GPS Data Points on Top of Street Layout
- 5-3 Relationship Between TRAKER I Signal Averaged over Entire Pass and TRAKER I Signal only Within 50 m of Master Tower
- 5-4 TRAKER Signal Averaged over Entire Pass and Averaged over only the Portion of Test Road in the Vicinity of Flux Towers
- 5-5 Ratio of Background Inlet PM₁₀ Concentration to Average of Left and Right Tire Inlet PM₁₀ Signals for TRAKER I passes
- 5-6 Time Series of Ratio of Pass-Averaged TRAKER I Right to Left Inlet Signal Ratios and Pass-Averaged Wind Speed
- 5-7 TRAKER I Signal Normalized to First TRAKER I Pass of the Measurement Set for Sets 4, 5, 6, 7 and 8
- 5-8 Normalized TRAKER I Decay Curve for Sets 5 and 7 & Hypothesized Aerodynamically Suspendable, Mechanically Suspendable, and Total Suspendable Road Dust Decay Curves
- 5-9 Normalized TRAKER I Decay Curve for Sets 4, 6, and 8 & Hypothesized Aerodynamically Suspendable, Mechanically Suspendable, and Total Suspendable Road Dust Decay Curves
- 5-10 Division of Set 13 into 4 Cycles, with Each Cycle Comprised of 6 Passes for TRAKER I

- 5-11 Speed Response of TRAKER I Signal
- 5-12 Relationship Between TRAKER II Signal Averaged Over Entire Pass and TRAKER II Signal only within 50 m of Master Tower
- 5-13 TRAKER II Ratio of Average of Left and Right Tire Inlet PM₁₀ Concentrations to Background Inlet PM₁₀ Concentration
- 5-14 TRAKER II Time Series of Ratio of Pass-Averaged Right to Left Inlet Signal Ratios and Pass-Averaged Wind Speed
- 5-15 Speed Response of TRAKER II Signal
- 6-1 Time Series of Pass-Averaged Horizontal Tower PM₁₀ Flux, Silt-Estimated AP-42 Emission Factor, TRAKER I, TRAKER II, and SCAMPER Raw Signals
- 6-2 Silt Depletion with Increasing Vehicle Passes
- 6-3 Comparison of Averaged AP-42 Emission Factors, in Gram/VMT, Computed from Silt Loadings for First Nine Passes, Compared to AP-42 Emission Factors for Remaining Passes
- 6-4 Comparison of TRAKER I Signal and Average North-South Silt Loading for all Vehicle Passes
- 6-5 Comparison of SCAMPER Signal and Average North-South Silt Loading for all Vehicle Passes
- 6-6 Time Series of Horizontal PM₁₀ Fluxes Measured with Tower Measurement System
- 6-7 Tower-Based PM₁₀ Emission Factors vs. Silt Based Emission Factors
- 6-8 Time Series of Measured Horizontal PM₁₀ Flux on the DRI Tower System and the Pass-Averaged TRAKER I Signal for Passes when the Horizontal Flux Measurement was Valid
- 6-9 PM₁₀ Emission Factors vs. TRAKER I Average Signal
- 6-10 Time Series of Measured Horizontal PM₁₀ Flux on the DRI Tower System and the Pass-Averaged TRAKER II Signal for Passes when the Horizontal Flux Measurement was Valid
- 6-11 PM₁₀ Emission Factors vs. TRAKER II Average Signal
- 6-12 Time Series of Measured Horizontal PM₁₀ Flux on the DRI Tower System and the Pass-Averaged SCAMPER Signal for Passes when the Horizontal Flux Measurement was Valid
- 6-13 PM₁₀ Emission Factors vs. SCAMPER Average Signal
- 6-14 Emission Factors for all Valid Passes
- 6-15 Comparison of Set-Averaged Emission Factors
- 6-16 Set Averaged TRAKER I EF, TRAKER II EF, and AP-42 Silt Based EF Plotted Against SCAMPER EF
- 6-17 Set Averaged TRAKER II EF, SCAMPER EF, and AP-42 Silt Based EF Plotted Against TRAKER I EF
- 7-1 TRAKER I Calibrations
- 7-2 Emission Factors from Phase II Clark County Study
- 7-3 Scatter Plot of TRAKER I EF vs. AP-42 Silt Based EF

LIST OF TABLES

- 3-1 Summary of Data Used to Determine 50th Percentile Silt Loading Value for Collector Roadways
- 3-2 Summary of Applied Silt Loadings During Phase IV Controlled Field Study
- 4-1 Validity Criteria Applied to Each 1 s TRACKER Data Point
- 5-1 Example of Vehicle Pass_ID Data
- 5-2 Summary of Set_ID's and Corresponding Pass_ID's for Phase IV Study
- 6-1 Summary of Tests During Field Study 9/11/06-9/15/06
- 6-2 Summary of Observed Silt Decay with Increasing Number of Vehicle Passes
- 6-3 Summary of Measured PM₁₀ Horizontal Fluxes
- 6-4 Summary of Equivalence Multipliers Between Mobile Measurement Systems and PM10 Emission Factors Assuming that the Raw Signal for the Mobile Systems is Linearly Related to Measured Emission Factors

1.0 INTRODUCTION

The Las Vegas Valley in Clark County, Nevada, is classified as a serious nonattainment area for federal fine particulate matter (PM₁₀) National Ambient Air Quality Standards (NAAQS). Clark County submitted a PM₁₀ State Implementation Plan (SIP) for this nonattainment area in June of 2001. As part of the SIP development, Clark County contracted with a consultant to collect 24 silt samples representative of Clark County roadways for estimating PM₁₀ paved road emissions. The silt measurements were significantly higher than EPA default values, and public works officials from four agencies and other stakeholders asserted that the Clark County SIP overestimated PM₁₀ emissions from paved roadways. Clark County committed to conducting quarterly silt sampling through the end of 2006 as part of the now federally approved PM₁₀ SIP. Sampling is ongoing and the current AP-42 data base includes sampling from the spring of 2000 through the spring of 2006. The PM₁₀ SIP also contained a research commitment to explore the feasibility of vehicle-based mobile sampling systems for development of improved paved road emissions inventories.

During this timeframe, Clark County has seen substantially improved air quality for the PM₁₀ pollutant, particularly from the year 2004 forward. Visually, it also appears that Las Vegas Valley roads have become cleaner, in part due to tightened controls on construction site track-out and an increased emphasis on enforcement, implemented in early 2003. However, statistical analysis performed by UNLV under contract has generally not shown statistically significant declines in paved road emission factors during this timeframe using silt sample data and AP-42 emission estimation methods. These results have reinforced Clark County's belief that the paved road emissions inventory developed using AP-42 methods for the PM₁₀ SIP overestimates actual emissions. In addition, silt measurements are time consuming, expensive, and frequently require the alteration of roadway traffic patterns while samples are being procured.

Initial work utilizing vehicle-based mobile sampling systems in Clark County occurred in 1999 as part of PM₁₀ SIP development. The test results showed even higher emission rates than corresponding AP-42 calculations and were not considered realistic. In addition, the need to complete an approvable PM₁₀ SIP was urgent and EPA approval of this new method was very unlikely based on work completed at that time. Phase I of the current research effort was initiated in 2004 and Phase II was completed in early 2005. Fieldwork for Phase III occurred in late 2005. Objectives for Phase IV are described below.

1.1 Study Objectives

- 1 Evaluate precision of all measurement methods under controlled conditions: Measurement methods include measurements from the tower sampling array, SCAMPER measurements, TRAKER measurements, and road silt measurements using AP-42 sampling methodology. Additional ancillary measurements include

- weights of silt material applied to test area, wind speed data, wind direction data, and relative humidity data.
- 2 Evaluate validity of original AP-42 emissions factor estimates: Compare measured tower emissions to AP-42 emissions calculated from silt loadings using the AP-42 equation.
 - 3 Calibrate mobile technologies systems to the tower emissions factors: Comparison of SCAMPER and TRAKER system measurements with external sampling array measurements in a controlled measurement environment, with defined vehicle movement, controlled speeds, and controlled road material loadings.
 - 4 Compare mobile technologies emissions factors to predicted AP-42 emissions factors: Determine relationships between roadway silt loading and measured SCAMPER and TRAKER particulate emissions under controlled conditions (standard vehicle speeds and weight). Compare SCAMPER/TRAKER measurements to AP-42 emission estimates under controlled conditions.
 - 5 Compare mobile technologies measurements: Comparison of SCAMPER to TRAKER measurements estimates under controlled measurement conditions, including defined vehicle movement, controlled speeds, and controlled road material loadings.
 - 6 Data assessment and review for recommendations on performance specifications: Assess data for accuracy and precision of vehicle-mounted mobile sampling systems and compare with other measurement methods. Prepare recommendations for the utilization of vehicle-mounted mobile sampling systems into AP-42.
 - 7 Characterization of silt depletion rate: Assess by number of vehicle passes with defined vehicle speeds and weight.

1.2 Study Design Overview

The five-day study included testing two vehicle-mounted mobile sampling systems, SCAMPER and TRAKER, under controlled road conditions. One SCAMPER and two TRAKER systems were utilized in this study. Comparative external measurements included upwind and downwind measurements with multiple samplers on twelve-meter towers and AP-42 silt sampling. Study objectives included a comparison of upwind/downwind source emissions measurements to SCAMPER/TRAKER measurements, a comparison of SCAMPER to TRAKER measurements, and AP-42 silt measurements/emission estimates under controlled conditions.

The sampling area consisted of two lanes of a four-lane divided highway with curbed median and curbed roadsides (see **Figure 3-1**). All road traffic was diverted to the

southeast-bound lanes, allowing the two northwest-bound lanes and the stabilized median area to be utilized exclusively for the five-day study. This diversion allowed us to limit vehicle passes between the external tower samplers to SCAMPER and TRAKER vehicles, with one sampling tower located on the median between the test area and adjacent traffic. It was anticipated that these controlled traffic and measurement parameters would enhance the quality of the upwind/downwind source emissions measurements compared to previous paved road dust studies.

Controlled road silt loading conditions were created through the application of known quantities of material onto the measurement section of the test area. The applied material approximated the sand and silt/clay percentages historically sampled on paved roads in the Las Vegas Valley. The test area was of sufficient length to allow for measurement at constant speeds of up to 45 miles per hour.

2.0 BACKGROUND

2.1 EPA AP-42 Development and Limitations

The United States Environmental Protection Agency (EPA) published a document entitled Compilation of Air Pollutant Emission Factors (AP-42) beginning in 1972. Since AP-42s inception as a tool for regulators, permit writers, and environmental planners, many have used this tool to account for emissions of air pollutants from a variety of sources in the human environment. EPA periodically reviews and updates the emission factors available in AP-42 to meet the needs of state and local air pollution control programs and industry. It wasn't until the late 70's that EPA, and others started looking at emissions from paved roads. Prior to this time, much of the work with respect to roadways was focused on unpaved roads. Prior to the March 1993 research findings¹, AP-42 contained two sections concerning paved road fugitive emissions. One of the early attempts to characterize paved road dust was addressed by EPA in 1983 with the inclusion of a Section 11.2.6 Industrial Paved Roads, and was slightly modified in 1988. Section 11.2.5, Urban Paved Roads, was first drafted in 1984 using the test results from public paved roads and was included in the AP-42, 4th Edition documentation in 1985. The emission factors included in Sections 11.2.5 and 11.2.6 were never quality rated "A" through "E." The updates proposed with the March 1993 report assumed there were no distinctions between public and industrial roads or between controlled and non-controlled test. These assumptions evolved into a single emission factor equation for all paved roads.

In July 1993, the AP-42 Section 13.2.1 (Paved Roads) was published to help better characterize the paved road dust source. The quantity of dust emissions from vehicle traffic on a paved road could be estimated using the following empirical expression:

$$E=k (sL/2)^{0.65} (W/3)^{1.5} \qquad \text{Equation 1.1}$$

¹ U.S. Environmental Protection Agency, Emission Factor Documentation for AP-42, EPA Contract No. 68-D0-0123, MRI Project No. 9712-44 dated March 8, 1993.

Where E = particulate emission factor (having units matching the units of k)
 k = base emission factor for particle size range and units of interest
 sL = road surface silt loading (grams per square meter) (g/m²)
 W = average weight (tons) of the vehicles traveling the road

This equation was slightly modified in 2004 to account for vehicle exhaust, tire and brake wear. In the most recent version the quantity of particulate emissions from re-suspension of loose material on the road surface due to vehicle travel on a dry paved road is estimated by using the following empirical expression.

$$E = k (sL/2)^{0.65} (W/3)^{1.5} - C^5 \quad \text{Equation 1.2}$$

Where E = particulate emission factor (having units matching the units of k)
 k = base emission factor for particle size range and units of interest
 sL = road surface silt loading (grams per square meter) (g/m²)
 W = average weight (tons) of the vehicles traveling the road
 C = emission factor for 1980's vehicle fleet exhaust, brake wear and tire wear

The AP-42 equation variable for weight of vehicle is defined as the average weight of all vehicles traveling the road. EPA did not intend that separate weights of vehicles be used to calculate a separate emission factor for each vehicle weight class. Instead, only one emission factor is calculated to represent the "fleet" average weight of all vehicles traveling the road or road network. The particle size multiplier (k) above varies with aerodynamic size range. The emissions factors for the exhaust, brake wear and tire wear are for a 1980's vehicle fleet (C), as calculated by EPA's MOBILE6.2 model.

The AP-42 paved road emissions equation is an arithmetic equation based on 65 tests conducted in the early 1990s. The test included measurements of vehicles moving at speeds of 10 to 55 miles per hour. The equation is intended for estimating emissions from free flowing traffic and is not intended to estimate emissions for stop and go traffic. Where road specific silt loading factors are utilized, the EPA assigns a quality rating of "A" provided the silt loadings, mean vehicle weight and vehicle speeds fall within the following parameters:

Silt loading:	0.02 - 400 g/m ² [0.03 - 570 grains/square foot (ft ²)]
Mean vehicle weight:	2.0 - 42 tons
Mean vehicle speed:	6 - 88 kilometers per hour (kph) [10 - 55 miles per hour (mph)]

Where the EPA recommended default silt loadings are used in place of locally measured silt loadings, the quality rating is reduced by one level (e.g. "B"). The EPA provides default values for High ADT and Low ADT roads. Each of these two ADT classes has a default silt loading for normal conditions and worst-case conditions.

The assumptions, limitations, and silt loading data collection requirements needed to utilize the equation considerably diminish the accuracy of emissions inventories for paved road emissions. Urban areas, where a majority of vehicle travel occurs in most airsheds, typically do not have free flowing traffic. Vehicle speeds have been shown to exert substantial influence on road dust emission rates, but the equation lumps all speeds from 10 to 55 mph into one emissions rate. Speeds above 55 mph, which may comprise a significant component of the vehicles miles traveled in an airshed; are not accounted for at all, introducing additional error into the emissions estimates.

The determination of correct silt loading values for each class of roadway and subclass of roadway is the most serious limitation of the AP-42 methodological approach. Road silt sampling is expensive, time consuming, and dangerous. As a result, only a few silt samples can be collected in each sampling quarter. Each sampling point is therefore used to represent hundreds if not thousands of miles of roadways. This limitation prevents emission inventory developers from obtaining a statistically valid number of silt samples for the roadways represented. Moreover, because of traffic congestion and safety concerns, department of transportation officials may not allow any sampling on some roadway classes such as freeways and major arterials. As a result, the silt loading data is always suspect for any paved road dust emissions estimate.

The inherent limitation on the feasible amount of silt sampling makes it impossible to accurately estimate future emissions from projected growth in vehicle miles traveled. This arises because sufficient silt loading data is not available to develop separate emissions rates for built-out areas and developing areas. Therefore, emissions for all future increases in vehicle miles traveled must be estimated using current emissions rates. This straight-line projection for future paved road dust emissions is at variance with observed real world conditions and can doom any transportation conformity finding for an airshed experiencing substantial growth.

In summary, the limitations of the arithmetically derived AP-42 paved road dust emissions equation combined with the infeasibility of collecting sufficient silt loading data to accurately represent all classes and subclasses of roadways make all current paved road dust emissions inventories highly suspect. The increased traffic congestion and personal safety issues associated with developing better silt loading data further reduce the utility of the current road dust emission estimating methodology. Finally, the challenges related to the successful maintenance of conformity make it imperative that an alternative approach to measuring and estimating paved road dust emissions be developed.

2.2 Clark County Background with AP-42

The Las Vegas Valley in Clark County, Nevada, is classified as serious nonattainment for federal fine particulate matter (PM₁₀) National Ambient Air Quality Standards (NAAQS). Clark County submitted a PM₁₀ State Implementation Plan (SIP) for this nonattainment area in June of 2001. As part of the SIP development, Clark County contracted with a consultant to collect 24 silt samples representative of Clark County roadways for

estimating PM₁₀ paved road emissions. The silt measurements were significantly higher than EPA default values, and public works officials from four agencies and other stakeholders asserted that the Clark County SIP overestimated PM₁₀ emissions from paved roadways. Clark County committed to conducting quarterly silt sampling through the end of 2006 as part of the now federally approved PM₁₀ SIP. Sampling is ongoing and the current data base includes sampling from the spring of 2000 through the spring of 2006. The PM₁₀ SIP also contained a research commitment to explore the feasibility of vehicle-based mobile sampling systems for development of improved paved road emissions inventories.

During this timeframe, Clark County has seen substantially improved air quality for the PM₁₀ pollutant, particularly from the year 2004 forward. Visually, it also appears that Las Vegas Valley roads have become cleaner, in part due to tightened controls on construction site track-out and an increased emphasis on enforcement, implemented in early 2003. However, statistical analysis performed by UNLV under contract has generally not shown statistically significant declines in paved road emission factors during the 1999 through 2006 timeframe using silt sample data and AP-42 emission estimation methods. These results have reinforced Clark County's belief that the paved road emissions inventory developed using AP-42 methods for the PM₁₀ SIP overestimates actual emissions. In addition, silt measurements are time consuming, expensive, and frequently require the alteration of roadway traffic patterns while samples are being procured.

Initial work utilizing vehicle-based mobile sampling systems in Clark County occurred in 1999 as part of PM₁₀ SIP development. The test results showed even higher emission rates than corresponding AP-42 calculations and were not considered realistic. In addition, the need to complete an approvable PM₁₀ SIP was urgent and EPA approval of this new method was very unlikely based on work completed at that time. Clark County DAQEM submitted the SIP using the current AP-42 methodology, and initiated a research effort to develop better methods to characterize paved road PM₁₀ emissions. Phase I of the current research effort was initiated in 2004 and Phase II was completed in early 2005. Fieldwork for Phase III occurred in late 2005 with augmentation work occurring in early 2006.

2.3 Paved Road Phase I-Phase III

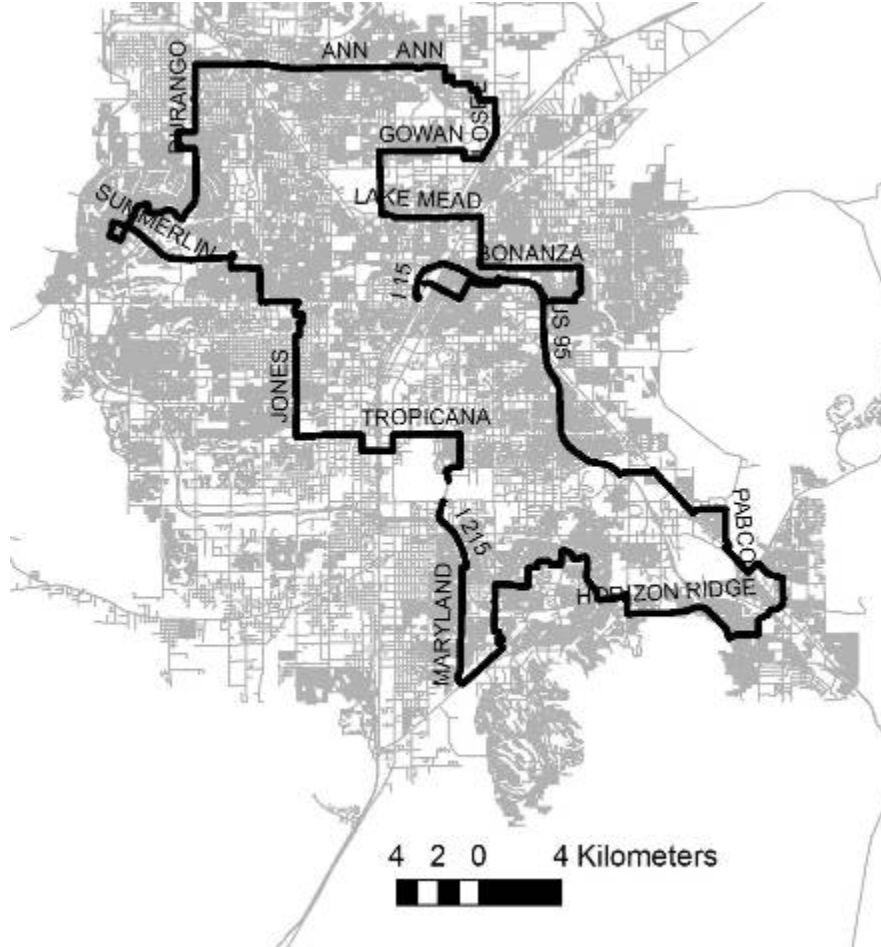
The Phase I study entailed a two-day field study utilizing a 107-mile sampling route. The purpose of the study was to determine the feasibility of vehicle-based mobile sampling system for use in Clark County to better characterize paved-road emissions and to develop real-time emissions of PM₁₀ for emissions inventory use. The sampling route was designed to include worst-case silt-impacted roads and best-case clean roads in order to evaluate the detection limits of the two systems. The route was further designed to include all political jurisdictions in the Las Vegas Valley. Several deviations from the original sampling route were required due to road closures resulting from road construction. An effort was made to note road infrastructure conditions and deposition sources during sampling using notepads and "wrist watch time." A total of sixteen AP-

42 silt samples were also collected on the sampling route. Phase I demonstrated the feasibility of using vehicle-based mobile sampling systems as an alternative to conventional AP-42 paved-road emissions estimating methods.

The Phase II study entailed four days of sampling on a 103-mile sampling route. The Phase II sampling route was designed to include a number of parameters. The route included the five classes of roadways (local, collector, minor arterial, major arterial, and freeway) and four political jurisdictions in the Las Vegas Valley. Consideration was given to development patterns in the Las Vegas Valley and the final sampling route included developing areas, older established neighborhoods, and newer planned communities that were completely built-out. The developing areas included a cross section of incomplete road infrastructure (e.g. unpaved road shoulders) and deposition sources such as vacant lots and construction activities. The built-out areas included completed road infrastructure, with few vacant lots, and little construction activity. The final route also included a cross section of soil classifications based on Clark County's Particulate Emission Potential (PEP) soil classification system². The sampling route included ten historical AP-42 sampling sites and eleven new sites that had not previously been sampled using AP-42 methodology. Relative humidity was measured during sampling at each AP-42 site. Specific road conditions and sources were not mapped or recorded during the study. The study was delayed for two weeks due to rain. The sampling route is shown in **Figure 2-1**. Staff from Maricopa County, U.S. EPA Region IX and U.S. EPA observed the field study. Limited notes on road infrastructure and silt deposition sources were made during development of the sampling route.

² Geotechnical and Environmental Services, Inc., *Presentation of Final Versions of Deliverables for Re-Evaluating and Updating the Particulate Emission Potential Map and Soil Classification for Dust Mitigation Best Management Practices Manual for Clark County*, dated September 26, 2003.

Figure 2-1. Map of Clark County 2/14/05 – 2/17/05 sampling route.



The Phase III study utilized only the SCAMPER and AP-42 emissions estimates. This study focused on development of specific emission factors for specific conditions and to assess measurement variability. A comparison of SCAMPER data to AP-42 emissions estimates was a second component of this study. To accomplish these objectives, the study occurred over seven consecutive days and utilized three sampling routes. Road infrastructure, adjacent land use (e.g. vacant land, residential, etc) and sources of deposition were comprehensively mapped prior to the study. In order to better evaluate site conditions during the study, a video camera was mounted externally on the driver's side of the vehicle. The video camera was linked to the SCAMPER GPS clock and camera sound was wired to a microphone located inside the vehicle to permit the operators to record comments and observations while operating the system.

The first sampling route (industrial route) was dominated by industrial haul roads with heavy silt loadings and was used to determine the precision of the SCAMPER unit. This route included local, collector and arterial roads. This route was sampled for most of day one of the study. The second route (transitional route) was a 7.3-mile track in a transitional area in the Las Vegas Valley. Development in the area is a mix of commercial, residential, rural residential and vacant land. Paved roads range from fully

improved with sidewalks, curbs and gutters to unimproved with unpaved shoulders on both sides. Sources of deposition included road construction, residential construction, vacant land used for storing fill soil, and vacant land with no active use. The area also has some of the highest PEP (Particulate Emission Potential) soils in the Las Vegas Valley. The transitional sampling area route was sampled for four consecutive days, including the weekend. This allowed a comparison of weekday and weekend paved road emission rates. The third route (developed community route) consisted of a 12.6-mile track traversing a newly developed planned community and contained local, collector and arterial roads. This route contained fully developed road infrastructure that was not impacted by any observable sources of silt deposition. The route included local, collector, and arterial streets, all of which contained very light silt loadings. In addition to providing baseline measurements for fully developed roadways with minimal silt deposition sources, this route was used to evaluate the sensitivity of the SCAMPER unit. Measurements were taken on this route for two full days. Relative humidity was measured during sampling at each AP-42 site and at a nearby DAQEM monitoring site. The study was coordinated with the cities of Las Vegas and North Las Vegas to insure that none of the streets were swept within three days prior to sampling.

3.0 METHODOLOGY

3.1 Experimental Design

3.1.1 Route Selection

Based on experience with previous studies and the sampling characteristics of the SCAMPER and TRAKER systems, DAQEM developed the following criteria selection of a study site:

1. The micro scale prevailing wind direction must be roughly perpendicular to the road direction at the study site.
2. The study site cannot have trees, buildings, or other obstructions in close proximity to the roadway.
3. The study site must not have significantly elevated topography in close proximity to the roadway on either side.
4. The study site must have a four-lane road divided by a median and the traffic conditions must make it feasible to block off two of the lanes on one side of the median during the study.
5. The study site must be located where there are no significant sources of PM₁₀ that may cause elevated PM₁₀ concentrations at the site during the study.
6. The study site must have an uninterrupted travel distance of at least $\frac{3}{4}$ of a mile.

Meteorological data from various sources was consulted to establish the road directional parameters for candidate sites. The requirements for no wind obstructions and particulate sources generally limited candidate sites to somewhat rural areas, whereas a majority of the roads in these areas did not meet the four lane and median separation criteria. Where all road and wind direction criteria were met, traffic volumes generally precluded blocking two travel lanes. After evaluating all available sites in Clark County, the Veterans Memorial Highway site in the City of Boulder City, Nevada, was the only site found that met all of the study criteria.

The study was conducted in the City of Boulder City, Nevada, on Veterans Memorial Highway, immediately west of Buchanan Boulevard. The sampling area consisted of two lanes of a four-lane divided highway with curbed median and curbed roadsides. Details are shown in the study plot plans and are also described below:

1. During the five study days, all road traffic was diverted to the southeast lanes, allowing the two northwest lanes and the stabilized curbed median area to be utilized exclusively for the five-day study. This allowed us to limit vehicle passes next to the external tower samplers to SCAMPER and TRAKER vehicles. These controlled traffic and measurement parameters enhanced the quality of the external source emissions measurements compared to previous paved road dust studies.
2. Tower sampling arrays were located on the median and sidewalk areas and were moved to achieve optimal orientation with the prevailing winds and sampling lane. Relocation of tower positions was logged throughout the study.

As shown in **Figure 3-1**, the course ran in a northwesterly direction approximately 4481' from the intersection of Buchanan and Veterans Memorial Hwy in the northwest-bound travel lanes. The 4481' course was divided into sections for testing purposes. The sections are described as follows:

Entire Length of Study Area: 4481'

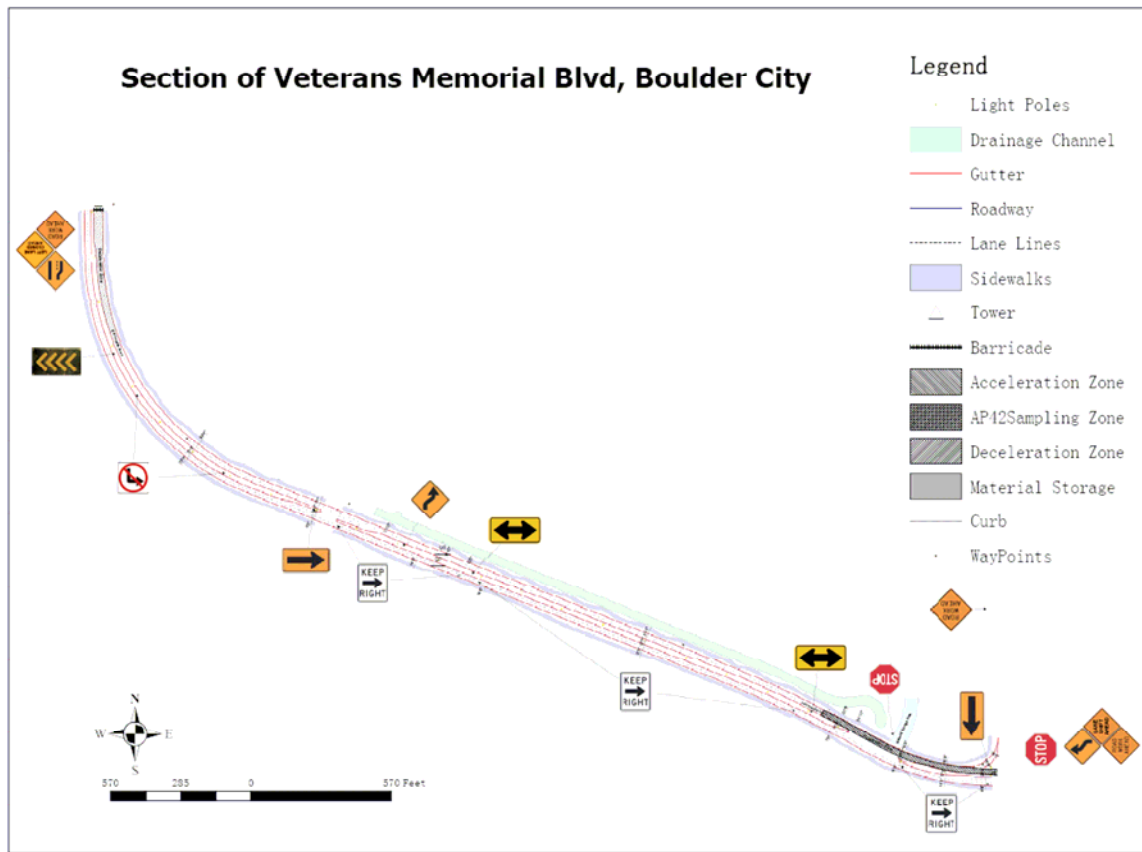
Acceleration Zone (Southern End of Course): 543'

Deceleration Zone (Northern End of Course): 500'

Constant Speed Zone/Sampling Zone: 3188'

AP-42 Sampling Zones: 120' each, located after acceleration zone and before deceleration zone at each end of the constant speed-sampling zone, for a total of 160 feet.

Figure 3-1. Phase IV route map.



3.2 Soil Selection and Application

3.2.1 Soil Sampling Site Selection

The 50th percentile silt content for collector roadways sampled in Clark County in 2005 and 2006 was used as a target value for silt content for selection of a candidate soil to be applied to the road surface for the Phase IV controlled study. Data summarizing the 50th percentile calculations are shown in **Table 3-1**. The 50th percentile silt content value for collector roads was 13%.

Table 3-1. Summary of data used to determine 50th percentile silt loading value for collector roadways.

Date	UNLV Site	Site Modifier	DAQEM location name	DAQEM Roadway Classification	Plot Number	Percent Gravel	Percent Sand	Percent Silt & Clay
3q-2005	24		Pabco	Collector		25.4	68.9	5.7
4q-2005	24		Pabco	Collector		17	76	7
1q-2006	23		Burkholder	Collector	4	11	77	12
3q-2005	23		Burkholder	Collector		20.1	75.6	4.3
4q-2005	23		Burkholder	Collector		7	80	13
1q-2006	15		lone	Collector	4	16	70	14
3q-2005	15		lone	Collector		13.3	75.7	11
4q-2005	15		lone	Collector		5	83	12
2q-2005	5		Washburn	Collector		15.6	55	29.4
3q-2005	5		Washburn	Collector		2.1	7.6	90.3
2q-2005	2		Marion	Collector		14.3	49.2	36.5
4q-2005	2		Marion	Collector		6	78	16
1q-2006	1		Gowan	Collector	4	8	79	13
2q-2005	1		Gowan	Collector		24.9	61.8	13.3
3q-2005	1		Gowan	Collector		17	78.5	4.5
geomean						11.4	61.4	13.1
10th pctile						5.4	51.5	5.0
50th pctile						14.3	75.7	13.0
90th pctile						23.0	79.6	33.7

* Gravel-sand boundary was 2.00 mm

* Sand-silt boundary was 75 microns

UNLV, in collaboration with Clark County DAQEM staff, surveyed four candidate field sites in southern metropolitan Clark County in July of 2006. Three candidate sites, in southwest Las Vegas, were not selected because either the silt content was incorrect, or because permission could not be obtained from either the US Bureau of Land Management or from private landowners for large-scale excavation.

A 21.9 kilogram sample of soil from a site located at Sunset Park, designated UNLV Road Dust site 29 (wet sieve) or 32 (dry sieve), in Wind Erodibility Group (WEG) 2, at an elevation of 1,988 feet, latitude N36° 3.792', longitude W115° 6.748' (Garmin eTrex®, WGS 84 datum) was collected on August 4, 2006. A 675 gram sample was sieved on August 11, 2006 and was found to be predominantly sand, with a 14% silt content.

A second group of samples were collected from (60 meters) 200 feet west of the original sampling site on August 23, 2006, designated as UNLV sites 38 and 39, at latitude N36° 03.777' and longitude W115° 06.824'. Volumetric soil moistures were found to range from 0.0% to 0.5%. Results of sieve analyses for silt content were similar to the first sample, and the decision was made to use this sandy WEG 2 deposit as the source material for the Phase IV controlled study.

3.2.2 Soil Excavation and Packaging

On Wednesday, September 6, 2006, a team of Clark County DAQEM and UNLV personnel, assisted by staff from Clark County Department of Parks and Recreation, excavated soil from the Sunset Park site. The excavation location was at latitude N36° 3.782' and longitude W115° 6.770', a location in between the two original soil collection sites.

A 0.38 cubic meter (0.50 cubic yard) bucket loader was used to remove soil from the site and deposit it in a loose pile. Soil was excavated to a depth of about 0.40 meters (18 inches). Round-end hand shovels were used to excavate soil from the pile and pour it through 30.1-centimeter (12 inch) diameter 1 mm sieves placed on top of tared plastic 19-liter (5-gallon) paint buckets. Three sets of 1 mm sieves and buckets were used in parallel to speed the bulk sieving process. The sieves and buckets were vigorously rocked from side to side to agitate fine soils through the sieve opening. Loose conglomerates of soil remaining on top of the sieves were hand-crushed to pass them through the sieves. Rocks, twigs, and other debris were shaken off the sieves and placed in a spoils pile at one side of the excavation site.

Tared and total bucket weights with soil were recorded on a calibrated Sunbeam Freightmaster® 150 scale to the nearest 0.1 kilogram and were logged into a bound laboratory notebook.

After total (tare + soil) bucket weight was calculated, each bucket was covered with a tight-fitting snap-down lid and moved to the bed of a pickup truck for transport to the Phase IV study site.

Fifty (50) covered buckets of sieved soil were prepared in this manner. They were then all simultaneously transported to the storage yard of the DRI Solar facility on Adams Boulevard in Boulder City, Nevada, and stored outside for four days until September 11, 2006, when the soil samples were applied to the Phase IV road site.

3.2.3 Soil Characterization

A soil sample with a mass of about 700 grams was extracted from each of six soil buckets with a trowel during the excavation process, sealed in plastic cash bags, and transported to Ninyo and Moore, the geotechnical company contracted to perform soils analysis, on September 6, 2007 for sieve analyses. Sampled soil masses were measured with a calibrated Sunbeam model 78411 postal scale. Every tenth bucket, corresponding to Bucket numbers 1, 11, 13, 17, 28 and 39, was sampled for soil (buckets were not filled in numerical order). Soil moistures were measured with a Dynamax HH2 TDR volumetric moisture meter. Values ranged from 1.9 to 4.1 volume%.

Ninyo and Moore sieved these samples, using a sieve stack consisting of number 16 (1.18 mm), 30 (0.600 mm), 50 (0.300 mm), 100 (0.150 mm) and 200 (0.075 mm) mesh sieves, and an eight-minute shake time, to determine silt contents. This non-AP-42 sieving

technique was used only for recovered field soil samples that were collected before the Phase IV AP-42 field study. Results using this method showed that the average silt fraction for the excavated soil was 14.3%.

3.2.4 Soil Application

Soil from 15 buckets (about 340 kilograms, or 750 pounds) was poured into a 12-foot wide Gandy 10T series fertilizer drop spreader at the Phase IV empirical study field site on the morning of 9/11/2006.

The Gandy spreader was then driven to the Veterans Memorial Boulevard (VMB) site. Prior to the first application of soil a group of preliminary measurements by the mobile PM₁₀ sampling vehicles were used to characterize the PM₁₀ emission rates of the natural road soil on the VMB site before and after two sweeper passes. Soil was first applied from the Gandy spreader at about 1120 in the morning of 9/11/2006 after 92 vehicle passes had been completed.

During the five days of the study, the spreader pull speed was kept constant at approximately 5 meters/second (16 kilometer/hour or 10 miles per hour over an 850 meter length of the course (2900 feet). The spreader was pulled by a Dodge MaxiVan on the first day while a large garden tractor was used on subsequent days. Spreader soil application was driven by geared wheel that turned an agitating feeder at a rate that is proportional to ground speed. The rate of application by the spreader is controlled by adjusting the size of the diamond-shaped openings that feed soil to the ground surface. The opening was held constant for each set. Opening size was varied for different sets to apply soil at different loadings to the test site.

Soil was applied from 26 meters (85 feet) before the start of the southern AP42 sampling zone to 15 meters (50 feet) after the end of the northern AP42 sampling zone.

3.3 Horizontal Flux Towers

The flux of PM downwind of the test roadway emissions was quantified using a flux measurement technique similar to that described in previous work by Gillies et al (2005). A “master” tower was erected downwind of the road (Between 4 and 6 m from centerline of test vehicle travel path) and aligned perpendicular to road (**Figure 3-2, Figure 3-3**). The trailer-mounted, 9 m-high tower was instrumented with DustTraks (Model 8520, TSI Inc., Shoreview MN) configured to measure PM₁₀ at five heights above the ground surface (0.7, 2.1, 3.4, 6.4, and 9.8 m). At one of the heights (3.4 m), a DustTrak equipped with a PM_{2.5} impactor inlet was collocated with the PM₁₀ DustTrak. The master tower also included a TEOM (R&P, Model 1400a), which measures PM₁₀ at a height of 2.3 m. The TEOM sampling inlet was nominally collocated with one of the PM₁₀ inlet-equipped DustTrak monitors (at 2.1 m above ground level).

The DustTrak monitor measurement is based on light scattering of particles which is dependent on the particle size-distribution and the optical properties of the emissions. The TEOM was intended to help account for differences between optical based measurement and mass based measurements. These data were used to confirm supplemental, controlled measurements conducted in a resuspension chamber and described below. This allowed for conversion of emission factors measured with the tower-mounted DustTraks into mass-based emissions factors (see Section 4.1). A wind vane was mounted at the top of the tower and one cup anemometer was approximately collocated with each pair of DustTrak samplers. All data from the PM samplers and meteorological instruments were telemetered and logged in 1-second intervals by a laptop located on the master tower.

Figure 3-2. Photograph of master (left) and satellite (right, not used in present study) towers showing locations of DustTrak PM_{10} monitors. For present study, only one $PM_{2.5}$ inlet-equipped DustTrak was used on the master tower at a height of 3.4 m above ground level.

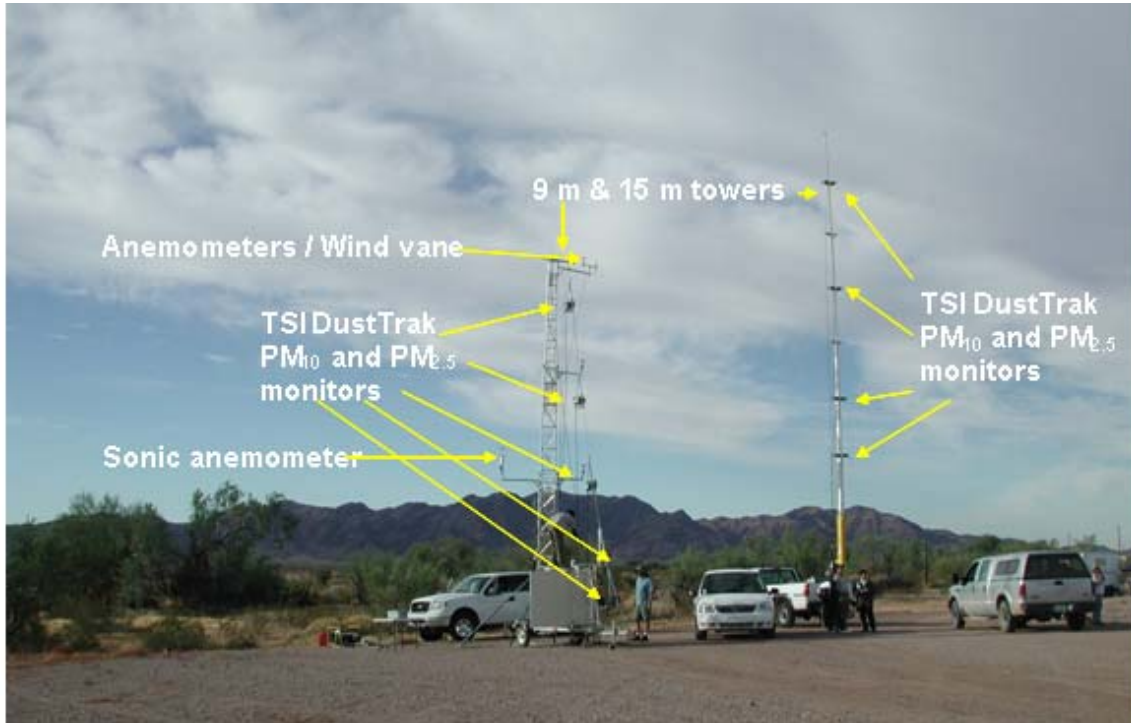
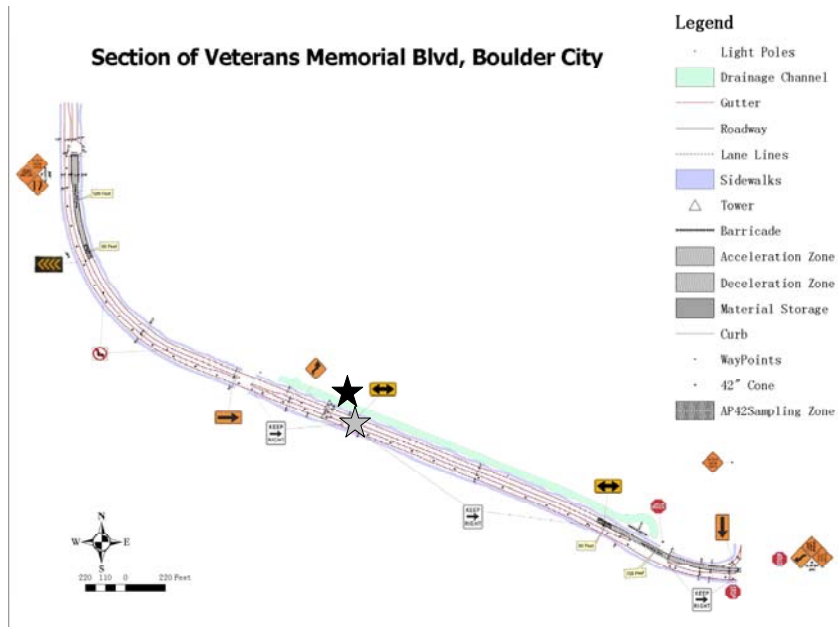
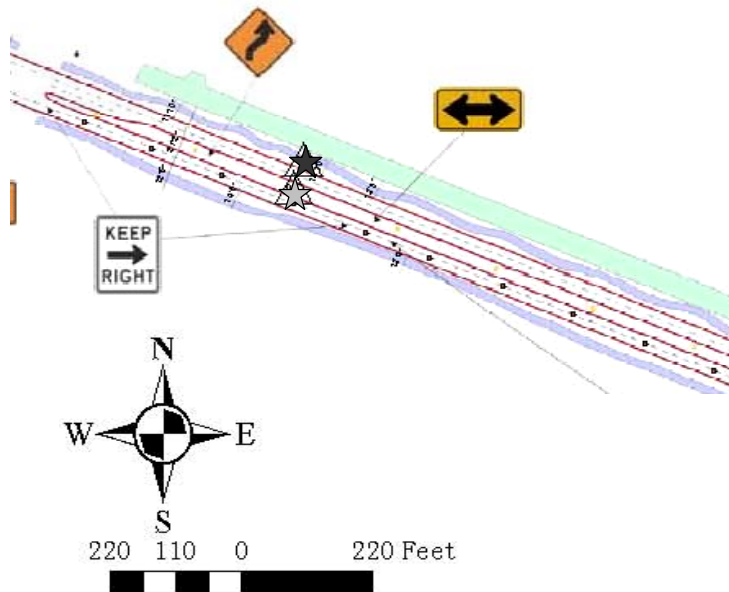


Figure 3-3. Schematic of field sampling layout. The gray star shows the location of the master tower on 9/11/06 and the black star shows the location of the master tower from 9/12/06 – 9/15/06.



a. View of entire test section



b. Close-up of section where tower was located

3.4 EPA Method AP-42

3.4.1 Plot Layout

Two zones of the course, called “south” and “north” were designated for silt recovery during controlled study.

The “near” end of the south AP-42 sampling zone was established 165 meters (543 feet) from the start of the course, as defined by the intersection of Veterans Memorial Dr. and Adams Drive. This distance was selected so that the mobile technologies vehicles could complete the acceleration portion of their pass before entering the soil sampling zone. The south AP-42 sampling zone was 36.6 meters (120 feet) long. The “far” end of the north AP-42 sampling zone was established 500 feet from the end of the course, just before the gradual curve in the roadway. GPS coordinates of the “near” and “far” corners of the sampling zones were measured using an un-corrected Garmin E-trex Global Positioning System receiver. Distances were also measured with a measuring wheel.

Seven 3.3 meter long x 4.1 meter wide (10 foot long x 13.5 foot-wide) plots were laid out in the south and north zones for soil recovery (**Figure 3-4**). Each of the AP-42 sampling plots was separated by a 2.4 meter (eight-foot) buffer zone. The buffer zone was used to allow field personnel and equipment to access the plots without disturbing the sampled area.

Two different plot layouts were used during the empirical study to collect soil samples:

1) A full size 3.3 meter long x 4.1 meter wide plot, with an area of 12.5 square meters was used to estimate soil and silt loading at the beginning and end of most of the mobile technologies sampling experiments. A 3.3 meter (10 foot) plot length was selected to remain consistent with recommended clean road plot length on page 7 of Appendix C.1, Procedures for Bulk Sampling of Surface Loading (US EPA 1993a) A 4.1 meter (13.5 foot) width was selected to recover soil from the edge of the asphalt (at the start of the concrete gutter) to the line dividing the eastern and western northwest-bound travel lanes on Veterans Memorial Boulevard.

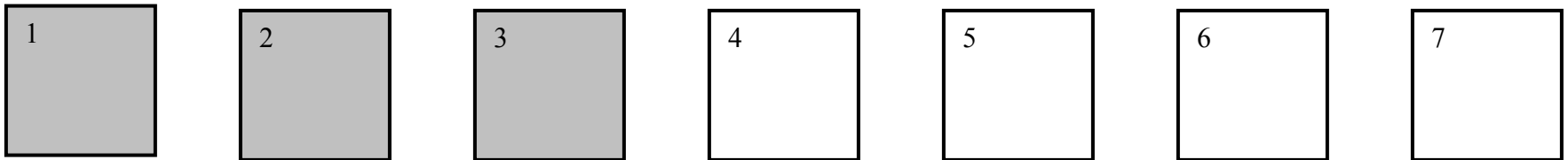
An array of seven (7) numbered full-size plots, with 2.4 meter (8-foot) spacing between the plots was laid out at each end (zone) of the driving course. Layout was established by first setting up a string rectangle consisting of colored surveyor’s twine wrapped around gravel-filled cans. The 3.3 meter and 4.1 meter lengths were different colors, and were tied to form a rectangle with an uncertainty of +/- 0.05 meters. White surveyors paint was used to establish the corners of the rectangles. The surveyors’ twines were pulled tight around the gravel-filled cans, and then 5.1 cm (2-inch) masking tape was applied from a roller dispenser to match the perimeter established by the colored surveyors’ twine.

2) For experiments evaluating the effects of vehicle passes on applied soil depletion, 0.61 meter (2 foot) wide “Quickie-Strips” (Etyemezian, personal communication, 2006) were

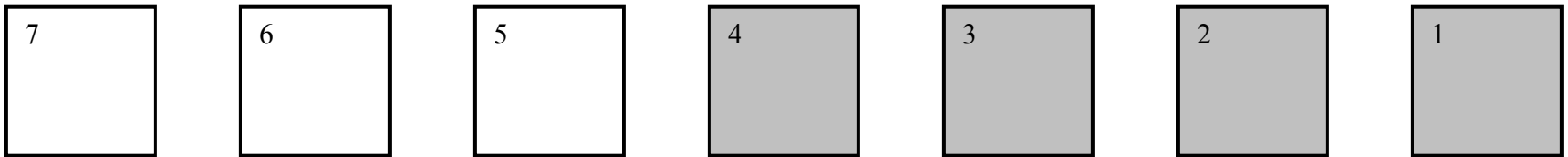
laid out in the zones between the full-size plots. Quickie-strip locations were marked on the concrete gutter and on the lane dividing line with white spray painted dots spaced every 2 feet apart. Painted lines or masking tape were not used to indicate boundaries of the Quickie Strips. Quickie Strip samples were also collected inside unused full-size plots, when needed. Although sampled in the “buffer” zones between AP-42 plots, the Quickie-strip samples were not collected in areas where there had been foot traffic, as the seven plots and, when needed, Quickie strips in the buffer zones were sampled in a progression from the near to far ends of the course (south zone) or far to near ends of the course (north zone).

Figure 3-4 - Phase IV Veterans Memorial Drive plot layouts

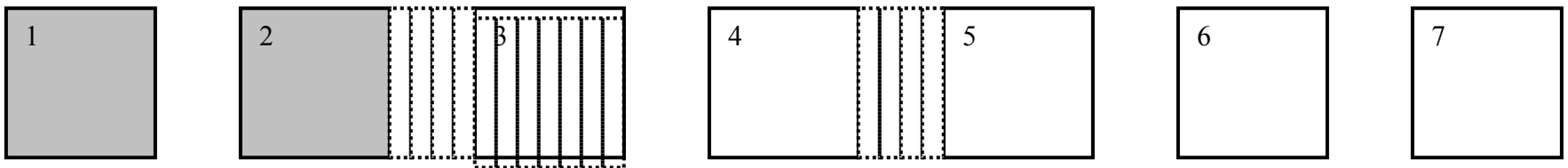
a) Schematic south zone plot layout (not to scale). Start of course is to left of Plot 1. Plots sacrificially sampled in ascending numerical order from 1 to 7, moving from left to right. Spaces between plots are eight-foot buffer zones for personnel and equipment access. Shaded plots indicate already sampled.



b) Schematic north zone plot layout (not to scale). End of course is to right of Plot 1. Plots sacrificially sampled in ascending numerical order from 1 to 7, moving right to left. Spaces between plots are eight-foot buffer zones for personnel and equipment access.



c) Example south zone quickie-strip plot layout (not to scale). Dotted lines show partitioning of un-used buffer zones or un-used plots into Quickie Strips for silt depletion sampling.



3.4.2 Vacuum Soil Recovery Methods

One Hoover Model S3636 Wind Tunnel Plus® and two Hoover Model S3639 Wind Tunnel Plus® canister vacuum cleaners, rated at 12 amperes, were used to recover applied soil from the roadway sites. The vacuum cleaners were connected by 50-foot or 100-foot 14-gauge extension cords to portable 3750-watt 120-volt Coleman generators. In cases where two samples were required at one point in time, two vacuum cleaners were simultaneously operated in parallel at the south zone of the site, and the northern vacuum cleaner would sample two test plots in sequence.

Soil samples were recovered into pre-tared (to +/- 1 gram using the Sunbeam 78411 postal scale) Hoover Type S Allergen Canister vacuum bags, model 4010100S. To determine the tare mass of the bags, the empty Hoover bags were removed from their plastic liner bags, weighed in the laboratory to within +/- 1 gram, labeled with a bag number and a tare mass, and replaced back in their plastic bags for interim storage until used in the field.

Vacuum hose-to-bag connections were sealed with low-density, high compression white foam polyethylene weather-stripping to minimize leakage of collected sample. New secondary motor filters were installed at the start of the study. They were cleaned every morning by removing and knocking the dust off. They were replaced every two days at a point when knocking the filter could not remove visible discoloration from soil.

Hoover Hard Floor Tools were used for soil recovery. Brushes on the Hard Floor tools are known to wear out quickly on asphalt. The most rapid wear occurred on the brush closest to the wand connection, with this brush worn down from about 9 mm to about 3 mm after 1/2 day's use in the field. Floor tools were replaced when visible wear of the brush below 3 mm was observed, typically every 1/2 day.

For full-size (12.5 square meters, 135 square feet) plots, two sets of twine wrapped around gravel-filled soup cans were used to visually partition the full-size plot into thirds across the direction of travel. Each partition was vacuumed twice with a curb-to-gutter vacuum stroke. After the curb-to-gutter vacuum strokes had been completed, the twine dividers were realigned along the direction of travel. Each partition was vacuumed twice with a front-to-back vacuum stroke. A total of four vacuum strokes were passed over each portion of the vacuumed plot, consisting of two curb-to-gutter strokes and two front-to-back strokes. Four vacuuming passes had been previously shown to recover 95-98% of applied mass on asphalt surfaces (UNLV unpublished data).

For Quickie-strip plots (area 2.51 square meters or 27 square feet), the hard floor tool was passed back and forth twice over each strip (Figure 2), first on the 1/2 of the plot nearest the curb, starting from the curb side towards the center of the road, and then on the 1/2 of the plot nearest the lane divider, starting at the lane divider and vacuuming towards the curb. Quickie-strip plots, comprised of five subsections of a standard plot, were not as well-marked as standard plots, so side to side variations in the swept width of

the Quickie-strips were larger than they were for the full-size plots. As a result, the absolute and relative uncertainty in the width of the Quickie-strip is larger than for the full-size plot.

Three soil recovery techniques were used during the study.

1) One plot per bag (Individual). Soil from one large heavily soiled plot would be recovered into one pre-tared bag, the bag would be weighed, sealed with plastic film to prevent leakage, and then placed in a labeled large brown 25 cm x 35 cm (10" x 14") office envelope. The envelope would then be held closed with its brass clasp. The date and time of the collection would be noted on the bag and on the log sheets.

2) Two large plots per bag (Cumulative). Soils from two lightly soiled large plots, sampled at the same time (before or after a particular vehicle pass) would be accumulated into one tared vacuum bag. The vacuum bag would be removed from the vacuum cleaner, weighed by one of the portable balances after the first soil recovery, and then reinstalled in the vacuum cleaner for sampling the second plot. After plot sampling was completed, the bag would be removed, sealed with film, placed in a labeled large brown office envelope and held in a sealed plastic storage container until needed for silt sampling analysis by Ninyo and Moore. The following formulae were used calculate the individual plot weights and silt loadings.

Silt mass plot 1 = (Ninyo and Moore silt fraction) x (Ninyo and Moore silt mass) x (Bag mass after plot 1 – Bag tare mass) / (Net mass for plot 1 + plot 2)

Silt mass plot 2 = (Ninyo and Moore silt fraction) x (Ninyo and Moore silt mass) x (Bag mass after plot 2 – Bag mass after plot 1) / (Net mass for plot 1 + plot 2)

3) Multiple small plots per bag (Cumulative). Soil masses from a series of Quickie strips, sampled in sequence after a specific vehicle pass.

Filled bag masses were recorded in the field after each vacuuming using the Pelouze SP5 and Sunbeam 78411 field scales. Scales were kept shaded from direct sun and measurements were made either inside a large plastic storage box or inside a closed 12-passenger cargo van to minimize effects of wind shake.

3.4.3 Field Soil Application History

The native road dust on Veterans Memorial Boulevard was first sampled by the AP-42 recovery technique before any passes were made by the mobile technologies vehicles.

Emissions from the native road soil were then measured by the mobile technologies sampling vehicles (DRI TRAKER I, TRAKER II, and UCR SCAMPER) and the DRI towers. After a series of 60 mobile technologies sampling passes, a PM-efficient sweeper was driven twice over the site to remove native road dust. Another 30 sampling passes by the mobile technologies vehicles then took place.

Soil from the Gandy spreader was first applied after vehicle pass 92. Pass 93 was the first mobile technologies measurement using the applied soil.

A summary of the applied soil loadings, vehicle passes and speeds is shown in **Table 3-2**.

Table 3-2. Summary of applied silt loadings during Phase IV controlled field study – Veterans Memorial Boulevard. Boulder City, NV

Date	Set #	Nominal Drive Speed (mph)	Spreader Setting	Net wt Applied, lbs	Spreader Path Length	Applied Soil Loading (gram/m ²)	Avg. Recovered Silt Loading, (gram/m ²)
9/11/06	3	35	15	45	2977	6.16	0.75
9/12/06	4	45	30	117	2775	17.17	2.48
9/12/06	5	25	30	113	2775	16.58	3.17
9/13/06	6	45	15	34	2775	4.99	0.88
9/13/06	7	25	15	32	2775	4.70	0.74
9/13/06	8	45	20	52	2775	7.63	1.14
9/14/06	9,10	35	20	53	2775	7.78	0.80
9/14/06	12	varying	30	120	2775	17.61	2.55
9/15/06	13	varying	35	194	2775	28.47	2.31

3.5 Mobile Technologies

3.5.1 SCAMPER

The SCAMPER determines PM emission rates from roads by measuring the PM concentrations in front of and behind the vehicle using real-time sensors. As a first approximation, the concentration difference (mg/m³) is multiplied by the vehicle’s frontal area (3.66m²) to obtain an emission factor in units of mg/m.

This SCAMPER includes five major components:

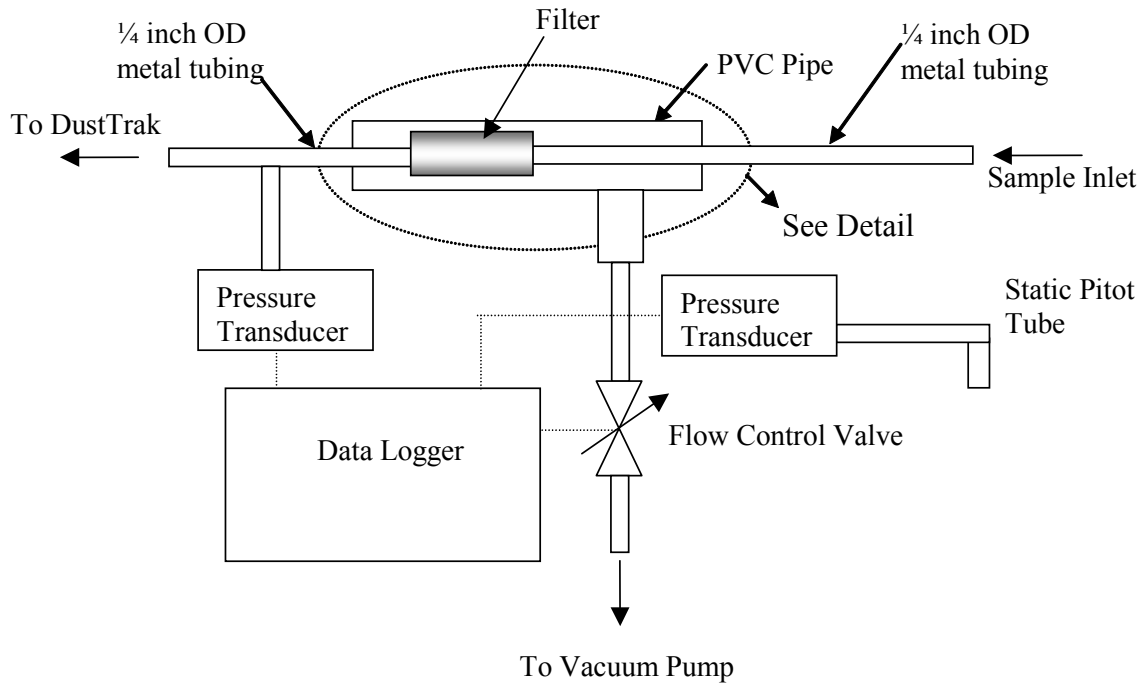
1) PM₁₀ Sensors

Thermo Systems Inc. (TSI Incorporated) Model 8520 DustTrak optical PM sensors with PM₁₀ inlets are used. These sensors are based on the principle that the amount of light scattered by particles is related to the particle concentration. Since the efficiency of light scattering depends on particle size, the response of the sensor depends on the particle-size distribution. Particles less than approximately 0.1µm diameter are not detected. The instruments are calibrated at the factory using NIST reference material 8632 Ultrafine Test Dust, more commonly known as “Arizona Road Dust”. The measurement range is from 0.001 to 100 mg/m³. The time constants are selectable from 1-60 seconds; the 1-second time constant is used on the SCAMPER. An impactor supplied with the instrument is used as a PM₁₀ size-selective inlet.

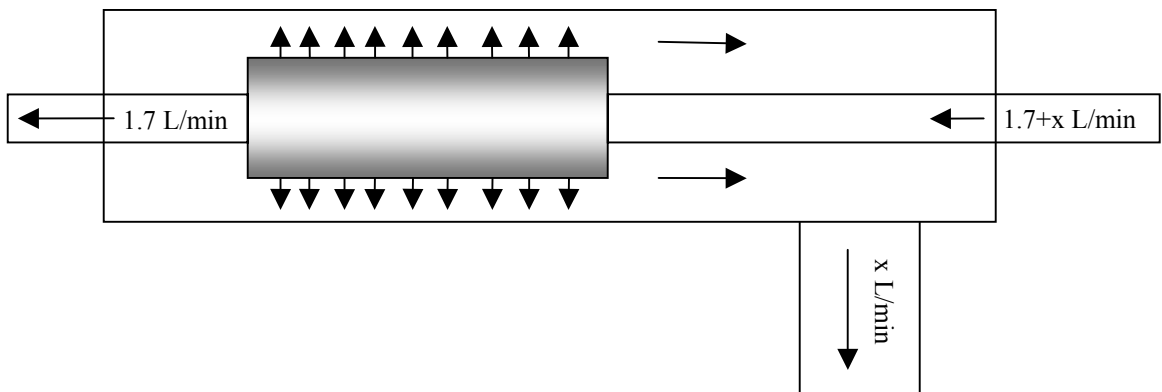
2) Sampling Inlet

An inlet for the real-time PM sensors was used that allowed sampling as isokinetically as possible over the full range of vehicle speeds. **Figure 3-5** shows the design of the inlet. Metal tubing is used to connect the sample inlet to the one end of a hollow cylindrical filter and from the other end to the DustTrak (the sampled air is not filtered, but travels from one end of the hollow cylinder to the other). To slow the flow to the sample flow rate of the DustTrak without creating a virtual impactor, excess air is pulled through the outside of the cylindrical filter with a vacuum pump that maintains the bulk air speed at the inlet equal to the speed of the air going past the inlet. The flow rate of the vacuum pump is adjusted by the data logging PC to produce a reading of zero pressure on the gauge. When the pressure equals zero, there is no pressure drop from the probe inlet to the tubing that leads to the DustTrak. This condition creates a no-pressure-drop inlet; therefore, the sampled air stream has the same energy as the ambient air stream.

Figure 3-5. Isokinetic inlet schematic diagram



Detail of Flow Splitting Section



3) Sampling Trailer

To determine PM_{10} concentrations in the vehicle wake, a DustTrak was mounted on a small trailer. The trailer has a flat bed four feet wide and six feet long, this configuration chosen such that the vehicle wake would be disturbed as little as possible. In addition, the trailer holds the bypass flow system. The trailer has a three foot extension on the hitch to place the DustTrak in a position ten feet behind the vehicle, which was shown to be representative of the PM_{10} concentrations in the wake and yet be safe to operate on public roads.

4) Position Determination

A Garmin GPS Map76 global positioning system was used to determine vehicle location and speed.

5) Data Collection

A PC was used to collect data from GPS and PM_{10} measuring devices. Data was stored as one-second averages. The PC also was used to automatically adjust the sample inlet bypass flow to maintain isokinetic particle sampling using a 10-second running average of vehicle speed based on the GPS.

Figure 3-6 shows front and rear photographs of the SCAMPER. The tow vehicle is a 2006 Ford Expedition with a custom trailer using an extended hitch.

Figure 3-6. Photographs of the front and rear of the SCAMPER.



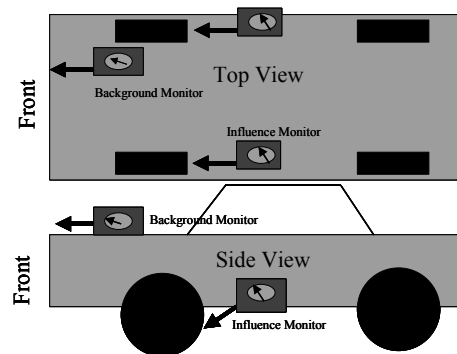
3.5.2 TRAKER I

The principle behind the TRAKER system is illustrated in **Figure 3-7**. The concentration of airborne particles is monitored through inlets that are mounted near the front tires of a vehicle. These particle sensors are influenced by the road dust generated through the tire contacting the road surface. A background measurement of particle concentrations is obtained simultaneously at a location on the vehicle farther away from the tires. The difference in the signals between the influence monitors and the background monitor is related to the amount of road dust generated:

$$T = T_T - T_b \quad \text{Equation 3.1}$$

where T is the “raw” TRAKER signal, T_T is the particle concentration measured behind the tire (average of left and right), and T_B is the background concentration.

Figure 3-7. TRAKER influence monitors measure the concentration of particles behind the tires. A background monitor is used to establish a baseline.



TRAKER I is comprised of a van that has been equipped with three exterior steel pipes acting as inlets for the onboard instruments (**Figure 3-8a**). Two of the pipes are located behind the left and right front tires and are used to measure emissions from the tires. The third pipe runs along the centerline of the van underneath the body and extends through the front bumper. This pipe is the inlet for background air. Dust and exhaust emissions from other vehicles on the road can cause fluctuations in the particle concentration above the road surface. The background measurement is used to correct the measurements behind the tires for those fluctuations.

The three exterior pipes enter the cargo compartment of the van through the underbody. Each pipe then goes into a plenum/manifold; the plenum can be used to distribute the sample air to up to five instruments (**Figure 3-8c**). For the present study, one TSI DustTrak with PM_{10} inlet was operated at each of the left and right inlet lines as well as on the middle inlet line. A central computer collected all the data generated by the onboard DTs as well as GPS coordinates, speed, and acceleration with 1-second frequency (**Figure 3-8d**).

All DustTrak monitors used for the study were calibrated by the manufacturer within 12 months of their use. Prior to each day of measurement, flows on the DustTraks were checked to ensure they were within manufacturer specifications and the instruments were “zeroed” with an inline HEPA filter as specified by the manufacturer.

Inlet configuration

Unlike gases, particles have inertia; as a result, the sampling of particles through an inlet results in some particle losses to inlet surfaces. These losses could be due to the diffusion of particles toward inlet walls or the impaction/settling of particles upon inlet walls. Diffusion is a phenomenon that governs the motion of very small particles (less than 0.1 μm). Since road dust is composed primarily of larger particles (greater than 0.3 μm), diffusion is not an important consideration for TRAKER. Impaction and gravitational settling, however, are important processes for sampling particles with aerodynamic diameters greater than 1 μm . Gravitational settling can be minimized by reducing the amount of time a particle spends in the inlet lines (e.g., by increasing the speed of the flow). On the other hand, particle impaction can be minimized by reducing the speed of the flow turns within the inlet lines.

The inlet lines, visible in **Figure 3-8a**, are 19 mm (3/4”) in diameter and 2.3 m (7.5’) long for the tire lines and 3.7 m (12’) long for the background line. The influence inlets on the right and left are in slightly different positions with respect to the tires. On the right, the inlet is 165 mm (6.5”) above the ground, 50 mm (2”) behind the tire, and 63 mm (2.5”) in (toward the center of the vehicle) from the outside edge of the tire. On the left, the inlet is 165 mm (6.5”) above the ground, 63 mm (2.5”) behind the tire, and 63 mm (2.5”) in from the outside edge of the tire. Because of the vehicle’s configuration, it is not possible to avoid bends in the inlet lines. However, the bends have been kept as shallow as possible in order to minimize losses of particles to the inlet walls. Each of the inlet lines feeds into a 600 mm (20”) long torpedo-shaped plenum (**Figure 3-8c**). All particle sampling instruments are connected through the plenum via short non-conductive tubes that are in turn attached to 20 mm (8”) long steel tubes that extend into the body of the plenum. Flowrates through the inlets, developed with a high vacuum pump, are 75 liters per minute (lpm), corresponding to an inlet face velocity of 4 meters per s (mps) and 0.3 mps in the plenum. Rotameters connected to each of the inlet lines are used to ensure that the flows through the inlets remain within 10% of the desired value. An independent rotameter equipped with stopper is used at the inlet lines to verify the readings of the onboard rotameters. Noting that in the seven years of experience using TRAKER I, the flowrate through the inlets has never drifted by more than a few percent of the desired value over the course of a day, the operator of the TRAKER can periodically check flows by examining the readouts on the rotameters in the vehicle’s rear-view mirror.

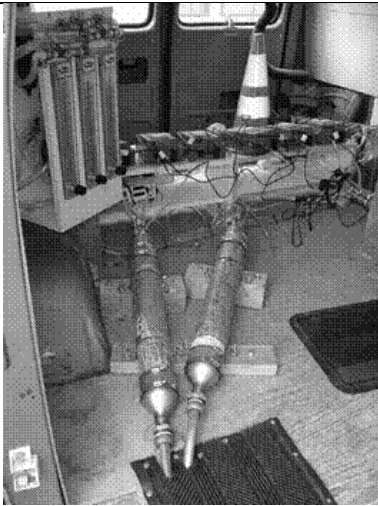
Figure 3-8. TRAKER vehicle and instrumentation: a) Location of inlets (right side and background shown); b) Generator and pumps mounted on a platform on the back of the van; c) Two sampling plenums (bottom), a suite of DustTrak particle monitors (top right), and three rotameters used for ensuring proper flows through the two plenums; and d) a dashboard-mounted computer screen used to view the data stream and a GPS to log the TRAKER's position every 1 second.



a.



b.



c.



d.

3.5.3 TRAKER II

In addition to the TRAKER I test vehicle described above, DRI also employed a prototype of a modified unit (TRAKER II). There are two major design differences between TRAKER I and TRAKER II. First, TRAKER II (**Figure 3-9** and **Figure 3-10**) uses low pressure-drop blowers to pull sample air in from behind the front tires and from the background instead of the high vacuum pump utilized by TRAKER I. This substantially reduces the power requirements of TRAKER II compared to TRAKER I and allows for the modified unit to be powered by onboard DC batteries that are recharged by the vehicle's alternator. Second, the TRAKER II inlet lines are configured so that on unpaved roads, where PM₁₀ concentrations behind the front tires could exceed the DustTrak instrument's upper limit (150 mg/m³), clean air can be mixed with air from the tire inlets in a controlled manner to achieve a desired amount of dilution.

There are also other minor differences between TRAKER I and TRAKER II. For example, a) the inlets behind the front tires in TRAKER II are located farther behind the tire than in TRAKER I; b) Instead of an onboard sampling plenum as in TRAKER I, a 10 cm diameter external pipe is used to channel/dilute inlet flow and instruments can sample the air within that pipe through small manifolds located on the floor of TRAKER II; c) The circular inlets used currently on TRAKER I are replaced by flattened manifolds on TRAKER II. Aside from these differences, TRAKER II is based on the same basic principle of operation as the TRAKER I.

In the present study, the use of TRAKER II is intended to obtain preliminary data for assessing if changes in design have achieved the desired outcome or if additional changes are needed. Like TRAKER I, TRAKER II was outfitted with PM₁₀ DustTraks on the left and right tire inlets as well as on the "Background" inlet, which in the case of TRAKER II resides above and slightly behind the driver-side and passenger-side doors (See **Figure 3-9**).

The electric blowers in the inlet pipes were turned on and fixed at a flowrate of 10 lpm. Within each inlet line, the flow rate is measured in 200 ms intervals by a small pitot tube attached to a pressure transducer (Dwyer Instruments, 1/4" of water max). An onboard laptop computer adjusts the power to the blower motor to maintain the flow at 10 lpm with a frequency of 200 ms.

As with TRAKER I, DustTrak monitors were zero- and flow-checked at the beginning of each sampling day. In operation, the DustTrak instruments extract particle-laden air from within the pipe that runs along the underside of the vehicle through non-conductive tubing. Optionally, TRAKER II can be equipped with other instruments such as filter samplers and particle size analyzers through additional sample ports on the inlet pipe. A GPS unit in TRAKER II provides geospatial coordinates, vehicle speed, acceleration, and wheel angle. These data, along with 1-second DustTrak measurements from the three inlet lines (left, right, and background) are displayed in real-time and logged by the laptop computer for subsequent analysis.

Figure 3-9. TRAKER II. Vertical inlet pipe near the passenger-side door is used to sample background air for the right side inlet.

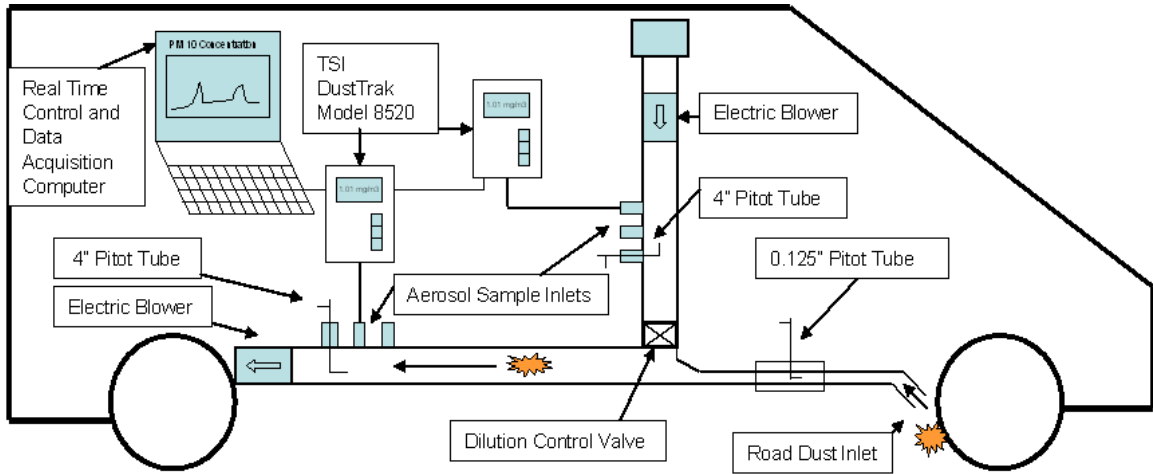


a. side view

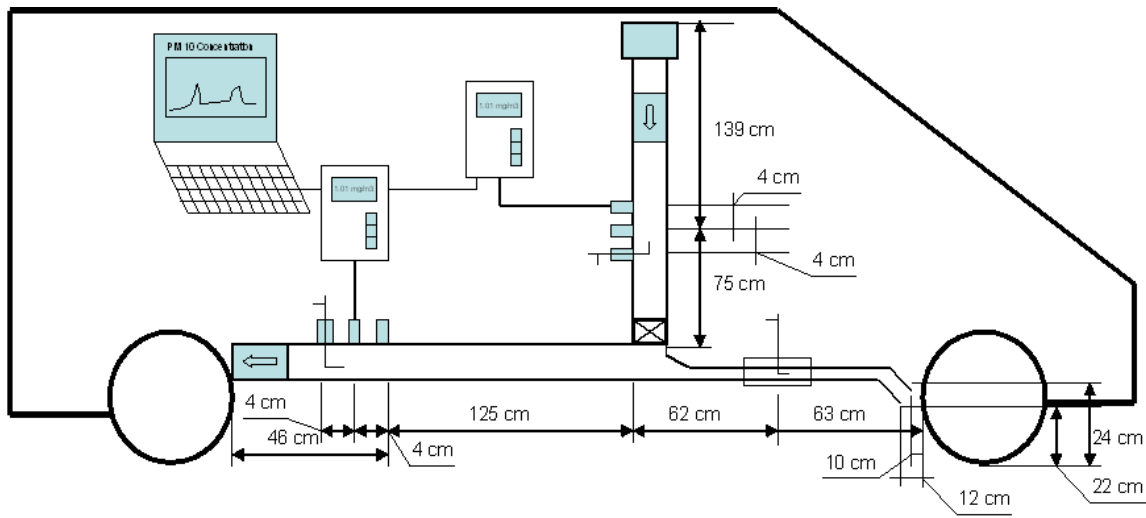


b. inlet close-up

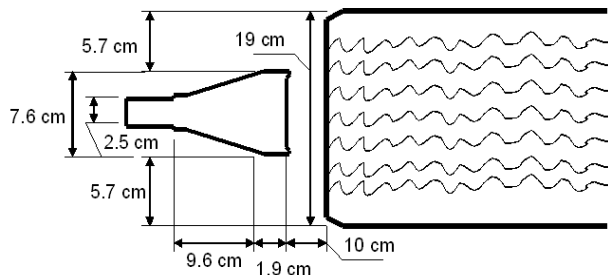
Figure 3-10. Schematics and dimensions of TRAKER II



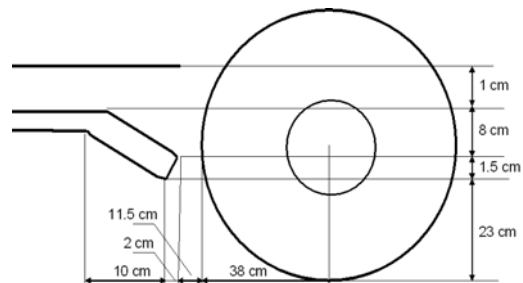
a. Functional TRAKER Diagram



b. Dimensions – Not drawn to scale



c. Inlet, Top View



d. Inlet, Side View

4.0 QA/QC

4.1 Horizontal Flux Towers

Horizontal fluxes of PM₁₀ (units of grams PM₁₀ per vehicle kilometer traveled – g/vkt) were calculated using data from the master tower. Level 0 data validation involved ensuring that instruments were operating properly and data were recorded correctly. This included cross-referencing the data recovered from computer files with dates and times of operation noted in field notebooks. Additionally, whenever new wire connections were made or modified or any part of the data acquisition was modified (change of communication ports on data acquisition system, replacement or exchange of DustTrak monitors, etc), the data files were spot-checked against the instrument visual display to ensure that readings in the data files corresponded to instrument labels.

Level I validation required visual as well as automated inspection of the data. The measured PM₁₀ concentrations at multiple heights, wind speeds, and wind direction were plotted with one-second resolution. In addition, the vehicle passage times that were manually noted by field personnel and verified with GPS data onboard TRAKER I and TRAKER II were also plotted on the same graph.

Two factors were used to determine if a specific flux measurement associated with a specific vehicle pass was valid. First, the one-second wind direction over the duration of the three intervals – pre-peak background, peak, and post-peak background was examined. In cases where the average wind direction over the three intervals was within 45 degrees of the perpendicular line drawn between the tower and the road segment and the wind speed was relatively constant (i.e. holding at > 1 m/s from the same general direction), the wind direction was considered valid. In cases where the average wind direction was outside of this 90-degree window (45 degrees in each direction about the perpendicular), one-second data were examined. If the wind direction was always less than 75 degrees from the perpendicular, the wind speed was relatively constant, and fluctuations in wind direction did not exceed 30 degrees, the wind direction was considered valid. In all other cases, wind conditions were considered to invalidate the horizontal flux measurement.

The second factor in determining the validity of a specific tower measurement was the noise level of the baseline PM₁₀ concentration. During periods of high wind, wind-entrained dust clouds often passed by the flux tower (especially true on 9/14/06 and 9/15/06). These high and spurious concentrations of PM₁₀ rendered the baseline from which peak values are estimated extremely noisy. In other cases, the passage of a large vehicle on the south side of Veterans Memorial Highway would sometimes result in a temporary spurious baseline reading. The entire time series of data from the flux towers was examined to flag periods when the baseline was too noisy for a measurement. Those data were considered invalid.

Note that an individual dust plume from a moving vehicle may exhibit a high degree of spatial heterogeneity, owing to the turbulent nature of air flow in the wake of a moving

vehicle. Thus, an actual plume consists of clouds of dust interspersed with comparatively clean background air. This is especially true close to the road; PM_{10} concentrations become more spatially continuous and smooth as the plume advects and disperses downwind. For the present study, in certain cases, baseline noise levels and the wind direction over the expected peak period were acceptable. However, a visible peak associated with the passage of a vehicle was not always clearly discernible. In those cases, the measurement was considered valid and the PM_{10} flux was calculated and reported. Though these cases could result in near-zero or negative fluxes, which are not physically reasonable, it is important to retain these measurements to avoid biasing the data. Estimation of peak duration (whether or not peak was visible) is discussed in Section 5.1.

DustTrak Mass Correction

PM_{10} measurements with the DustTrak were compared to two types of mass-based PM_{10} measurements. First, the DustTrak located at 3.4 m on the master flux tower was compared to the TEOM measurements at the same height, also located on the master tower. Second, in-lab tests were used to more accurately obtain a relationship between the DustTrak measurements and mass-based measurements. The correlation between the DustTrak and TEOM on the master tower is quite noisy, but shows that DustTrak values would have to be multiplied by a factor of 2.8 ± 0.6 to obtain mass-equivalent PM_{10} . (See **Figure 4-1**)

In the laboratory, we constructed a chamber in which silt material that was used to seed the road at the Boulder City site was injected and suspended. Measurements of the PM_{10} and $PM_{2.5}$ inside the chamber were made with the DustTraks as well as filter samples. The dust-laden air from the chamber was drawn through size-selective impactors and subsequently directed to Teflon-membrane filters in Savillex filter holders. These filters were submitted for gravimetric analysis to allow us to compare mean PM concentrations measured with the DustTrak and the mass-based measurement obtained using the filters. We also evaluated the $PM_{2.5}:PM_{10}$ ratio developed from the field data with these additional laboratory measurements.

Results of this laboratory experiment showed that the DustTrak instruments have very good measurement consistency with $PM_{2.5}$ being highly correlated with the PM_{10} measurements ($PM_{2.5} = 0.501 PM_{10}$, $R^2 = 0.955$) (**Figure 4-2**). The relationship between gravimetric mass concentration and DustTrak concentrations are also very good. For PM_{10} filtered mass concentration versus DustTrak we observed the relationship PM_{10} (gravimetric) = $2.4 \pm 0.2 \times PM_{10}$ (DustTrak) with a correlation coefficient (R^2) of 0.84 (**Figure 4-3**). For the $PM_{2.5}$ the relationship between gravimetric and DustTrak derived mass concentrations was $PM_{2.5}$ (gravimetric) = $0.7 \times PM_{2.5}$ (DustTrak) with a correlation coefficient (R^2) of 0.891 (**Figure 4-4**).

Based on these two sets of collocated tests, one conducted in the field and the other in the lab, we chose a DustTrak correction multiplier of 2.4 corresponding to the in-lab measurements. Noting that the uncertainty in the regression between the DustTrak and

the TEOM in the field encompasses this value (2.8 ± 0.6), the in-lab measurements were chosen for correcting the DustTraks because the correlation was much better than in the field. This was likely due to the fact that in the field, the DustTrak and TEOM were only nominally collocated whereas in the lab, the two instruments were sampling a well mixed controlled volume of air.

Figure 4-1. Scatter plot of DustTrak PM₁₀ average concentrations and TEOM PM₁₀ measurements. Both measurements were collected at 3.4 m height on the master flux tower. Red dot shows averages for all sets of measurements over the course of the study.

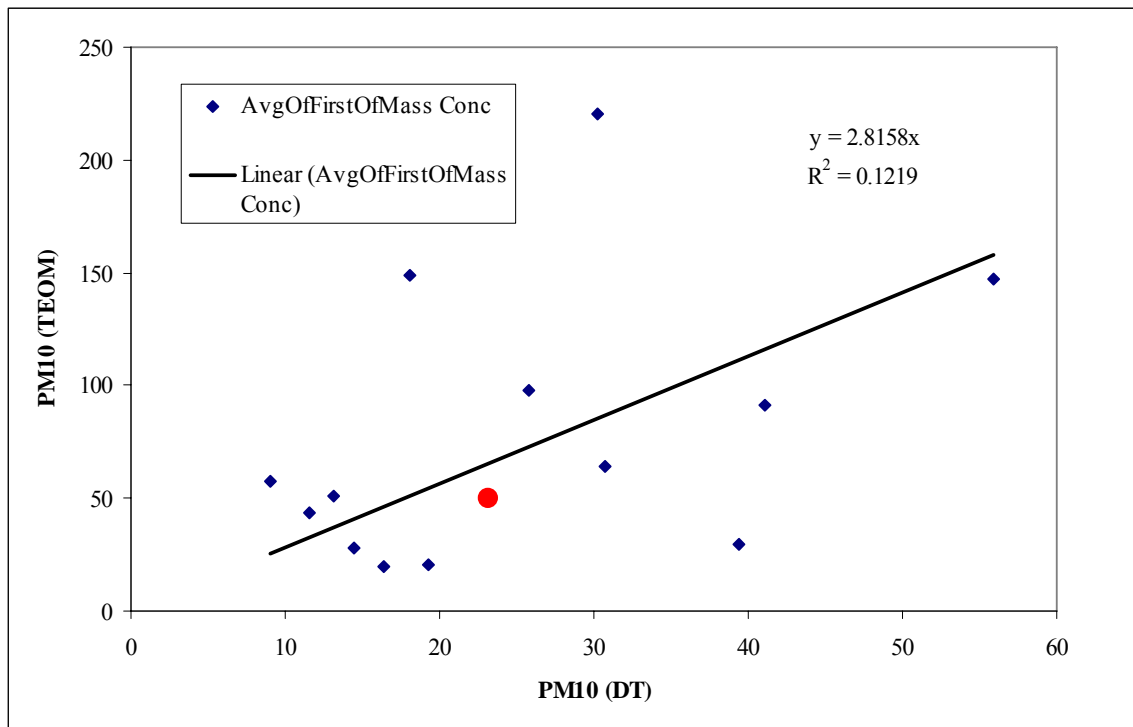


Figure 4-2. Scatter plot of DustTrak monitor outfitted with PM_{2.5} inlet versus DustTrak with PM₁₀ inlet. Both instruments sampled silt material from the Phase IV tests that was resuspended in a specially designed chamber.

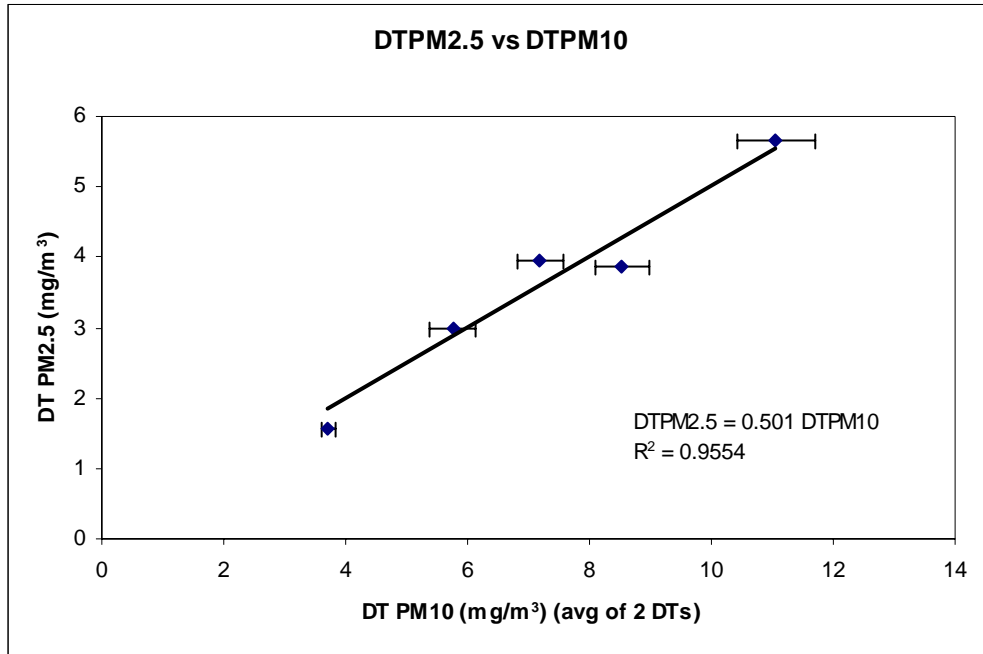


Figure 4-3. Comparison of filter-based PM₁₀ measurements with DustTrak outfitted with PM₁₀ inlet. Both instruments sampled silt material from the Phase IV tests that was resuspended in a specially designed chamber.

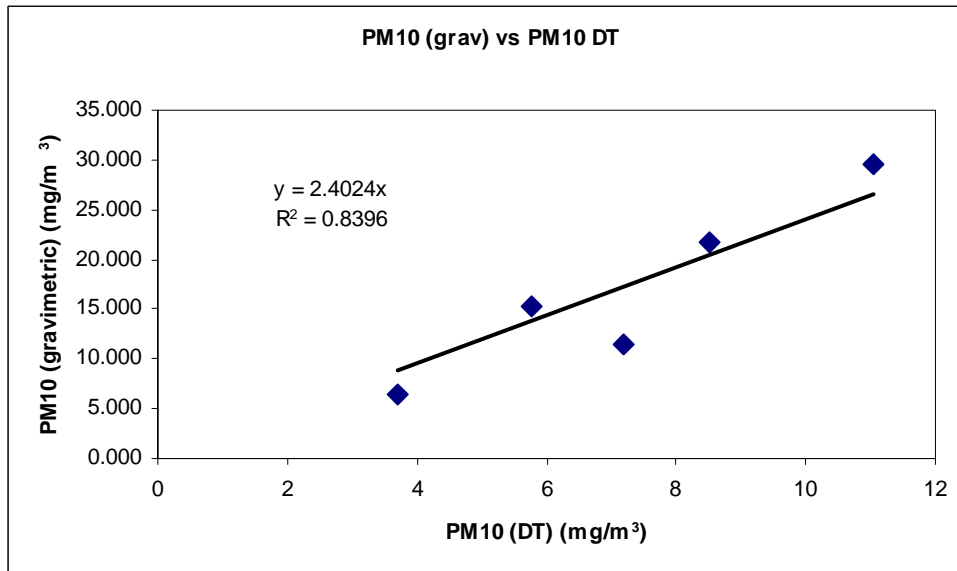
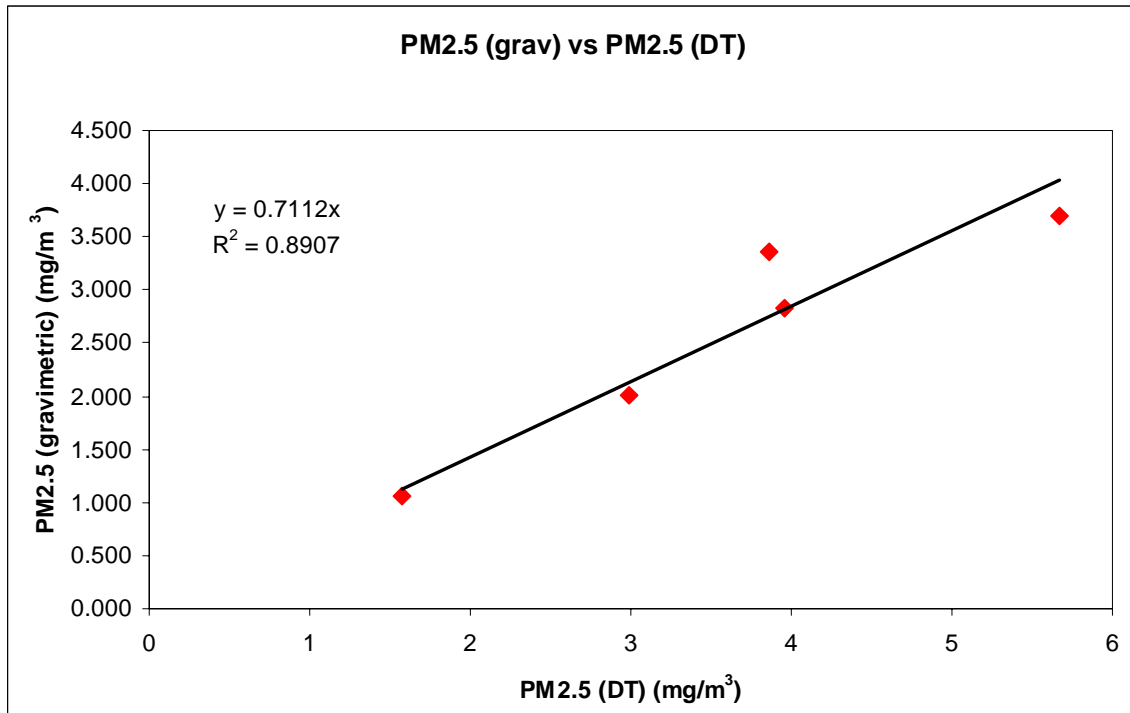


Figure 4-4. Comparison of filter-based PM_{2.5} mass measurement with DustTrak outfitted with PM_{2.5} inlet. Both instruments sampled silt material from the Phase IV tests that was resuspended in a specially designed chamber.



4.2 EPA Method AP-42

4.2.1 Field Balance Mass Calibration

Calibration of all postal measurement scales was carried out with Rite-O-Weigh® brass weights meeting ASTM Class 6 adjustment tolerances.

The Sunbeam 78411 postal scale has a readability of +/- 1 gram and was found to read within 1 gram of the true weight from 0 gram to 200 grams, and within 2 grams of the true weight from 200 grams to 1,000 grams.

The Pelouze SP5 Postal scale has a readability of +/- 1 gram was found to read within 1 gram of the true weight from 0 grams though 1,000 grams.

The Sunbeam Freightmaster® 150 scale for soil sample excavation has a readability to +/- 0.1 kilogram. It was calibrated with the Rite-O-Weigh® brass weights over the 0.1 kilogram to 4.0 kilogram range and found to deviate less than 0.2 kilogram.

4.2.2 Road Plot Marking Uncertainty

Full size roadway plots 10 feet (3.05 meters) long by 13.5 feet (4.12) meters wide were

marked with 3.05 meter and 4.12 meter string lengths were different colors, and were tied to form a rectangle with an uncertainty of +/- 0.05 meters (5 centimeters). Corners were squared so that the string was taut with standard building bricks, and then 2-inch masking tape was applied from a roller dispenser to match the perimeter established by the colored surveyors' twine. The tape perimeter was then marked with white surveyors paint and the tape was removed. White surveyor's paint spots are laid out at one foot (0.305 meter) intervals across the road way at each end of the 3.047 meter long plot to delineate the area to be vacuumed.

“Quickie strip” roadway plots 2 feet (0.610 meter) long by 13.5 feet (4.115 meters) wide were laid out between the full size plots. White surveyor's paint was used to mark the corners of the quickie strip plots. Painted lines or masking tape were not used to indicate boundaries of the quickie strips. As a result, vacuum path width for the quickie strips, guided only by the eye of the operator from the inside curb to the lane divider, tended to deviate by up to 1/6th of the 30 cm (12 inch) width of the Hard Floor tool, or about 5.0 cm or 2 inches. This deviation in path width results in a proportionately larger single sample uncertainty in the vacuumed area of the quickie-strip plots compared to the vacuumed area of the full size plots.

4.2.3 Sieve Analysis Calibration

Collected soil samples were held in sealed plastic containers for three weeks in a climate-controlled laboratory at UNLV. Ninyo and Moore's laboratory in Las Vegas, Nevada, performed sieve analyses. Sieves are manufactured to ASTM standard E-11:87 and to AASHTO M-92. Sieves are calibrated annually by a calibration laboratory following ATM Manual 32. All sieved masses are determined to +/- 0.1 gram on a calibrated electronic balance.

The eight-inch (20.3 cm) sieve stack recommended in AP-42, Section 13.2.1, Appendix C.2. (US EPA 1993b), consisting of sieve numbers 3/8 inch, 4 mesh, 10 mesh, 20 mesh, 40 mesh, 100 mesh, 140 mesh, and 200 mesh, plus pan, was used to sieve all recovered soil samples. A standard sieve time of 10 minutes was used, per AP-42 13.2.1 Appendix C.2. The sieves were agitated on a Tyler Ro-Tap® RX-29 mechanical Test Sieve shaker, operating at a fixed speed of 278+/- 10 revolutions per minute with 150 taps +/- 5 taps per minute. Silt masses were reported as the mass passing the number 200 (75 micron) sieve.

Upon review of AP-42 methods for minimum soil required sample masses (Appendix C.2, US EPA 1993b, page 7), where “100 to 300 grams may be sufficient when 90% of the sample passes a No. 8 (2.36 mm) sieve,” soil masses for simultaneous parallel bags from the same sampling location and vehicle pass were combined for sieving to make total sieve masses exceeding 100 grams, if individual bag masses were less than 50 grams.

Sieving analyses by Ninyo and Moore were “blind” in that they did not know the location or expected composition of the recovered soil samples.

All sieving work was completed by the end of October 2006. Ninyo and Moore transmitted soils data back to UNLV as multi-page PDF files, with one page for each sample. Each page of the PDF file contained results for one sample, organized by UNLV site identification number.

4.3 Mobile Technologies

4.3.1 SCAMPER

The zero response and flow rate of each DustTrak was recorded at the beginning and end of each day. In prior studies the response of the rear DustTrak was compared to mass determined by collocated filter samples. The average response factor based on a linear regression was approximately 3. Given the scatter of the data, this is in general agreement with the correction factor described previously. The response of the DustTraks was therefore less than when calibrated using Arizona Road Dust. This most likely is due the PM₁₀ behind the SCAMPER consisting of a greater fraction of larger particles than the Arizona Road Dust. The mass-specific light scattering response drops rapidly with increasing particle size for particles larger than 1µm diameter, thus a small change in the particle-size distribution can change the response significantly.

The data acquisition system recorded all data digitally at one-second intervals. Data was downloaded from the PC and entered into an Excel worksheet where all of the calculations were made. Quality control data such as inlet pressure and various voltages were also entered into the master worksheet in addition to GPS location, time, speed, and DustTrak values.

Data was validated to Level 0 and then Level 1 status from QC pressure and voltage data, logbook entries, and by observing time series, to determine if the results made physical sense. The data was flagged as follows in the Excel worksheet:

- 0 or blank: valid data
- 1: missing or erroneous
- 2: DustTrak on filtered air for zero check- not moving control
- 3: DustTrak on filtered air for zero check-moving control
- J: DustTrak values not changing for 30 seconds of more

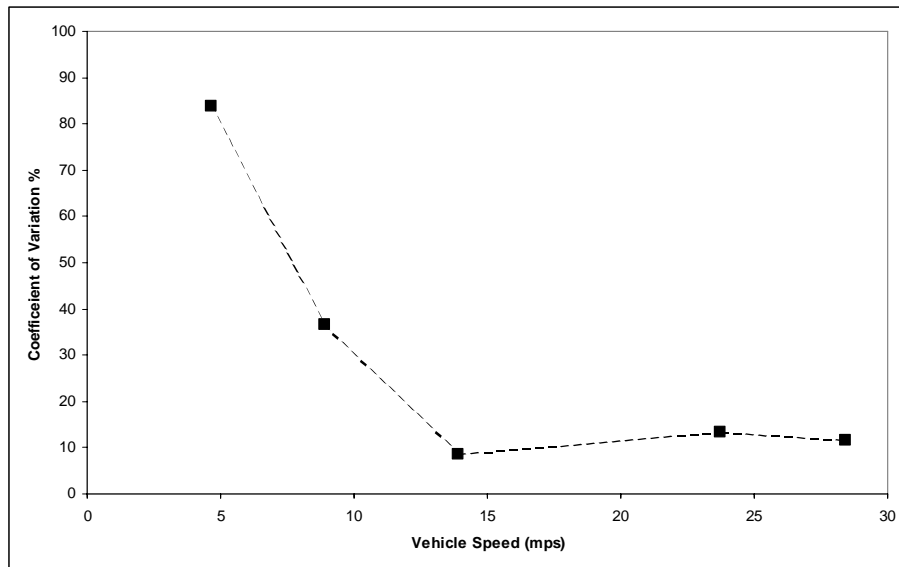
4.3.2 TRAKER I

The DustTrak instrumentation onboard the TRAKER vehicle has a resolution of 1 µg/m³. Thus, the smallest measurable difference in concentration between the tire and the background monitor locations is 1 µg/m³. This corresponds approximately to a single-point minimum detection limit equivalent to an emission factor of 0.0005 g/VKT (0.0008 g/VMT) for paved roads, meaning that any 1 s measurement can be resolved to within this value only. In practice, emission factors from real roads are generally higher than

0.01 g/ VKT (0.016 g/VMT). At the other end of the measurement range, DustTrak readings above 150 mg/m³ are not reliable. This corresponds to an emission factor for PM₁₀ of approximately 75 g/VKT (120 g/VMT). Again, in practice, 20 g/VKT (32 g/VMT) represents an upper limit to paved road PM₁₀ emissions.

Figure 4-5 shows the TRAKER coefficient of variation calculated from the left and right PM₁₀ DustTrak signals as a function of vehicle speed. The coefficient of variation is a measure of the relative precision and is equal to the standard deviation of the measurement divided by the average of the measurement. In the figure, the measurement corresponds to multiple passes on the same 1-mile stretch of road (Etyemezian et al., 2003). The figure shows that the precision of the measurement improves with increasing vehicle speed. The precision is 84% at 5 m/s, 30% at 9 m/s, and approximately 10% above 14 mps. Note that most TRAKER measurements occur at speeds greater than 9 m/s (approximately 20 mph). The poor precision at low speeds is probably due to the influence of fluctuating ambient winds on the flow regime behind the front tires. As the vehicle speed increases, such fluctuations become less important compared to the speed of the vehicle.

Figure 4-5. TRAKER coefficient of variation expressed as a percentage for left and right PM₁₀ DustTrak signals as a function of speed. The data represent left and right PM₁₀ DustTrak signals averaged over a 1-mile stretch of road near Boise, Idaho (Etyemezian et al., 2003). The coefficient of variation provides an estimate of the precision and is equal to the standard deviation of a measurement divided by the average.



The vehicle speed can become important in moderate to high winds. If the TRAKER is not moving fast enough, crosswinds and fluctuations in the ambient winds can lead to unsteady flow conditions between the front tire and the inlet. To avoid this possibility, a minimum speed of 5 m/s is required to consider a data point valid. Acceleration/deceleration criteria ($<0.7 \text{ m/s}^2$) are also applied to the TRAKER

measurement. During periods of high acceleration, the flow regime around the inlets may be transient; during periods of deceleration, dust from the brakes may influence the particle concentrations behind the front tire. Note that in the prior work of Etyemezian et al. (2003a, 2003b) and Kuhns et al. (2001) the criterion for acceleration was 0.5 m/s^2 . Due to the start and stop nature of the loop selected for the present study, that criterion had to be relaxed slightly in order to avoid losing much of the data collected. This relaxation of the criterion should not affect the measurement significantly since the original criterion was set to be overly conservative.

In addition, the wheel angle must be less than 3 degrees with respect to the vehicle body. This is to ensure that the orientation of the inlets with respect to the front tires is not changing over the course of the measurements. The criteria shown in **Table 4-1** are based on empirical observations and statistical analyses of the TRAKER measurement under a variety of driving regimes. These criteria are applied to the one-second data prior to any further aggregating or averaging. They are conservative and intended to ensure that the measurements used in this study are valid.

Table 4-1. Validity criteria applied to each 1 s TRAKER data point.

Parameter	Criterion	Threshold	Description
Speed	>	5 m/s – paved roads (~11 miles/hr)	Minimize disturbances due to ambient winds.
Acceleration	<	0.7 m/s^2 (~1.3 miles/hr/s)	Lateral shear during acceleration and transient airflow around the TRAKER inlets render TRAKER measurements during times of high acceleration unreliable.
Deceleration	<	0.7 m/s^2 (~1.3 miles/hr/s)	Applying the brakes releases dust particles and may result in false high road dust readings.
Wheel Angle	<	3 degrees with respect to the vehicle body	Turns cause the front wheels to form an angle with the vehicle body. This in turn changes the orientation of the TRAKER inlets with respect to the front tires. Data associated with sharp turns are not valid.

Level 0 validation was performed by examining the DustTrak and GPS time series for the entire study. The data were examined for completeness and correspondence with known sampling times. GPS data were checked by mapping coordinates from the GPS receiver on a spatially referenced GIS map. Any documented deviations in flow rate or procedure were examined to ensure that they did not affect data quality. For the entire study, all instruments were found to be logging as expected and no deviations from normal operating procedure were noted. In addition, the DustTrak zero-check on all days indicated that there was not significant instrument drift from day to day (i.e. correction required was less than $3 \mu\text{g/m}^3$)

Level I validation included examination of the time series for each pass that was completed through the test course. We looked for sudden jumps (spikes or troughs) in

the DustTrak record as well as in the GPS time series. In TRAKER I, the DustTrak samples air from a plenum with an approximate residence time of 2 seconds. Thus, spikes in PM₁₀ concentration that appear for only one second are considered suspect data. No such data were found for the present study.

Level II validation included examining relationships between the signals on the left and right TRAKER inlets as well as over the course of a measurement set. The ratio of PM₁₀ concentrations measured behind the tires to those measured at the background (bumper) inlet was also examined to ensure that the TRAKER signal was substantially above background.

4.3.3 TRAKER II

Noting that the use of TRAKER II as part of this study was experimental and that this updated version of TRAKER I has not been as extensively characterized, TRAKER II data were handled in a manner similar to TRAKER I. The same speed, acceleration and wheel angle criteria applied to TRAKER I (Table 4-1) were also applied to TRAKER II on a one-second basis.

Level 0 validation included ensuring that all instruments were operating and logging data during the measurement period. Level I validation included examination of time series of DustTrak concentrations and GPS data. Time series of the flow rates through the left and right inlets were also examined for deviation from the fixed value of 10 lpm. It was discovered during this examination that for all of 9/11/06 and a portion of 9/12/06 the flowrate through the inlets was not being properly maintained at 10 lpm, but rather was held at 6 lpm. This problem was attributed to a glitch in the software that controls the TRAKER II data acquisition system and repaired in the field. In summary, TRAKER II passes with Pass IDs of 170 and higher were considered level I valid whereas those with Pass ID lower than 170 were considered invalid.

Level II validation was conducted as part of the data analysis for this study and the outcomes of that effort are summarized in a later section along with other study findings.

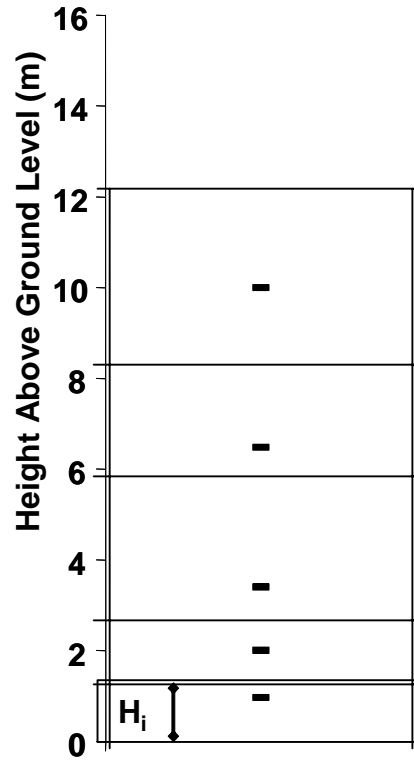
5.0 DATA HANDLING

5.1 Horizontal Flux Towers

Horizontal PM₁₀ fluxes were calculated from the tower data for all individual passes that met the validation criteria outlined in Section 4.1. As mentioned in that section, the two factors that were used to determine whether a data point was valid or not were the wind direction/speed and the background noise level, determined from periods with no influence from any of the test vehicles. The general approach for calculating the horizontal PM₁₀ flux was to assume that the master tower was located in a flux plane parallel to the road and that the multiple vertical measurements of wind speed, wind direction, and DustTrak PM₁₀ concentrations each represented a discrete section of the tower height. This is illustrated in **Figure 5-1** which shows instruments mounted at 0.7,

2.1, 3.4, 6.4, and 9.8 m above ground level representing the sections spanning 0 – 1.4, 1.4 – 2.75, 2.75 – 5.9, 5.9 – 8.1, and 8.1 - 12 m, respectively.

Figure 5-1. Illustration of portions of flux plane represented by DustTrak and wind instruments at each height. The dots shoe the instrument locations and the horizontal lines show the height range that the instruments represented in calculating flux.



An emission factor (EF , g/km) for each vehicle pass was calculated using the equation:

$$EF = \alpha \left[\sum_{i=1}^5 \sum_{t=t_{begin}}^{t_{end}} u_{t,i} \cdot (C_{t,i} - C_{0,i,t_{begin}-t_{end}}) \cdot H_i \cdot \cos(\theta) \right] \times 1000 \quad \text{Equation 5.1}$$

where: i refers to the vertical section represented by the DustTrak height, t is the time (sec), t_{begin} is the peak start time, t_{end} is the peak end time, u is the wind speed (m sec^{-1}), C is the measured concentration (g m^{-3}), C_0 is the background concentration over the period $t_{begin} - t_{end}$ (g m^{-3}), and H is the height of the section of the flux plane represented by position i , θ is the angle of the 1-sec wind direction relative to the flux plane, and α is a constant used to convert DustTrak-measured PM_{10} concentrations to mass equivalent PM_{10} and has a value of 2.4 (See Section 4.2).

In some cases, DustTrak concentration peaks were clearly discernible and associated with the known passage of a vehicle. In practice, this required that DustTrak concentrations departed from baseline values on multiple DTs within 15 seconds of the passage of a test vehicle in front of the master tower. In those cases where peaks were clearly associated with the test vehicle, the peak curves were divided into three intervals. The first interval corresponded to the background PM₁₀ concentration prior to the peak and included the 10 – 30 second period that ends with the peak start time. The second interval was bounded by the peak start and stop times (giving the values of t_{begin} and t_{end}), which were determined visually as the instance when any of the tower-mounted DustTraks began exhibiting a peak in concentration to the instance when all of the tower-mounted DustTraks exhibited a return to baseline concentration values. The third interval corresponded to the background PM₁₀ concentration after the end of the peak and included the 10 – 30 second period after the peak stop time. The first and third intervals were aggregated to estimate the baseline average PM₁₀ concentrations (C_0 in Equation 1) for each DustTrak and the noise level (standard deviation) exhibited by the background signal. For cases where a peak was not clearly discernible, the peak duration was assumed to span 20 seconds that were centered on the recorded vehicle passage time.

Horizontal fluxes calculated using Equation 1 yielded an emission factor in units of gram PM₁₀ per kilometer traveled for every time a test vehicle passed through the test course and wind conditions and background PM₁₀ levels were considered acceptable for providing a valid measurement.

5.2 EPA Method AP-42

5.2.1 Organizing Bag Data

Soil sample bag data, consisting of a bag number, its assigned UNLV site number, date and time, tared mass, and final mass were entered into a the MS Access® database. This database was used to organize and print out bag identification data in tables were transmitted with the soil samples to Ninyo and Moore’s geotechnical laboratory for soil sieve analysis.

5.2.2 Organizing AP-42 Emission Factor Data

Returned silt masses from AP-42 sieving conducted by Ninyo and Moore were manually entered into the Access® bag database.

The Access® database table was then exported to an Excel® database to facilitate calculation of AP-42 Emission Factors. The silt recovery time that most closely matched the time of a particular vehicle pass identification number, taken from the DRI Excel® vehicle Pass_ID and time database, was used to match silt recovery to a mobile technologies event. An entry was made in the AP-42 Excel® database to indicate if the silt recovery had taken place before or after the vehicle Pass_ID. Where available, separate silt mass values were entered for each corresponding Pass_ID for both the south and north zones. Silt mass data were then converted into silt loadings by dividing by the corresponding plot area in square meters. Uncertainties in individual silt loadings were

computed using root-mean square (RMS) error analysis of the uncertainty in the silt mass and the uncertainty in the plot area.

AP-42 emission factors were then calculated for the silt loadings using the AP-42 emission factor equation.

$$EF = k * (SL/2)^{0.65} (W/3)^{1.5} - C, \quad \text{Equation 5.2}$$

where:

EF is the computed AP-42 PM₁₀ emission factor in gram/VMT or gram/VKT,

k is the coefficient for PM₁₀, with values of
7.3 gram^{0.35}-m^{1.30}/(VMT-ton^{1.5}) or
4.6 gram^{0.35}-m^{1.30}/(VKT-ton^{1.5}),

SL is silt loading in gram/m² calculated from field measurements,

W is a fleet average vehicle weight in U.S. short tons, and

C is the brake and tire wear correction factor, with values of:

0.2119 gram/VMT, or
0.1317 gram/VKT.

A weight of 2.88 tons, based on the arithmetic average of the reported weights of the three mobile source vehicles (SCAMPER 2.5 tons, TRAKER I 3.4 tons, and TRAKER II 2.75 tons) was used to calculate the AP-42 emission factors from the silt loadings.

Uncertainties in the individual emission factors were computed using root-mean square error analysis of the uncertainty in silt loading. Fleet vehicle weight was assumed to be known exactly, with an uncertainty of zero.

In cases where multiple silt loading measurements, in the north or south, were available for a particular Pass_ID, the average north or south silt loading measured for that pass was used to compute the AP-42 emission factor. Standard deviations of the north and south silt loadings were calculated, and for each zone, the larger value of the individual RMS silt uncertainty or the plot-to-plot silt standard deviation was used in a root mean square computation of the AP-42 emission factor uncertainty.

Averages and standard deviations of the silt loading and AP-42 Emission factors for each Pass_ID were computed from the combined north and south zone data, where available. The larger uncertainty of the RMS error calculation or the north-south standard deviation was used as the uncertainty of the AP-42 emission factor measurement.

The Excel® database containing date, time, vehicle Pass_ID, vehicle speed, silt loadings and silt loading uncertainties, and AP-42 emission factors and emission factor uncertainties was then transmitted to all cooperating agencies for data analysis.

5.2.3 Unification of Data Sets

DRI combined the following data sets using Vehicle Pass_ID as a common variable into a master Excel database that was used for joint data analysis:

- 1) UNLV AP-42 emission factor data, averaged north and south for each pass,
- 2) Tower mass emission rate data, averaged for each pass,
- 3) SCAMPER, TRAKER I and TRAKER II mobile technologies data, averaged for each pass.

5.3 Mobile Technologies

5.3.1 SCAMPER

All data with a flag of (1) were removed from the data that was submitted. The master Excel worksheet shows all the calculations and all flags. Data for the test track were selected from the GPS coordinates of the test track boundaries and the heading of the SCAMPER. The differences between the front and rear DustTraks were calculated and the results were multiplied by the frontal area of the Ford Expedition (3.66m^2), to yield the emission factor in mg/m. Averages and standard deviations of this emission rate data were calculated for each test pass and for the entire test set.

There were occasional periods when the GPS did not report data, most likely due to interferences in the sight path to a satellite. In these cases the cell was filled with the average of the position before and the position after. The same was done for speed and PM10.

We found that the output of the rear DustTrak occasionally spiked, either positive or negative, most likely due to physical shock. These spikes always showed up for two consecutive seconds. These were unlikely to be associated with an actual PM₁₀ concentration as concentrations rarely change to that degree in less than one second. This two-second characteristic of this noise spike is also expected from the internal averaging and output characteristics of the DustTrak. On the time constant we selected (which is the shortest available) the DustTrak output is a two-second running average that is updated every second. A large spike in a one-second period will therefore show up as two smaller spikes for two consecutive seconds. To filter this noise we tabulated the data as five-second running medians. Two-second anomalous spikes therefore would be removed from the data set. At the same time we calculated the running medians we also corrected for the zero response for each analyzer. The final data was submitted as five-second running means of the five-second running medians to further filter noise.

5.3.2 TRAKER I

Following validation of individual one-second TRAKER I data, several steps were taken to align and aggregate the data points for data analysis. First, the GPS time stamp was retarded 3 seconds and linked to the DustTrak data using the retarded time. This was

done to account for the discrete amount of time (3 seconds) that it takes for the air at the inlets of the TRAKER I to move through the inlet lines and plenum and the DustTrak sampling nozzle. That is, data logged by the DustTrak at time t_0 corresponds to the dust that was channeled to the inlet of the TRAKER (either behind a tire or through the bumper at time $t_0 - 3$ seconds).

Next the TRAKER signal was calculated for all valid data points using the equation:

$$T_t = (C_{R,t} + C_{L,t})/2 - C_{B,t} \quad \text{Equation 5.3}$$

Where T_t is the TRAKER signal in mg/m^3 at time t and C_R , C_L , and C_B are the concentrations (mg/m^3) respectively measured at the right, left, and middle (background) inlet. The quantity T in Equation 1 is the main entity that is provided by the TRAKER measurement system and is the “raw” TRAKER signal.

Next, only data that correspond to the test route were selected for analysis. This was accomplished by imposing limits on the latitudes and longitudes of the GPS coordinates as well as the direction of travel of the vehicle (See **Figure 5-2**). After extracting only data that correspond to measurements along the test route, each data point was associated with a Pass ID number common to all study participants. Depending on the speed of travel on the test route, between 28 and 57 points were associated with each Pass ID that was assigned to TRAKER I. An example of the raw vehicle Pass ID data is shown in Table 5-1. Pass durations are about 1.5 minutes at 35 mph intervals between successive vehicle passes within a given Run ID.

Table 5-1. Example of Vehicle Pass_ID data. Pass durations are about 1.5 minutes at 35 mph intervals between successive vehicle passes within a given Run ID

Date	Set_ID	Test_type	Run_ID	Pass_ID	Vehicle	Speed (mph)	Drive Direction	Time (Local)	Exact time?
9/11/2006	1	Pre-sweep	1	1	UC	35	N	11:56:20	Y
9/11/2006	1	Pre-sweep	1	2	TR1	35	N	11:57:32	Y
9/11/2006	1	Pre-sweep	1	3	TR2	35	N	12:02:49	Y
9/11/2006	1	Pre-sweep	1	4	UC	35	S	12:04:25	Y
9/11/2006	1	Pre-sweep	1	5	TR1	35	S	12:05:53	Y
9/11/2006	1	Pre-sweep	1	6	TR2	35	S	12:07:09	Y
9/11/2006	1	Pre-sweep	2	7	UC	35	N	12:08:49	Y
9/11/2006	1	Pre-sweep	2	8	TR1	35	N	12:10:18	Y
9/11/2006	1	Pre-sweep	2	9	TR2	35	N	12:11:42	Y
9/11/2006	1	Pre-sweep	2	10	UC	35	S	12:13:23	Y
9/11/2006	1	Pre-sweep	2	11	TR1	35	S	12:15:04	Y
9/11/2006	1	Pre-sweep	2	12	TR2	35	S	12:16:26	Y
9/11/2006	1	Pre-sweep	3	13	UC	35	N	12:18:00	Y
9/11/2006	1	Pre-sweep	3	14	TR1	35	N	12:19:27	Y
9/11/2006	1	Pre-sweep	3	15	TR2	35	N	12:20:25	Y

There are 476 total passes in the database that covers the five days of Phase IV experiments. Data in Table 5-1 are shown only for the first 15 passes of Set 1.

Experimental Set_ID numbers describe different experiments that took place during the Phase IV experiments. Each Set number describes a different experimental condition. Usually, each Set ID number describes a unique combination of applied silt loading and mobile technology vehicle speed.

A summary of the Pass_ID numbers that correspond to each Set_ID in the Phase IV study is shown in Table 5-2.

Table 5-2. Summary of Set_ID's and corresponding Pass_ID's for the Phase IV study

Date	Set #	Experiment Name	Start Pass_ID	End Pass_ID	Nominal Drive Speed (mph)	Applied Soil Loading (gram/m ²)	Avg. Recovered Silt Loading, (gram/m ²)
9/11/06	1	Pre-Sweep	1	60	35	N/A	0.17
9/11/06	2	Post-Sweep	63	92	35	N/A	N/A
9/11/06	3	Apply silt #1	93	139	35	6.16	0.75
9/12/06	4	Apply silt #2	140	169	45	17.17	2.48
9/12/06	5	Apply silt #3	170	211	25	16.58	3.17
9/13/06	6	Apply silt #4	212	241	45	4.99	0.88
9/13/06	7	Apply silt #5	243	272	25	4.70	0.74
9/13/06	8	Apply silt #6	273	308	45	7.63	1.14
9/14/06	9	Apply silt #7 - Depletion, one vehicle	309	318	35	7.78	0.80
9/14/06	10	Apply silt #7- all vehicles	319	331	35	7.78	0.80
9/14/06	11	Post-sweep	334	364	35	N/A	
9/14/06	12	Apply silt #8 - strong winds	365	391	Repeat 25,35,45, 45,35,25 cycle twice	17.61	2.55
9/15/06	13	Apply silt #9 - strong winds	392	476	Repeat 25,35,45, 45,35,25 cycle 4 1/2 times	28.47	2.31

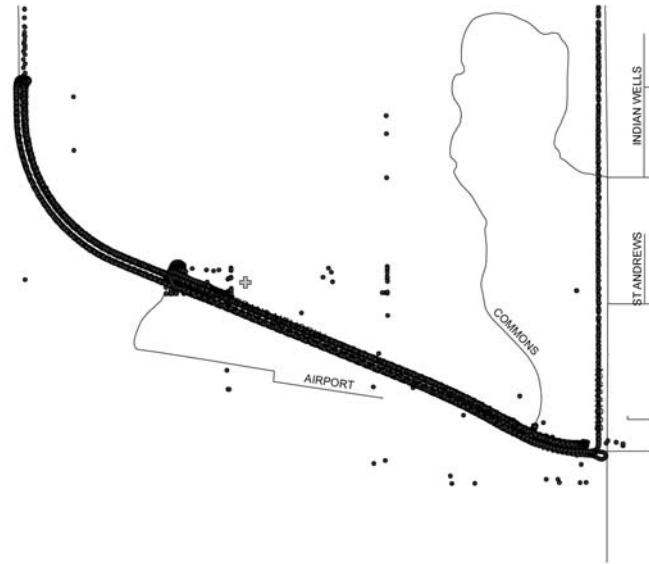
To facilitate comparison among the different measurement systems (TRAKER II, SCAMPER, Tower measurements, and silt measurements), all real-time data were aggregated by vehicle pass. For the remainder of data analysis, pass-averaged TRAKER signals are used. That is, the TRAKER signal (Equation 5.3) was averaged over all real-time data points acquired during a specific Pass ID, and the resulting average value was used to represent the TRAKER I signal for that Pass ID. The effects of this assumption/simplification were examined by comparing pass-averaged TRAKER I signals to the averages of data points that correspond only to measurements taken within 50 m of the master tower (See **Figure 5-2b**). **Figure 5-3** shows that there is a good correlation ($R^2 = 0.82$) between the pass-averaged TRAKER I signal and the TRAKER I signal averaged only over data points that correspond to measurements within 50 m of the master tower. Nevertheless, the relationship does exhibit substantial noise (note: in log scale) indicating that a number of factors can change over the length of the test route including the road dust loading and the portion of the lane where the driver is driving the vehicle.

Figure 5-4 shows a time series of pass-averaged TRAKER I signal over the whole length of the test road section (between the longitudes: -114.854849 and -114.847239) as well as averages in the vicinity of the DRI flux towers (between longitudes of -114.853817 and -114.852524, See also **Figure 5-2**). The “Tower-averaged” TRAKER signals tend to exhibit more pass-to-pass variability than the “pass-averaged” signals. This is to be expected since the former are averages over a smaller number of individual one-second measurements (5-12) compared to the latter which include many more data points (25 - 60). Larger numbers of data points in the average mitigate variations in driving technique and road dust distribution on the test road surface. In some cases, (e.g. Set 3 and Set 12), the “pass-averaged” TRAKER I signal is consistently higher than the tower-averaged signal, indicating that silt was probably not applied uniformly over the length of the test road. In addition, prior to application of silt (i.e Sets 1 and 2), there are substantial differences between the TRAKER I signal over the entire test road length and the TRAKER I signal in the vicinity of the towers. This is true for both eastbound and westbound travel. This suggests that the “natural” condition of Veterans Memorial Highway around the area of the measurements consists of a high degree of spatial variability with respect to road dust emissions. However, overall, agreement between TRAKER I signals averaged over the two different lengths of road is quite good (See **Figure 5-3**).

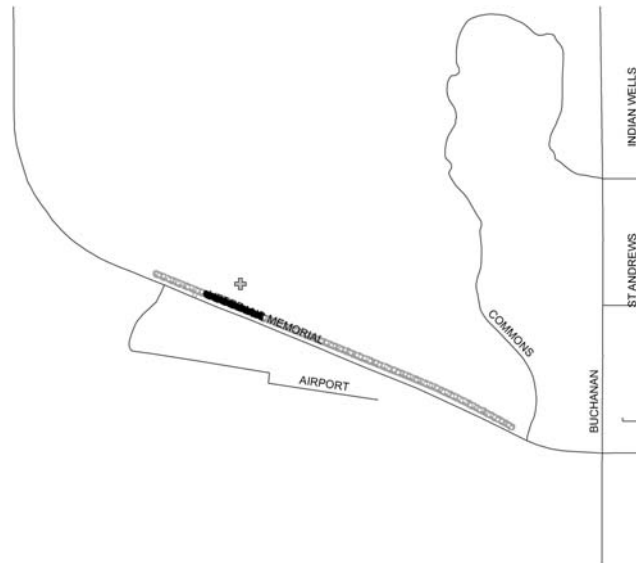
In applying Equation 5.3 to obtain the TRAKER I signal, two observations are worth noting. First, the value of C_R and C_L were substantially higher than C_B for all TRAKER I passes (**Figure 5-5**). This indicates that the “influence” measurements behind the two front tires were able to resolve a signal substantially above background (minimum of a factor of 10) for even the cleanest road conditions encountered over the duration of the study.

Second, the signals (concentrations) measured behind the right and left tires were not equal over the course of the study. While the ratio of the right to left signal fluttered about unity for many of the test passes, for some measurement sets (11 and 13), the right signal was considerably higher than the left signal and for other measurements sets (1 and 2) the opposite was true. **Figure 5-6** shows a time series of the ratio of the TRAKER I right inlet signal to the left inlet signal. The vertical lines in the Figure indicate the beginning of a new measurement set and the gray squares indicate passes along the same test route in the eastbound (instead of the primarily used westbound) direction. Note that eastbound passes were conducted in the lane adjacent to the one where westbound passes were completed. The figure shows that the ratio of right to left inlet signals can vary substantially. This variation does not appear to be caused by moderate cross-wind (< 6 m/s or < 13 mph), but rather by variations in the distribution of road dust material on the road as well as variations in where the vehicle tires are with respect to the lane (i.e. where the driver guides the vehicle with respect to previous passes and drivers of other test vehicles). Having noted these asymmetries, the actual PM_{10} emissions are a combination of the signals from both sides of the vehicle. Thus, using the average of the left and right signals as is done in Equation 1 is appropriate for estimating road dust emissions.

Figure 5-2. Schematic of GPS data points on top of street layout. a. All TRAKER I GPS data and b. only data that correspond to the test route or data collected within 50 m of the master tower (black dots). The gray cross shows the approximate location of the master tower.



a. all TRAKER data points



b. Data filtered for validity and location on test route and/or within 50 m of master tower.

Figure 5-3. Relationship between TRAKER I signal averaged over entire pass (route length) and TRAKER I signal only within 50 m of master tower.

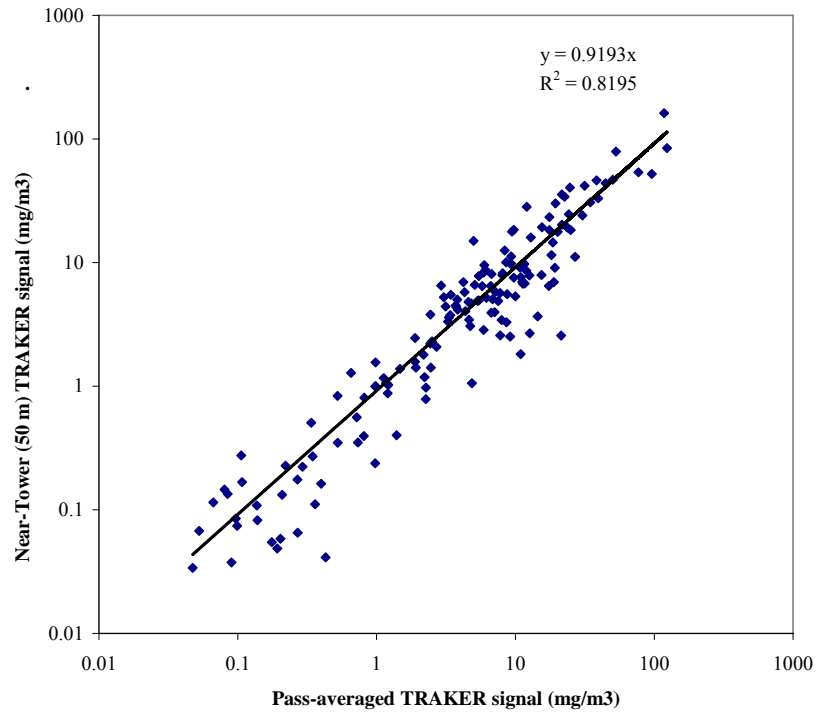


Figure 5-4. TRAKER signal (left and right) averaged over entire pass (pass-ave) and averaged over only the portion of test road in the vicinity of flux towers (Tower-ave).

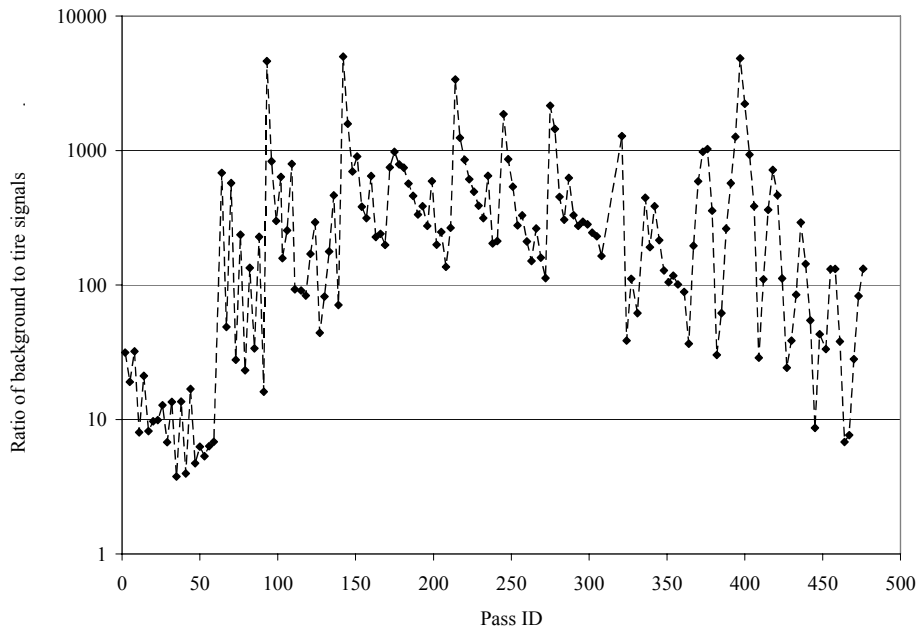


Figure 5-5. Ratio of background (middle) inlet PM₁₀ concentration to average of left and right tire inlet PM₁₀ signals for TRAKER I passes.

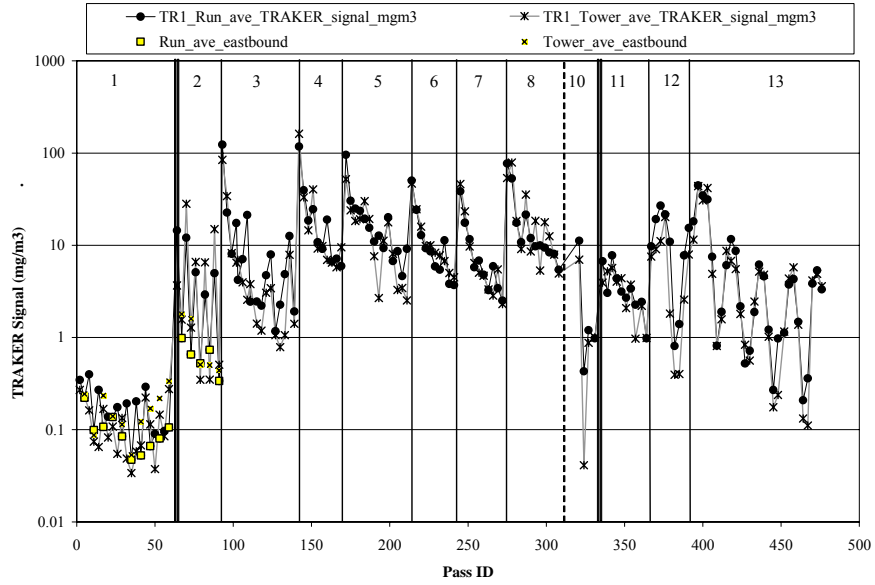
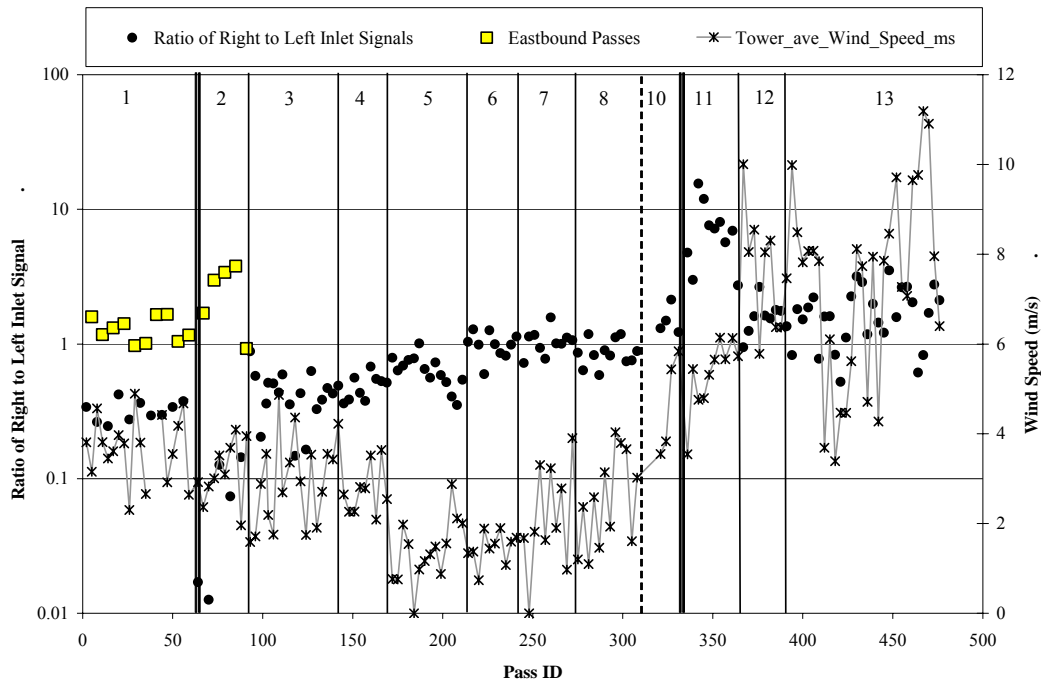


Figure 5-6. Time series of ratio of pass-averaged TRAKER I right to left inlet signal ratios and pass-averaged wind speed (m/s). Squares denote passes where travel was in the eastbound direction. Vertical lines represent times when the road was swept and silt was applied, while double vertical lines represent times when the road was swept only. Numbers at the top correspond to different measurement sets.



Sets 4, 5, 6, 7, and 8 were analyzed further to examine the rates of decay as measured by TRAKER I. Sets 1, 2, and 3 were not associated with uniform road silt coverages. Sets 9 – 13 were associated with rather variable loadings, owing perhaps to the redistribution of road material by high winds. For each of Sets 4- 8, the first TRAKER measurement was taken to be the baseline reading and a measure of the amount of measurable road dust at the beginning of the set – i.e. immediately after silt material was laid on the road. Thus, all measurements within the same set were divided by this value to normalize the rate of decay across the different sets. **Figure 5-7** shows the normalized decay curves for Sets 4 – 8. The solid black circles and triangles in the figure represent the average normalized decay for sets completed at a 25 mph measurement speed (Sets 5 and 7) and Sets completed at a 45 mph measurement speed (Sets 4, 6, and 8), respectively. In examining the average decay curves for the 25 mph Sets (**Figure 5-8**) and the 45 mph sets (**Figure 5-9**) separately, it appears that in both cases, the decay rate can be described by two separate decay processes.

We hypothesize a conceptual mechanism for the reduction in TRAKER-measured road dust emissions over the course of a measurement set. The roadway surface is not

completely smooth and there are pits and protrusions on even the smoothest asphalt surfaces. When road silt material is placed onto the road by the spreader, a portion of the material nestles into the pits and a portion settles on protrusions in the asphalt. The suspendable material that is associated with the protrusions is more exposed than the material that is nestled in the pits. We hypothesize that aerodynamic forces generated by the passage of the vehicles are able to influence the road dust associated with the protrusions and entrain a portion of that road dust. In contrast, road dust material that is nestled in the pits is protected somewhat from aerodynamic stress generated by the movement of the test vehicles through the air above the surface. Road dust material in the pitted portions can only be entrained through contact with (or more generally influence from) the tire surface. With this conceptual model, we can propose a mathematical reconstruction of the removal of road dust from the driving surfaces.

First, we assume that road dust placed on the road surface is either associated with protrusions in the road and is referred to in our model as “aerodynamically suspendable” road dust (RDA) or nested into the pits of the asphalt surface and referred to as “mechanically suspendable” road dust (RDM). These two categories sum to the total suspendable road dust (RDT):

$$RDT = RDA + RDM . \quad \text{Equation 5.4}$$

$$RDT_0 = RDA_0 + RDM_0 = 1 \quad \text{Equation 5.5}$$

Equation 5-5 above reflects that at time 0, before any vehicles traverse the tests course, the normalized sum of RDA and RDM is unity. Second, assume that the decay curves for RDA and RDM are first-order. In words, this means that each time a test vehicle passes over the road surface, some percentage of the RDA and some percentage of the RDM are suspended. Mathematically, this is written as

$$RDA(X) = RDA_0 \cdot EXP(-a_{aero} \cdot X) \quad \text{Equation 5.6}$$

$$RDM(X) = RDM_0 \cdot EXP(-a_{mech} \cdot X) \quad \text{Equation 5.7}$$

where X is the number of test vehicle passes after road silt material has been applied, a_{aero} is the coefficient of decay for aerodynamically suspendable road dust, and a_{mech} is the coefficient of decay for mechanically suspendable road dust. These two decay coefficients can be thought of as the fraction of suspendable road dust (either aerodynamically or mechanically) that is removed (suspended) each time a vehicle passes over the road surface.

The data shown in **Figure 5-8** and **Figure 5-9** fit this hypothesized conceptual model quite well. The implications of this model may be quite important for road dust management practices. In the context of the present study, these data indicate that dust emissions occur under a different regime during the first 9 vehicle passes than in ensuing passes. Since for a paved road, the volume of vehicles is generally much higher than 9, the first 9 passes after silt material application probably do not reflect the regime under which real-world dust emissions occur. It is more likely that the latter passes (greater than 9) more accurately reflect the slower, steadier emissions of PM₁₀ road dust that occurs on paved roads. Note that this observation does not depend on whether or not our earlier hypothesis regarding the separation of “aerodynamically suspendable” road dust

(RDA) and “mechanically suspendable” road dust (MDA) is deemed physically plausible. It is clear from Figures 5-7, 5-8 and 5-9 that the rate of road dust emissions changes after the first 9 (or so) vehicle passes. This phenomenon is seen not just through the TRAKER I measurements, but from the results of all of the measurement techniques, namely AP-42 silt, SCAMPER, TRAKER II, and tower horizontal PM₁₀ flux measurements (Illustrated in Chapter 6 of this report).

Figure 5-7. TRAKER I signal normalized to first TRAKER I pass of the measurement set for sets 4, 5, 6, 7 and 8. The black circles and triangle represent averages for speeds of 25 mph (circles) and 45 mph (triangles)

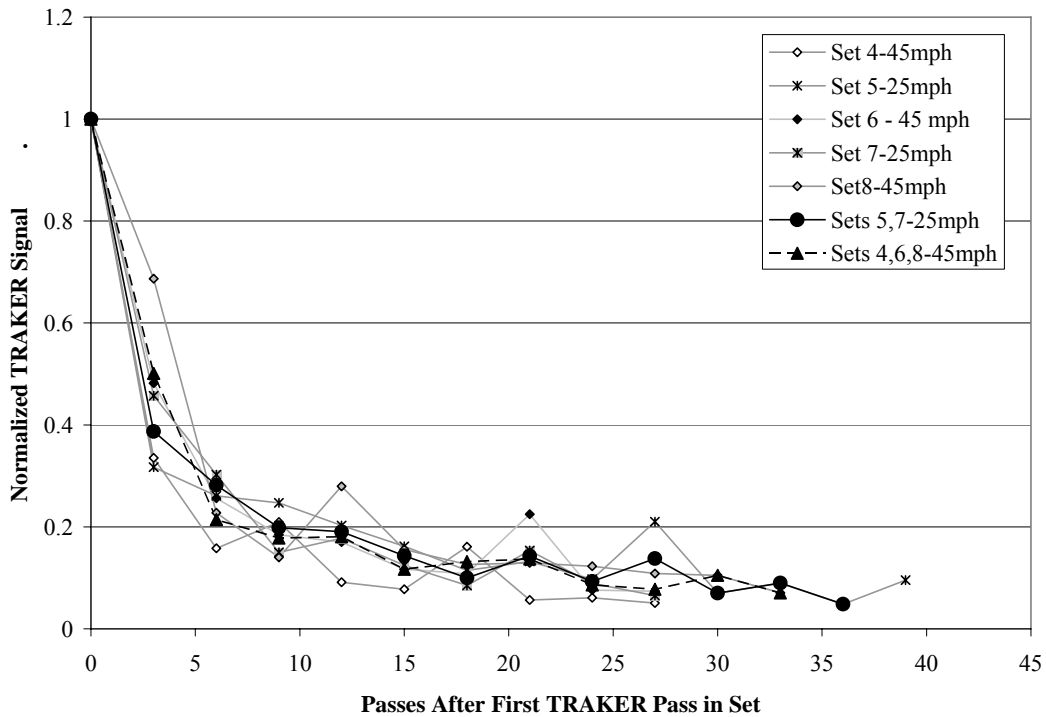


Figure 5-8. Normalized TRAKER I decay curve for Sets 5 and 7 (25 mph measurement) and hypothesized aerodynamically suspendable, mechanically suspendable, and total suspendable (aerodynamic plus mechanical) road dust decay curves.

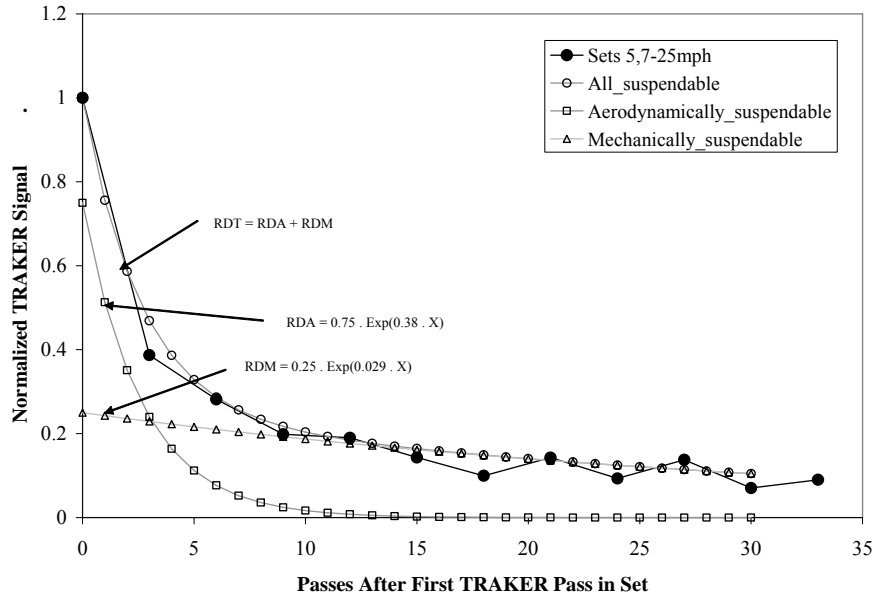
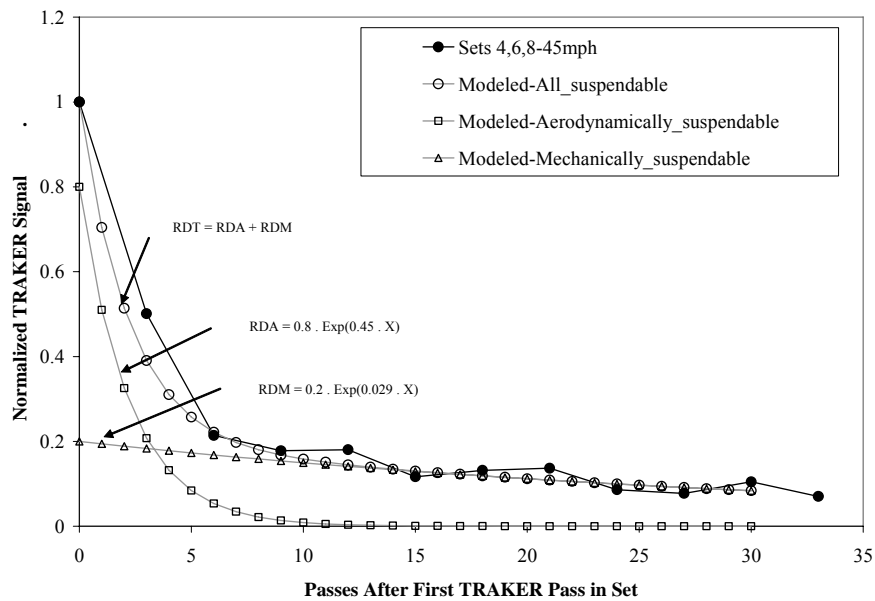


Figure 5-9. Normalized TRAKER I decay curve for Sets 4, 6, and 8 (45 mph measurement) and hypothesized aerodynamically suspendable, mechanically suspendable, and total suspendable (aerodynamic plus mechanical) road dust decay curves.



In prior work, it was observed that the TRAKER I signal was dependent on the speed of travel on the road that was being measured. Those speed response relationships summarized in prior work were obtained by traversing the same section of road several times at varying travel speeds (15 – 60 mph). The underlying assumption behind those tests was that the test road was essentially unaffected by the passage of the TRAKER I and provided a constant “loading” of road dust, allowing us to isolate the effect of traversal speed on the TRAKER I signal (i.e. road “dirtiness” was constant throughout speed tests). In several of the prior studies, it was found that the TRAKER I signal for a given, time-invariant test road, was approximately proportional to the speed of traversal raised to the third power (cubed).

It is instructive to extract a similar speed response relationship from the present study for comparison. However, there are some complicating factors. First, the only full set of speed tests were completed on the last day of the field study during Set 13. Second, owing to the high winds on that day, the ratio of right to left inlet signals was quite variable (See **Figure 5-6**). Third, owing to the nature of the field study, the road dust loadings were constantly changing over the course of the Set 13 measurements. In order to extract speed response information comparable to the speed tests reported in earlier work, it was necessary to account for these three non-idealities. Set 13 TRAKER I passes were separated into 4 complete cycles, with each cycle consisting of 2-25 mph, 2-35 mph, and 2 – 45 mph passes (See **Figure 5-10**). Using only the TRAKER I signal from the right side of the vehicle (the side sheltered from direct southerly crosswinds which were prevalent during Set 13), the TRAKER I signal from the two 25 mph measurements within each cycle were averaged and assumed to reflect the average condition of the roadway over the cycle. The two 35 mph measurements within each cycle were averaged together as were the two 45 mph measurements. To account for cycle-to-cycle changes in road conditions, these averages were normalized to the 25 mph average for each cycle. The results of this normalization for each of the four cycles appear in **Figure 5-11** as do the normalized data averaged over all four cycles. A least-squares power-fit to the 4-cycle average suggests that the TRAKER I signal for Set 13 data approximately obeys a cubic (regression exponent = 3.1) relationship with speed, though we note that there are some differences from cycle to cycle.

Figure 5-10. Division of Set 13 into 4 cycles, with each cycle comprised of 6 passes for TRAKER I.

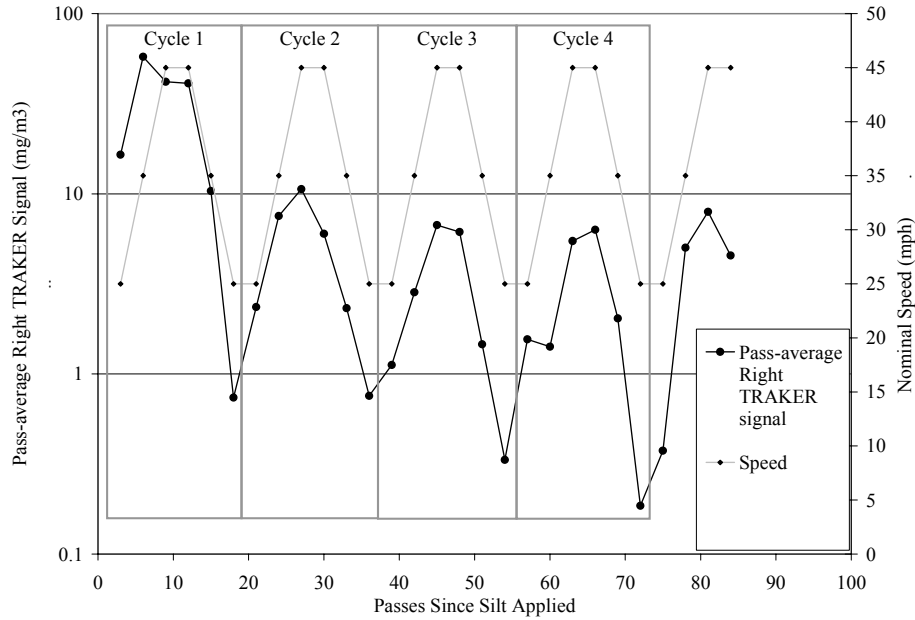
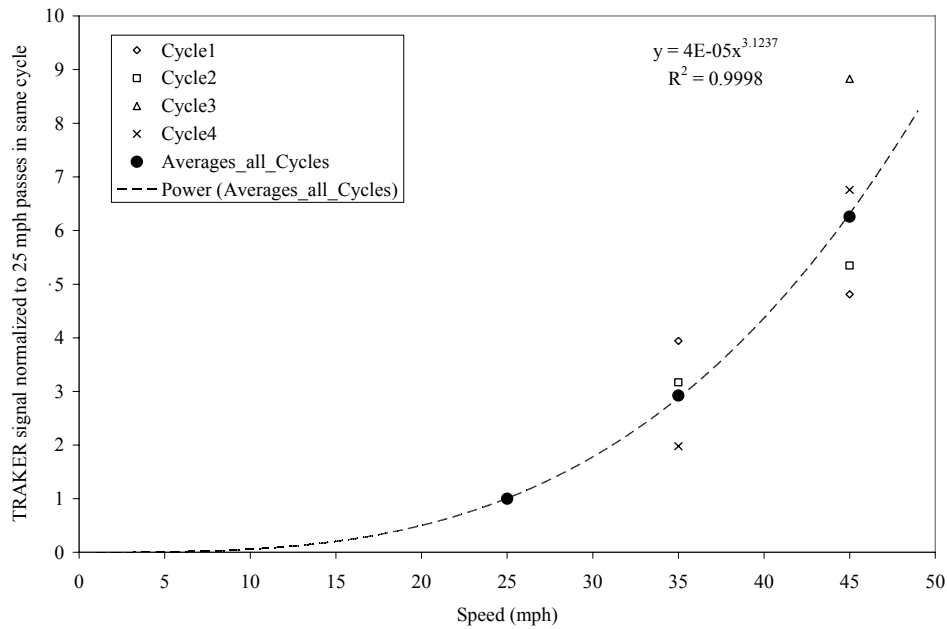


Figure 5-11. Speed response of TRAKER I signal. Figure shows the TRAKER I signal at each speed normalized to the average signal at 25 mph in the same cycle. Data are shown for 4 consecutive cycles as well as the average value for all cycles.



5.3.3 TRAKER II

Data alignment and aggregation for TRAKER II were conducted almost identically as for TRAKER I. Starting with all valid 1-second data, the GPS time was retarded by 3 seconds and then re-associated with DustTrak data. The TRAKER II 1-second signal was calculated with equation 1 for each valid data point. Only data associated with measurements on the test route were considered for further analysis and each of those data points was linked with a Pass ID. Pass-average values were calculated from the 1-second data points for further data analysis.

As with TRAKER I, some differences were evident between the TRAKER II signal averaged over an entire pass and the signal averaged only over data points corresponding to measurements within 50 m of the master tower (**Figure 5-12**). Also, the concentrations measured in the left and right tire inlets were always substantially higher than those measured in the background (**Figure 5-13**).

Examination of the ratio of the right to left inlet signals indicated that overall, the signal from the left side was higher than the signal from the right side (**Figure 5-14**). Unlike the near-unity values for Sets 4 – 8 exhibited by the TRAKER I data (**Figure 5-6**), TRAKER II data suggest that for almost all passes, the signal from the left side was higher than from the right (less than unity ratio). Moreover, the ratio is much more variable for TRAKER II. There are several possible reasons for this. First, the cargo bay in TRAKER II was heavily loaded on the left side with tools and equipment with an approximate mass of 300 kg. This may have resulted with a higher signal on the left. Second, the inlets for TRAKER II are further behind the tire than TRAKER I, resulting perhaps in a generally noisier signal. Third, the signal values from TRAKER II were consistently lower than TRAKER I, also perhaps contributing to greater noise in the ratio for right to left inlet signals. Fourth, TRAKER II was operated by a different driver than TRAKER I and it is possible that small differences in the paths that the vehicle tires followed could have caused higher signals on the left side of TRAKER II compared to the right side. The difference between the left and right signals in TRAKER II deserves further attention in future work. However, for the present study, we note again that the road dust emissions from the TRAKER II will be a combination of the emissions from the left and right sides of the vehicle and that it is appropriate to apply Equation 1 to obtain a representative TRAKER II signal for the whole vehicle.

Finally, **Figure 5-15** shows the speed response of the TRAKER II signal (same as **Figure 5-11** for TRAKER I). The relationship between speed and TRAKER II signal is close to the cubic relationship (exponent of speed term is 3.3 according to regression) exhibited by TRAKER I.

Figure 5-12. Relationship between TRAKER II signal averaged over entire pass (route length) and TRAKER II signal only within 50 m of master tower.

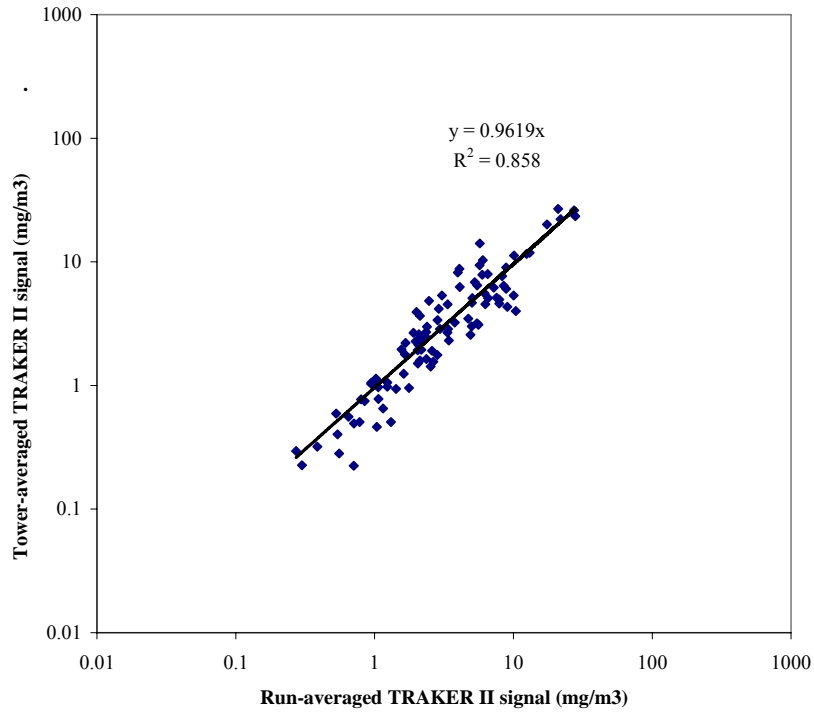


Figure 5-13. TRAKER II Ratio of average of left and right tire inlet PM₁₀ concentrations to background (middle) inlet PM₁₀ concentration.

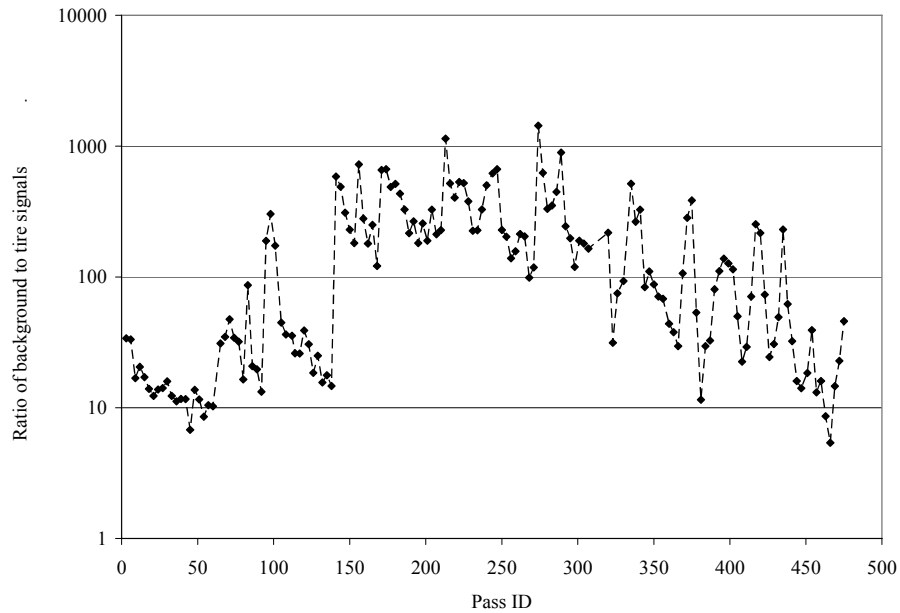


Figure 5-14. TRAKER II time series of ratio of pass-averaged right to left inlet signal ratios and pass-averaged wind speed (m/s). Vertical lines represent times when the road was swept and silt was applied, while double vertical lines represent times when the road was swept only. Numbers at the top correspond to different measurement sets.

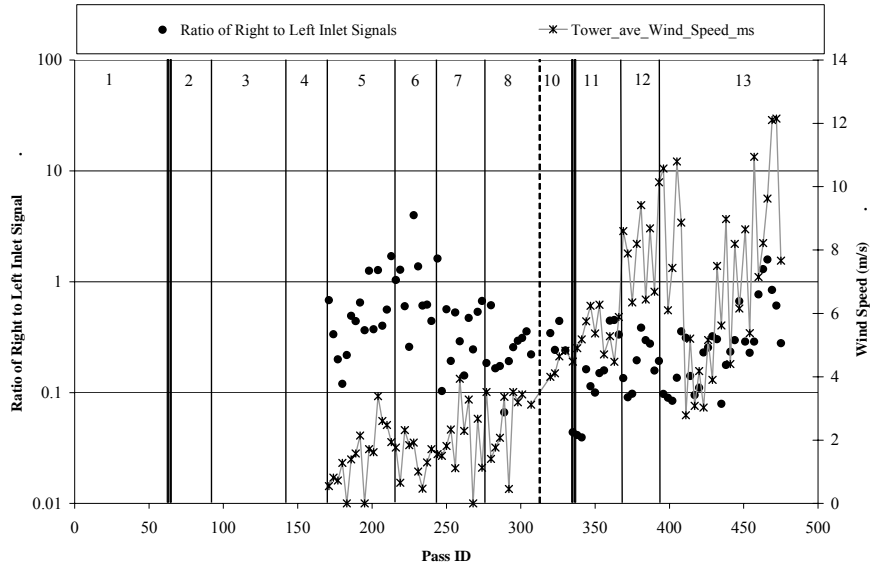
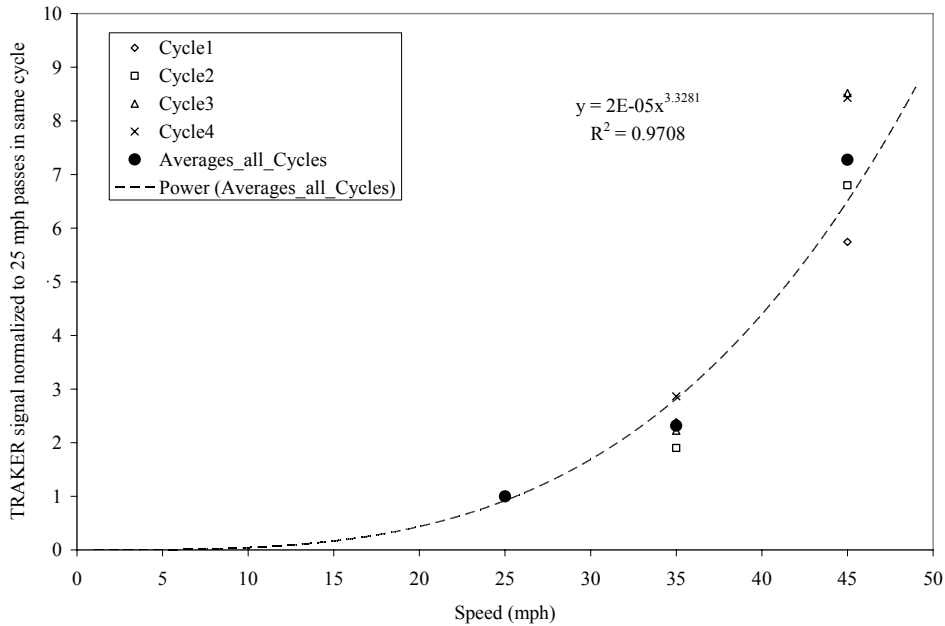


Figure 5-15. Speed response of TRAKER II signal. Figure shows the TRAKER II signal at each speed normalized to the average signal at 25 mph in the same cycle. Data are shown for 4 consecutive cycles as well as the average value for all cycles.



6.0 RESULTS

The test types, times, vehicles involved, and number of vehicle passes are summarized in **Table 6-1**. The total number of traversals through the test course for each test vehicle were: TRAKER I – 154, TRAKER II – 152, SCAMPER – 162. The distribution of nominal speeds at which measurements were conducted was approximately: 25 mph – 24%, 35 mph – 47%, and 45 mph – 29%. Except for the first two sets of measurements, where test vehicles traversed the test course in both directions, vehicles traversed the course from the eastern end of Veterans Memorial Highway by the Command Center (CC) towards the west/northwest.

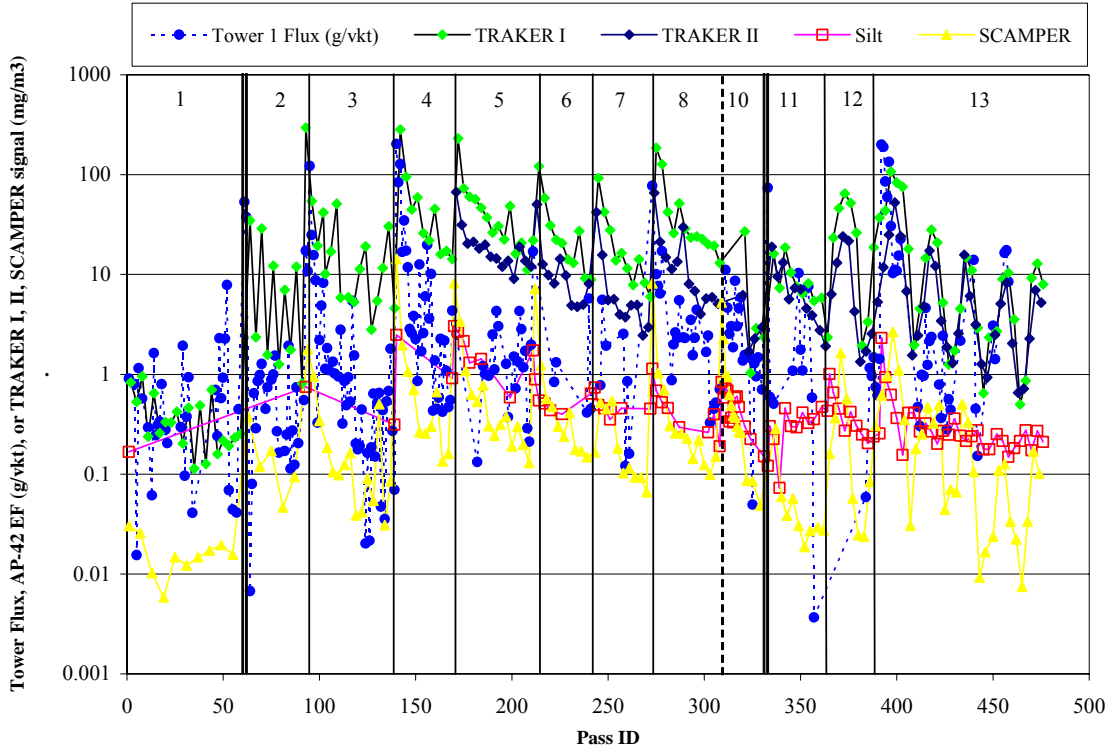
Results from AP-42 silt measurements and the three mobile systems used in this study (TRAKER I, TRAKER II, and SCAMPER) are discussed in individual sections below. In addition to providing data summaries, those sections assimilate the different methods for road dust emission estimation with horizontal PM₁₀ tower flux data. In the case of AP-42 silt sampling, this provides a basis for comparing the AP-42 methodology to emission factors measured on-site. In the cases of the mobile systems, the horizontal flux measurements which represent an independent measure of PM₁₀ emission factors are used to calibrate the three systems used as part of this study.

One important finding deserves discussion here since it applies to all the mobile systems as well as the AP-42 silt sampling. It was noted when examining the time series of the tower flux, TRAKER I, TRAKER II, SCAMPER, and even the AP-42 silt measurements that the application of silt material to the test road section led to an initial surge in PM₁₀ emissions. This can be seen in **Figure 6-1** where the pass-averaged time series for all of these data sets are plotted. Starting with measurement Set 3 - the first instance when silt was applied to the test road - the first several passes in the set exhibit comparatively very high road dust emissions or mobile system raw signals. Subsequently, emissions begin to stabilize at a lower though not necessarily constant value. Measurement Sets 12 and 13 deviate somewhat from this pattern because during those sets, the travel speeds of the test vehicles were varied over the course of the Sets. We alert the reader at this time that for comparing the signals from the mobile systems to those measured on the horizontal flux towers, the first 9 vehicle passes will not be considered for sets where road silt material was applied to the surface. The justification for this was provided in an earlier section (Section 5.3.2).

Table 6-1. Summary of tests during field study (9/11/06 – 9/15/06)

Set ID	Date	Approximate Time (local)	Activity	Vehicles used	Nominal speed (mph)	Total passes/passes per vehicle
1	9/11	11:55 - 13:15	Test: Baseline road conditions - No Sweep, No silt	All test vehicles	35	60/20
	9/11	13:35	Sweep	Street Sweeper	NA	NA
2	9/11	13:52 - 14:18	Test: After Sweeping, No silt applied	All test vehicles	35	30/10
	9/11	14:30	Silt applied to test road	Tractor/spreader	NA	NA
3	9/11	15:17 - 26:30	Test: After application of silt, 35 mph	All test vehicles	35	27/9
	9/11	17:00	Sweep	Street Sweeper	NA	NA
4	9/12	9:15	Silt applied to test road	Tractor/spreader	NA	NA
	9/12	10:15 - 11:00	Test: After application of silt, 45 mph	All test vehicles	45	30/10
	9/12	11:05	Sweep	Street Sweeper	NA	NA
	9/12	13:00	Silt applied to test road	Tractor/spreader	NA	NA
5	9/12	13:35 - 14:40	Test: After application of silt, 25 mph	All test vehicles	25	42/14
	9/12	15:00	Sweep	Street Sweeper	NA	NA
	9/13	9:00	Silt applied to test road	Tractor/spreader	NA	NA
6	9/13	9:40 - 10:25	Test: After application of silt, 45 mph	All test vehicles	45	30/10
	9/13	11:09	Sweep	Street Sweeper	NA	NA
	9/13	12:15	Silt applied to test road	Tractor/spreader	NA	NA
7	9/13	12:45 - 13:35	Test: After application of silt, 25 mph	All test vehicles	25	30/10
	9/13	14:00	Sweep	Street Sweeper	NA	NA
	9/13	14:45	Silt applied to test road	Tractor/spreader	NA	NA
8	9/13	15:20 - 16:15	Test: After application of silt, 45 mph	All test vehicles	45	36/12
	9/13	17:00	Sweep	Street Sweeper	NA	NA
	9/14	8:00	Silt applied to test road	Tractor/spreader	NA	NA
9	9/14	8:40 - 9:20	Test: Depletion of silt resulting from vehicle passes	SCAMPER Only	35	10/10
10	9/14	9:20 - 9:50	Test: Measure emissions prior to sweeping	All test vehicles	35	12/4
	9/14	10:05	Sweep	Street Sweeper	NA	NA
11	9/14	10:25 - 11:20	Test: Measure emissions after sweeping	All test vehicles	35	30/10
	9/14	11:30	Sweep	Street Sweeper	NA	NA
	9/14	12:30	Silt applied to test road	Tractor/spreader	NA	NA
12	9/14	13:10 - 14:05	Test: Speed tests	All test vehicles	25 - 45	27/9
	9/14	14:30	Sweep	Street Sweeper	NA	NA
13	9/15	8:00	Silt applied to test road	Tractor/spreader	NA	NA
	9/15	8:30 - 11:15	Test: Speed tests	All test vehicles	25 - 45	84/28
	9/15	11:30	Sweep	Street Sweeper	NA	NA

Figure 6-1. Time series of pass-averaged horizontal tower PM₁₀ flux (g/vkt), Silt-estimated AP-42 emission factor (g/vkt), TRAKER I, TRAKER II, and SCAMPER raw signals (mg/m³). Vertical lines represent times when the road was swept and silt was applied, while double vertical lines represent times when the road was swept only. Numbers at the top correspond to different measurement sets.

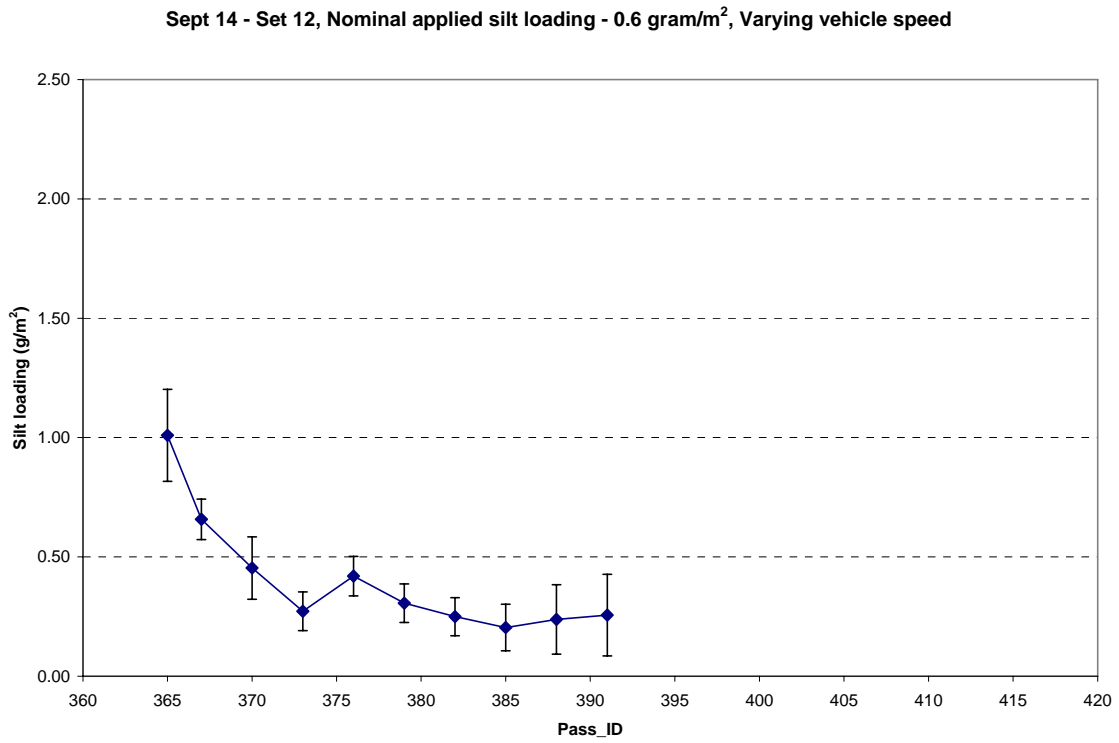


6.1 Short-Term Emission Factor Decay and Silt Loading Depletion

6.1.1 Silt Loading Depletion

Figure 6-2 shows a typical pattern of silt loading depletion for Set 12, at a low initial applied silt loading of 0.6 g/m² depleted at cyclically varying vehicle travel speeds of 25, 35, and 45 mph. Silt loading undergoes a rapid decay to about for the first nine passes, and then stabilizes at a low constant value that is about one-third of the initial value.

Figure 6-2. Silt depletion with increasing vehicle passes.



This pattern was observed in five of the nine data sets for which sufficient silt loading information is available. Results are summarized in **Table 6-2**.

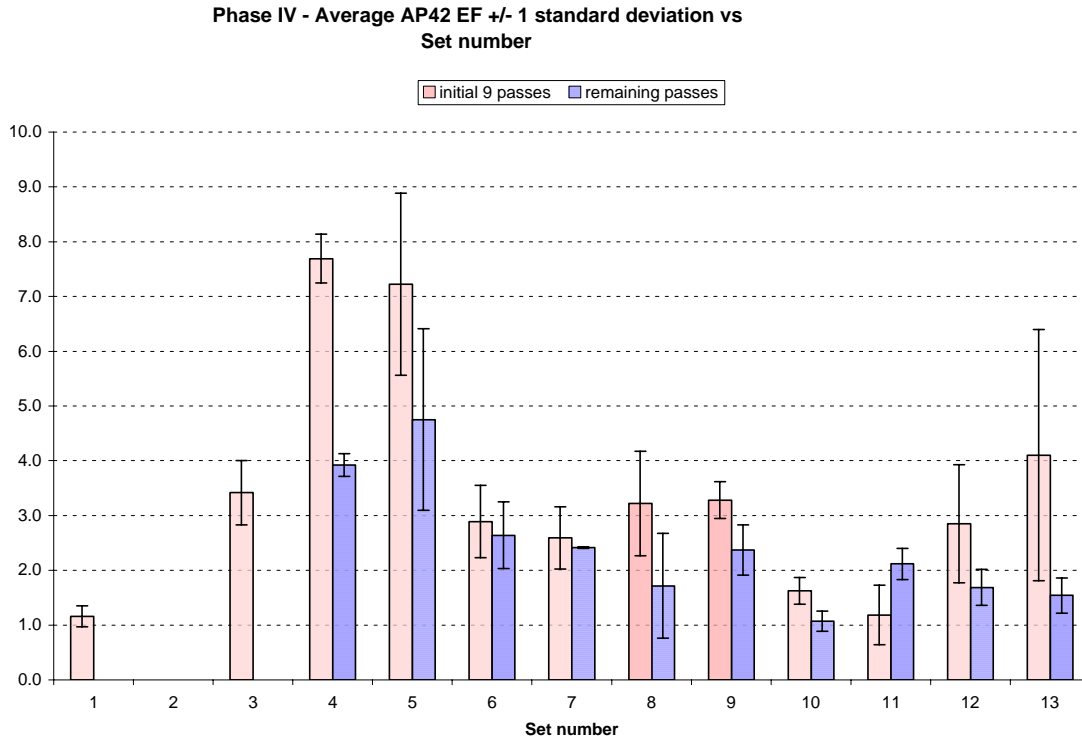
Table 6-2. Summary of observed silt decay with increasing number of vehicle passes.

Set	Initial Loading (gram/m ²)	Vehicle Speed (mph)	Decay First Nine Passes?	Ratio Last Pass Avg./ first 9 Pass Averages	Comments
4	2.5	45	N/A		decay observed, but only 2 data points
5	2.3	25	Yes	0.55	
6	0.6	45	No	0.87	
7	0.5	25	Yes	0.89	first 6 passes
8	0.7	45	Yes	0.41	
9	0.7	35	Yes	0.63	
10	0.3	35	Yes	0.57	9 passes total
11	0.2	35	No	2.11	
12	0.6	varying	Yes	0.47	Strong cross winds at end of experiment
13	1.1	varying	Yes	0.23	Strong cross winds throughout experiment

A comparison of AP-42 Emission factors computed separately for the first 9 passes and for the remaining vehicle passes (**Figure 6-3**) shows that AP-42 emission factor values for the first 9 passes, were (with the exception of Run 11) higher than values for the remaining passes.

The rapid decay in silt loading over the first few passes lends support to the DRI/UCR hypothesis that two separate mechanisms, aerodynamic (first 9 passes) and mechanical (subsequent passes) may be responsible for suspending PM₁₀ from paved road surfaces.

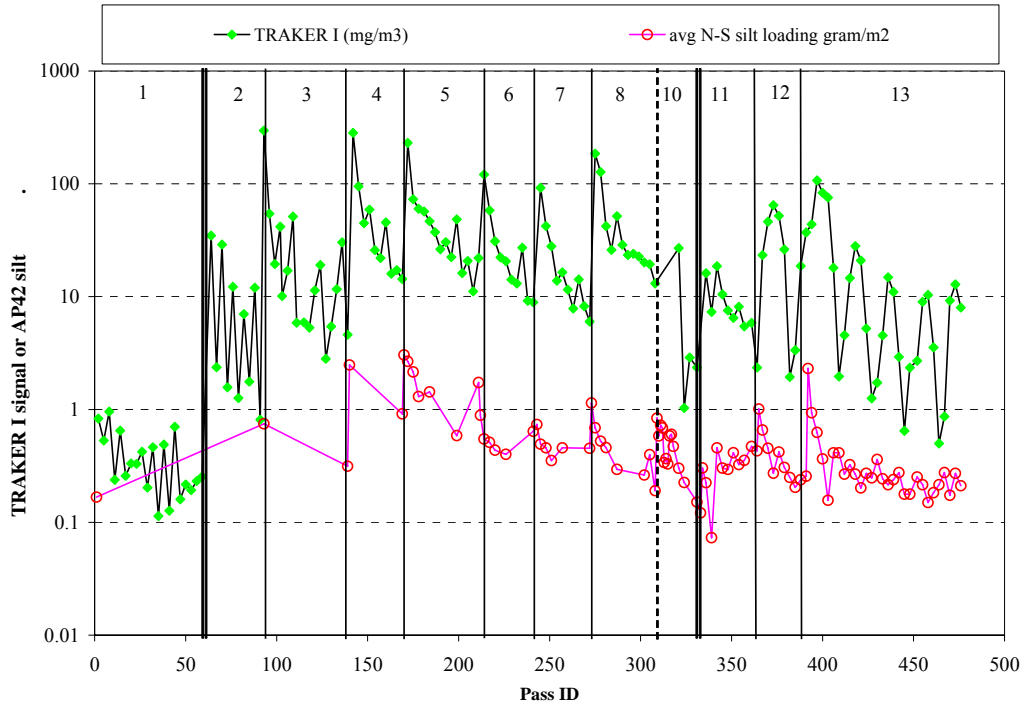
Figure 6-3. Comparison of averaged AP-42 emission factors, in gram/VMT, computed from silt loadings for first nine passes, compared to AP-42 emission factors for remaining passes.



*Error bars are +/- one standard deviation

Signals from the mobile technologies systems also showed high initial decay within several experimental sets. **Figure 6-4** compares TRAKER I signal to AP-42 silt over all observed experimental runs.

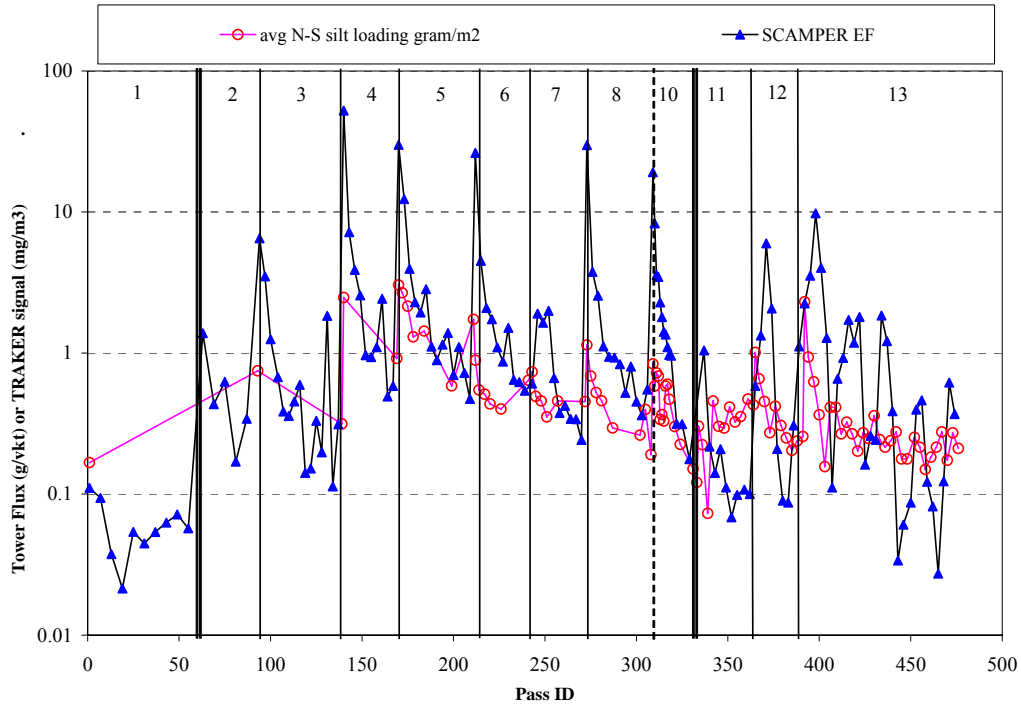
Figure 6-4. Comparison of TRAKER I signal and average north-south silt loading for all vehicle passes.



The TRAKER I signal decay with vehicle passes matches AP-42 silt loading decay in Sets 5, 8 and 10 for cases of constant vehicle speed. However, TRAKER I measured emissions also showed, in sets 12 and 13, clear vehicle travel speed dependence that is not accounted for in the current AP-42 emission factor equation. The rising and falling TRAKER I signals in Sets 12 and 13 are a result of systematically varying vehicle speeds first rising from 25 to 35 to 45 mph, then declining from 45 to 35 to 25 mph. Silt loadings in Set 12 declined throughout the experiment, even though TRAKER I emissions increased with increasing vehicle speed. Silt loadings in Set 13 declined rapidly to a steady state value, while TRAKER I emissions fluctuated regularly with rising and falling vehicle speed.

TRAKER II and SCAMPER signals showed similar behavior. The SCAMPER signal is plotted alongside silt loading in **Figure 6-5**.

Figure 6-5. Comparison of SCAMPER signal and average north-south silt loading for all vehicle passes.

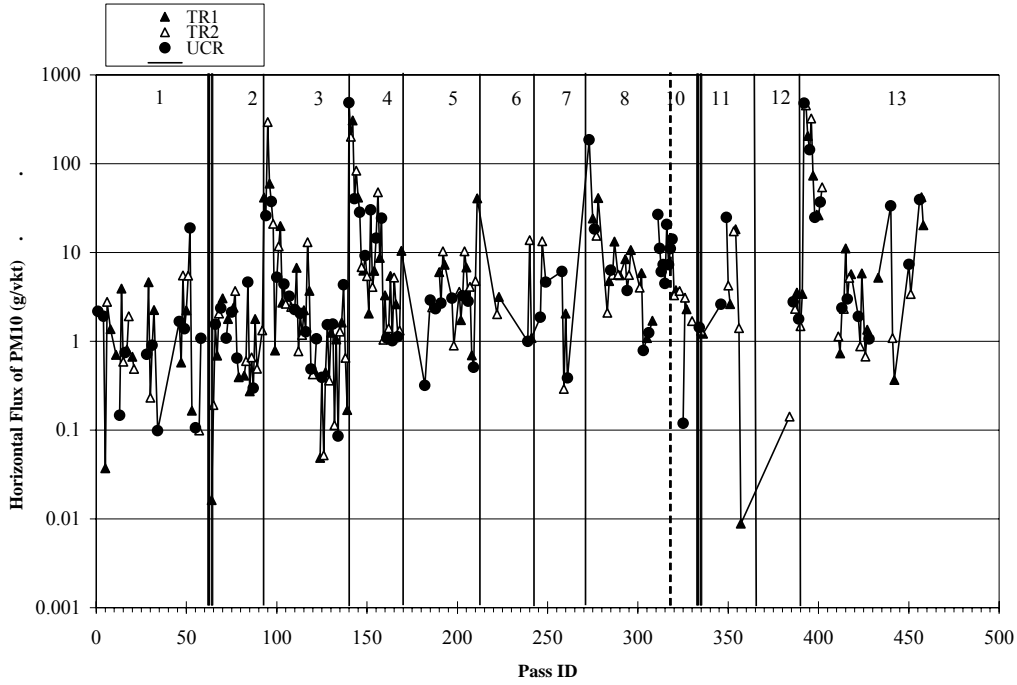


The SCAMPER signal tracks decay in AP-42 silt loading with vehicle speed in Sets 5, 8 and 10 for cases of constant speed. However, just as in the case for TRAKER I, SCAMPER measured emissions showed, in sets 12 and 13, clear vehicle travel speed dependence that is not accounted for in the current AP-42 emission factor equation.

6.2 Comparison of Horizontal Flux Tower Emission Factors to EPA Method AP-42

Plumes from point and line sources are often modeled as exhibiting smooth, Gaussian concentration distributions. This type of representation has been adequate over long spatial and time scales, where dispersive forces from random turbulent eddies are allowed to proceed for long periods and average out. In practice, individual, non-steady plumes such as from a point puff or a moving line source are quite erratic and the instantaneous spatial distribution of concentration does not at all resemble a Gaussian profile. Furthermore, owing to the random nature of plume dispersion, the flux measured at a point in space is likely to vary considerably from one event (e.g. passage of a vehicle) to the next. This can be seen in **Figure 6-6** where individual tower flux measurements associated with the passage of the test vehicles are plotted. The figure (Note log y-axis scale) shows that individual flux measurements exhibit substantial pass-to-pass variability.

Figure 6-6. Time series of horizontal PM₁₀ fluxes measured with Tower measurement system.



The inherent variability of tower flux measurements requires that data be aggregated (averaged) over several replicate measurements in order to filter out some of the measurement noise. In the case of the present study, this poses a slight challenge because the road dust loading on the test road was not constant over the course of the field study and indeed was changing over the course of a single set of measurements. This can be seen quite clearly in (See **Figure 6-2**) where, as the number of vehicle passes within a measurement set increases, the signals from the three mobile systems decrease, indicating a decay in road dust loading over time. (Please refer to **Figure 5-8** and **Figure 5-9** in Section 5.3.2) The observed decay pattern suggests that there are two modes for this decay. During the first several vehicle passes after silt is applied to the surface, road dust loading appears to diminish quickly. Earlier, we termed this “aerodynamically suspendable” road dust. After 9 or so vehicle passes, the road dust loading decreases much more slowly as the “mechanically suspendable” material is all that remains on the test road surface. As discussed earlier, for the purpose of reporting emissions from the different test vehicles used in this study, we consider only the horizontal PM₁₀ fluxes for times when the number of vehicles passing over the road after silt application was greater than 9 (Note that this does not affect Sets 1 and 2 when silt was not applied to the surface). This serves to both mitigate the large range of emissions factors that were measured (if first 9 passes are included) as well as separate the “mechanically

suspendable” road dust from the “aerodynamically suspendable” road dust – the former being more likely to prevail on well traveled roads.

The average horizontal fluxes (emissions) by measurement set, and test vehicle are reported in **Table 6-3**. With some set-to-set variation in the emissions magnitude, in general all three vehicles exhibit approximately the same emissions within the standard error of the measurement set. If averaged over all valid horizontal flux measurements, mechanically suspended PM₁₀ dust fluxes are 4.1 ± 0.7, 5.0 ± 1.2, and 5.0 ± 2.0 g/vkt for TRAKER I, TRAKER II, and UCR SCAMPER, respectively – not statistically significant differences.

Table 6-3. Summary of Measured PM₁₀ Horizontal Fluxes. Data shown are averages for all passes following the ninth pass after silt application.

Set	TRI Valid Flux Count	TRI Flux ave (g/vkt)	TRI Std err (g/vkt)	TRII Valid Flux Count	TRII Flux ave (g/vkt)	TRII Std err (g/vkt)	UCR Valid Flux Count	UCR Flux ave (g/vkt)	UCR Std err (g/vkt)	All Valid Flux Count	All Flux ave (g/vkt)	All Std err (g/vkt)
1	7	1.32	0.62	4	1.66	1.28	7	0.59	0.36	18	1.11	0.38
2	5	1.53	0.58	5	0.94	0.70	5	0.72	0.65	15	1.06	0.36
3	13	3.04	1.50	12	1.91	1.05	12	1.89	0.42	37	2.30	0.63
4	7	5.53	1.19	7	9.44	6.39	7	11.64	4.51	21	8.87	2.57
5	6	10.53	6.13	8	4.51	1.40	8	2.23	0.41	22	5.32	1.80
6	2	2.13	1.04	2	7.90	5.88	1	0.99	NA	5	4.21	2.42
7	1	2.05	NA	1	0.29	NA	2	3.24	2.86	4	2.21	1.36
8	8	6.40	1.48	5	4.57	0.69	4	3.02	1.27	17	5.07	0.82
9	NA	NA	NA	NA	NA	NA	1	11.04	NA	1	11.04	NA
10	4	1.18	1.11	4	2.94	0.43	4	3.32	3.60	12	2.48	1.18
11	5	3.70	3.78	5	4.53	3.32	4	6.46	6.24	14	4.79	2.33
12	3	0.40	3.08	3	1.31	0.63	2	2.28	0.50	8	1.21	1.07
13	9	5.47	2.25	10	11.03	6.26	9	13.88	5.77	28	10.16	2.96

“NA” indicates that either there were no valid flux measurements during the indicated period or silt was not applied to test road prior to measurements.

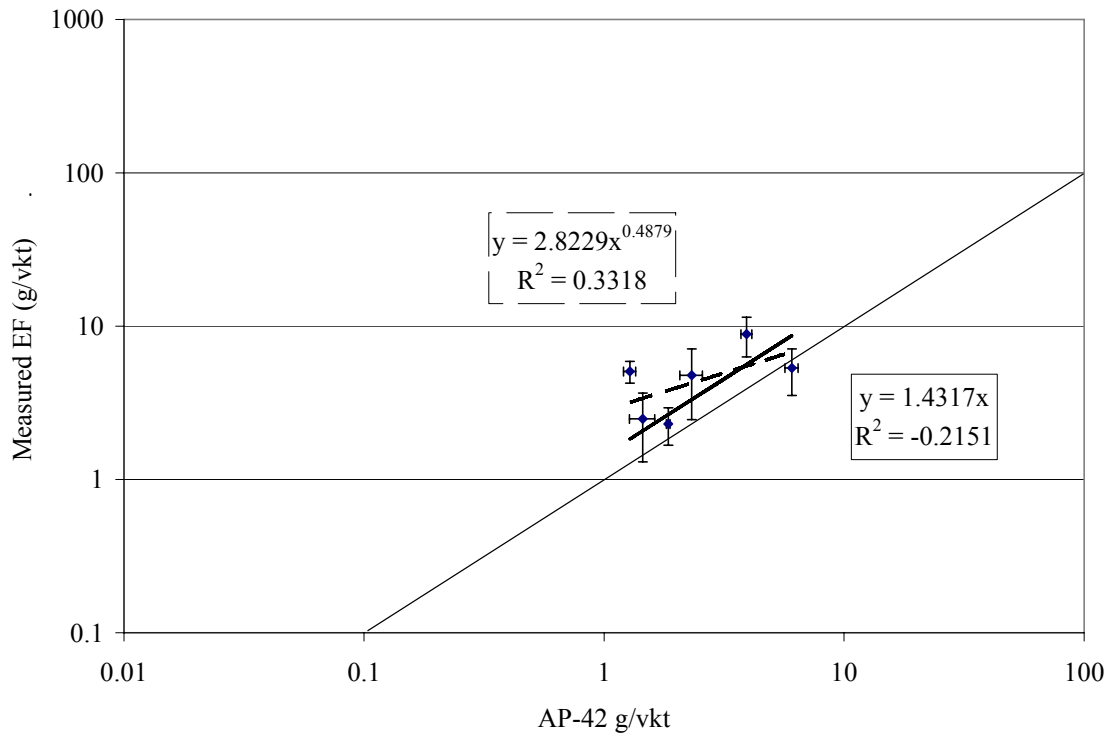
Silt measurements were conducted at various point in time over the course of measurement sets and within measurement sets (Please refer to **Table 6-1**). Full silt sampling (as opposed to “quickie strips”) was primarily conducted at the beginning and end of measurement sets. The silt sample procured at the beginning of measurement sets where silt was applied to the road contain significant fractions of “aerodynamically suspendable” road dust. This can be seen in **Figure 6-1** in Section 6.0 where it is clear that at the beginning of those measurement sets, the rate of decay of silt loading is high compared to later periods (i.e. after the first 9 vehicle passes). Silt samples procured at the end of those measurement sets represent, in principle, the lowest emission factors of the measurement set. Referring again to **Figures 5-8** and **5-9** in Section 5.3.2, the rate of decay of “mechanically suspendable” road dust is much lower than that of “aerodynamically suspendable” road dust. If for the purposes of the present effort, we accept the decay rates shown for mechanically suspendable” road dust (**Figures 5-8** and **5-9** in Section 5.3.2), namely an exponential decay of -0.029 X, where X is the number of

passes since silt application, then the difference in mechanically suspendable road dust between $X=10$ and $X=25$ is about a factor of two. Considering that PM_{10} emission fluxes from consecutive passes can vary by an order of magnitude or more (**Figure 6-6**), the error introduced by assuming that the silt sample procured at the end of the measurement set represents all passes where “mechanically suspendable” road dust was dominant (i.e. from > 9 passes after silt until set completion) is acceptably small.

To compare PM_{10} tower flux measurements with AP-42 silt methodology and mobile system measurements, data were averaged by measurement set. For each set all tower flux measurements were averaged together regardless of the test vehicle. Thus, tower flux measurements represent average fluxes for all vehicles. This was to ensure that all methods examined would be calibrated (or compared in the case of AP-42) against the same standard and results from future measurements can be compared using a common basis. In examining **Table 6-3** (three rightmost columns), it is clear that the number of valid flux measurements varied from set to set. A minimum criterion of 10 valid vehicle passes was applied to the tower flux average value. This invalidated sets 6, 7, 9, and 12. In addition, data from set 13 were considered invalid because wind speeds were very high during that period and neither the mobile systems nor the tower flux measurement system measurements are trustworthy at high winds. The remaining valid sets for comparison were 1, 2, 3, 4, 5, 8, 10, and 11. These measurement sets were used to compare AP-42 silt-based emission factors estimated from the AP-42 emission factor equation (See Section 5.2.2 for full equation) to PM_{10} emission factors measured with the horizontal flux towers. Silt measurements at the end of a set were available for Sets 3 – 13. Thus, the measurement sets that remained for comparison between the AP-42 methodology and the tower data were 3, 4, 5, 8, 10, and 11.

Comparison of AP-42 silt based emission factors and set-averaged PM_{10} emission factors are shown in **Figure 6-7**. The solid line in the Figure represents a least-squares linear fit to the data with a zero intercept while the dashed line represents a power law fit. The power law fit appears to accommodate the data better than the linear fit ($R^2 = 0.33$ compared to -0.22). In general, AP-42 estimated emission factors appear to be substantially lower than measured tower-based PM_{10} emission factors for all measurements sets by about 40%.

Figure 6-7. Tower-based PM₁₀ emission factors versus AP-42 silt based emission factors. Solid squares represent emission factors that are averages of all valid tower measurements for sets 3, 4, 5, 8, 10, and 11. AP-42 data shown are averages of the north and south sample measurements procured at the end of the measurement sets. The solid line in the Figure represents a least-squares linear fit to the data with a zero intercept while the dashed line represents a power law fit. A one-to-one line is included in the Figure for comparison.



We hypothesize in Section 7.2 that an altered distribution of freshly applied road silt on a low roughness experimental road surface increased mobile PM₁₀ emission factors compared to AP-42 PM₁₀ emission factors.

1) On the Phase IV road surface, soil was freshly-applied and had not yet been swept by repeated vehicle passes into the “pits” between asphalt-embedded aggregate “protrusions,” as would occur on normally traveled road surfaces. As a result, for the same silt loading, a greater proportion of the freshly applied silt would be located on the “protrusions” of the road surface, and would less sheltered from conditions of applied mechanical or aerodynamic shear than is the case for a well-traveled road where road silt has been generated by natural processes.

2) The road surface used in this experiment was recently paved, is very smooth, and is in better condition than the normally traveled road surfaces studied in earlier phases of this project. The road surface “pits” were therefore shallower and the silt that is deposited in the valleys would be less sheltered than would normally be the case on a well-traveled road with silt generated by natural processes.

The combined effects of 1) and 2) are to make the freshly-applied PM₁₀ on the experimental road more “exposed” to suspension during conditions of mechanical vehicular shear and moderate vehicular aerodynamic than the amount of more “sheltered” PM₁₀ mobilized into the air from a normally traveled, rougher typical road surface.

Compared to the moderate shears developed by vehicles, vacuum cleaners apply much higher shears during AP-42 silt recovery (Bettancourt Rodriguez, 2006). Silt recoveries of greater than 99% were observed after four vacuum cleaner head passes (Rodrigues, 2006) on both smooth and rough road surfaces. As a result, both silt recoveries and calculated AP-42 PM₁₀ emissions factors would not be as sensitive to silt distribution or road surface condition as mobile technologies emission factors.

When simultaneously measuring AP-42 emissions factors and mobile technologies emission factors that are sensitive to roughness and silt spatial distribution on a smooth road with freshly applied silt, we hypothesize that, compared to what would be observed on a well-traveled road, mobile technologies PM₁₀ emissions factors would increase relative to AP-42 emissions factors.

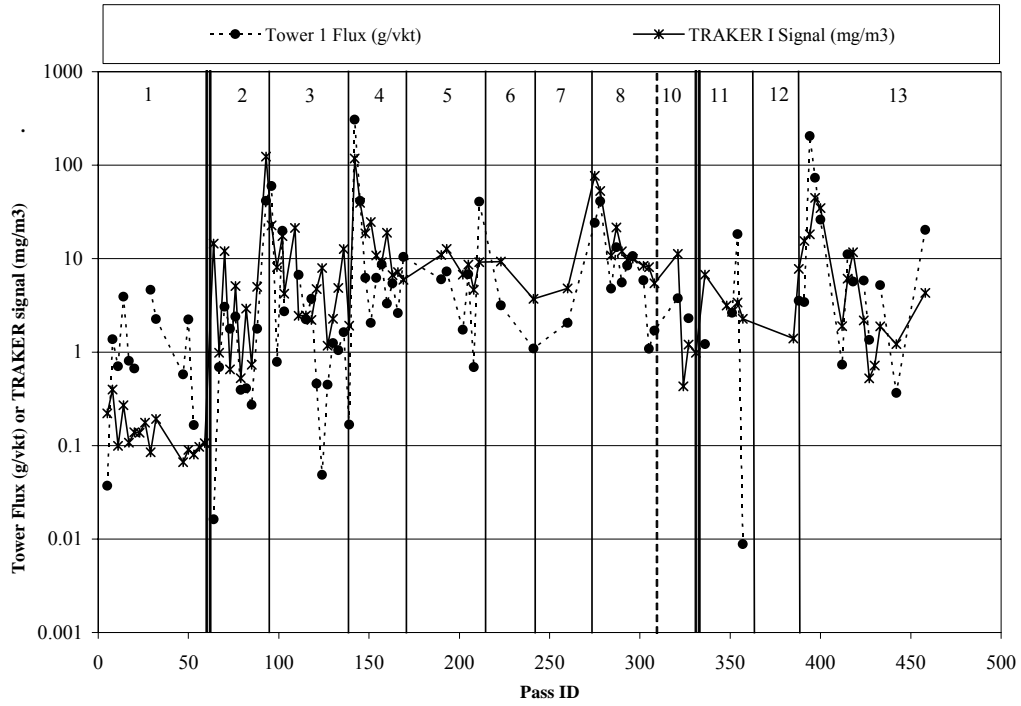
Recommendations of experiments that could be performed to test this hypothesis are proposed in Section 8.2

6.3 Comparison of Horizontal Flux Tower Emission Factors to Mobile Technologies Emission Factors

TRAKER I

Figure 6-8 shows the pass-averaged PM₁₀ emission factor measured by the tower system and the pass-averaged TRAKER signal for cases where both data sets were valid. Overall, the flux measurement and the TRAKER signal track reasonably well, though on a point-to-point basis, the relationship between the two measurements is somewhat noisy. To compare PM₁₀ tower flux measurements with AP-42 silt methodology and mobile system measurements, data were averaged by measurement set. For each set valid, tower flux measurements for all passes excluding the first 9 following silt application were averaged together regardless of the test vehicle. A minimum criterion of 10 valid vehicle passes was applied to the tower flux average value. This invalidated sets 6, 7, 9, and 12. In addition, data from set 13 were considered invalid because wind speeds were very high during that period. The remaining valid sets for comparison of TRAKER signal to PM₁₀ flux were 1, 2, 3, 4, 5, 8, 10, and 11.

Figure 6-8. Time series of measured horizontal PM₁₀ flux on the DRI tower system and the pass-averaged TRAKER I signal for passes when the horizontal flux measurement was valid.



Comparison of set-averaged TRAKER I data and set-averaged PM₁₀ emission factors are shown in **Figure 6-9**. The solid line in the Figure represents a least-squares linear fit to the data with a zero intercept while the dashed line represents a power law fit. The power law fit appears to accommodate the leftmost data point better than the linear fit, though we note that the linear fit provides a better R² value (0.57 compared to 0.48). However, it is unknown whether the leftmost data point is an outlier. The white squares also shown in the figure were collected on a road near Lake Tahoe, California as part of an earlier study (Kuhns et al., 2004). Whereas these earlier data are not fully comparable owing to a slightly different field setup, they tend to indicate that the linear fit (or a near-linear fit) to the data from the present study is more reasonable than the power law fit which exhibits an exponent of 0.38. Of course, without a mechanistic understanding of the road dust emission process, there is no a priori reason to anticipate a specific form for the equation that best represents a calibration of TRAKER I. In the absence of further information, we assume for simplicity that the TRAKER I signal is related to PM₁₀ emission factors through the simple linear relationship:

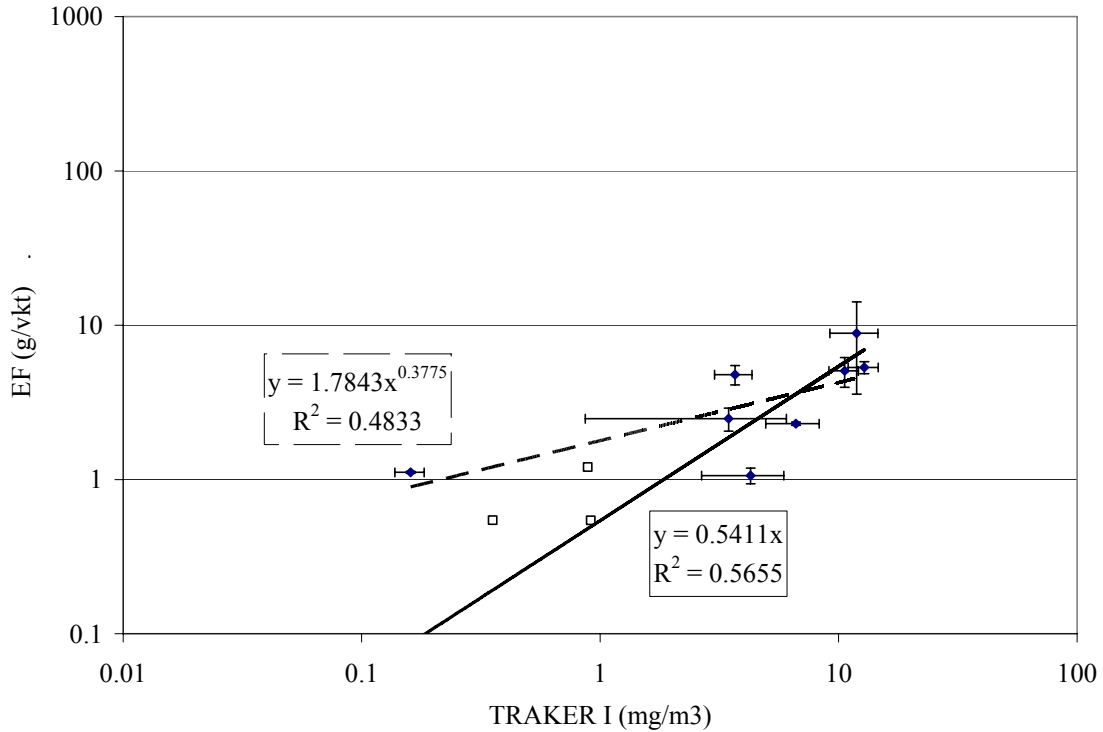
$$EF_{10} = 0.54 \times T \quad \text{Equation 6.1}$$

where

EF_{10} is the PM₁₀ mass emission factor from the tower data for all the vehicles used as test vehicles in the present study, and

T is the TRAKER signal defined simply as the background corrected average of the concentrations measured behind the left and right tires (Equation 5.3).

Figure 6-9. PM₁₀ emission factors versus TRAKER I average signal. Solid squares are data from the present study and represent emission factors that are averages of all valid tower measurements for sets 1, 2, 3, 4, 5, 8, 10, and 11. TRAKER I data shown are averages of TRAKER I passes during the respective set. Averages include only passes after the ninth pass following silt application for sets when silt was applied to the test road. The solid line in the Figure represents a least-squares linear fit to the data from the present study with a zero intercept while the dashed line represents a power law fit. The white squares are data collected during an earlier study near Lake Tahoe, California.



TRAKER II

Figure 6-10 shows the PM₁₀ horizontal fluxes and the TRAKER II signal averaged by pass when both measurements were valid. As with the TRAKER I data, the two measurements tend to follow each other, though not consistently owing to the noise that is inherent to both measurements, especially the tower fluxes. As with the TRAKER I data, to obtain a correspondence between tower measured PM₁₀ emission factors and the TRAKER II signal, we compared set-averaged tower data to set averaged TRAKER II signal. Only Sets with at least 10 valid tower measurements corresponding to “mechanically suspendable” road dust (i.e. more than 9 passes after silt application) were considered (1, 2, 3, 4, 5, 8, 10, and 11). Although the TRAKER II data for pass IDs lower than 170 were considered of suspect validity because of a malfunction in the inlet flow control, they have been included in the comparison shown in **Figure 6-11**. If not included, only a few points for comparison would be available. Thus, the relationship

between the TRAKER II signal and the PM₁₀ emission factors should be considered preliminary.

Unlike TRAKER I, the power law fit for TRAKER II provides a substantially higher R² value than the simple linear fit (0.90 compared to 0.75). It would be interesting as additional research becomes available to re-examine the relationship between the TRAKER II signal and tower measured emission factors. For the purposes of comparison with TRAKER I and SCAMPER (below), we propose to use the same simple linear form that was presented for TRAKER I in Equation 1 above, namely,

$$EF_{10} = 0.92 \times T_{II} \quad \text{Equation 6.2}$$

where T_{II} is the TRAKER II signal.

Figure 6-10. Time series of measured horizontal PM₁₀ flux on the DRI tower system and the pass-averaged TRAKER II signal for passes when the horizontal flux measurement was valid.

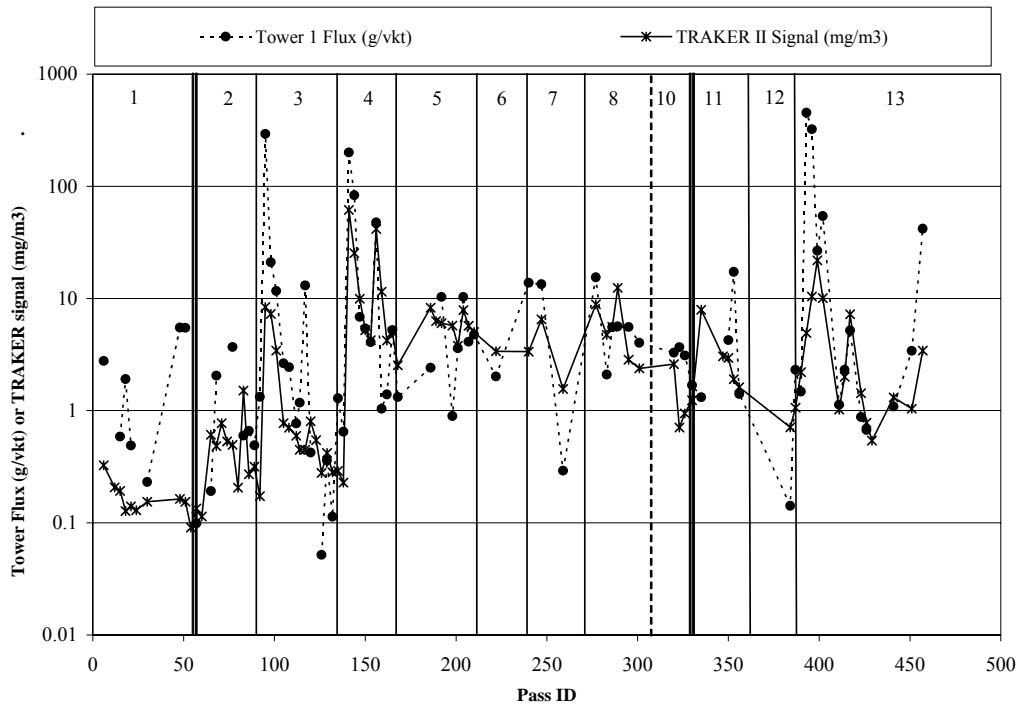
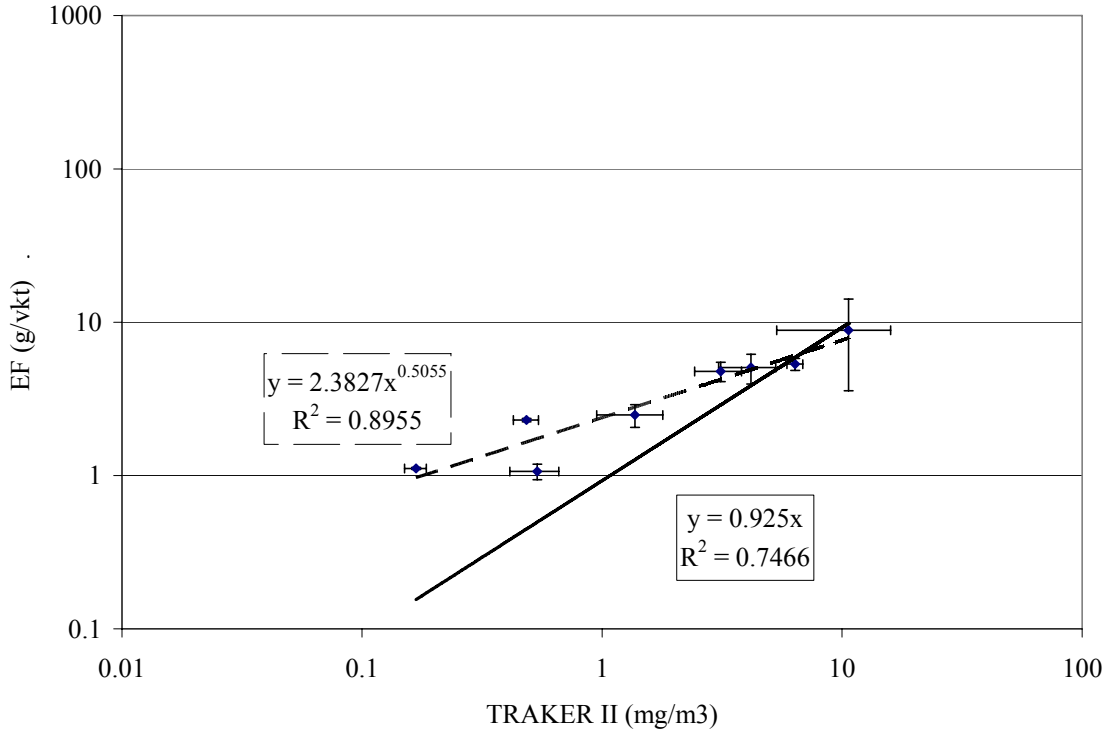


Figure 6-11. PM₁₀ emission factors versus TRAKER II average signal. Solid squares represent emission factors that are averages of all valid tower measurements for sets 1, 2, 3, 4, 5, 8, 10, and 11. TRAKER II data shown are averages of TRAKER II passes during the respective set. Averages include only passes after the ninth pass following silt application for sets when silt was applied to the test road. The solid line in the Figure represents a least-squares linear fit to the data with a zero intercept while the dashed line represents a power law fit.



SCAMPER

Figure 6-12 shows the time series of pass-averaged net (rear – front DustTrak signal) SCAMPER signal and PM₁₀ horizontal flux measurements when both types of measurements were valid. As with TRAKERS I and II, the UCR SCAMPER follows the general trend of emission factors captured by the tower system. For comparing the SCAMPER signal to PM₁₀ emission factors measured by the towers, only Sets with at least 10 valid tower measurements corresponding to “mechanically suspendable” road dust (i.e. more than 9 passes after silt application) were considered (1, 2, 3, 4, 5, 8, 10, and 11). Set averaged PM₁₀ emission factors are plotted against set-averaged SCAMPER signal in **Figure 6-13**. As with TRAKER I and TRAKER II, we show both a linear fit and a power law fit in the Figure. Similar to TRAKER I, there was no benefit in terms of R² values in a power law fit (0.40) over a linear fit (0.47). Assuming a linear relationship between PM₁₀ emission factors and the SCMAPER signal, the following empirical equation can be used to relate the two quantities:

$$EF_{10} = 20 \times SC$$

Equation 6.3

where *SC* is the SCAMPER signal.

In the SCAMPER the net signal is multiplied by the frontal area of the tow vehicle (maximum height * maximum width), 3.66 and the DustTrak “calibration factor”. The later is determined from PM₁₀ filter sampling collocated with the rear-mounted DustTrak. Due to a leak in the PM₁₀ sampler during this study, we did not determine a calibration factor. In previous studies conducted in Clark County NV and in Maricopa County AZ the average factor has been measured as 3.4 with an estimated uncertainty of 1. Therefore the emission factor based on this method is given by:

$$EF_{10} = 12 \times SC$$

Equation 6.4

This is within a factor of two of the value determined by the tower measurements and given the scatter in both data sets, they are in reasonable agreement.

It is interesting to note the multipliers for the different mobile systems that are needed to obtain the same emission factors (**Table 6-4**), especially in the context of the distance of the mobile measurement from the road dust source. The inlets of TRAKER I are located closest to the vehicle’s front tires. In TRAKER II, the distance between the inlet and the vehicle front tires is almost twice that of TRAKER I. For SCAMPER, the distance between the “influence” DustTrak mounted on the trailer behind the vehicle and the vehicle tires is more than an order of magnitude that of TRAKERs I and II. These simple observations suggest that the differences in the signals from these three mobile systems are closely related to the distances between where the “influence” measurement is taken compared to the locations of the tires.

Table 6-4. Summary of equivalence multipliers between mobile measurement systems and PM₁₀ emission factors assuming that the raw signal for the mobile systems is linearly related to measured emission factors.

System	Raw Signal (mg/m ³) Multiplier to get PM ₁₀ Emission Factor (g/vkt or g/vmt)
TRAKER I	0.54 (0.86)
TRAKER II	0.92 (1.5)
SCAMPER	20 (32)

Figure 6-12. Time series of measured horizontal PM₁₀ flux on the DRI tower system and the pass-averaged SCAMPER signal for passes when the horizontal flux measurement was valid.

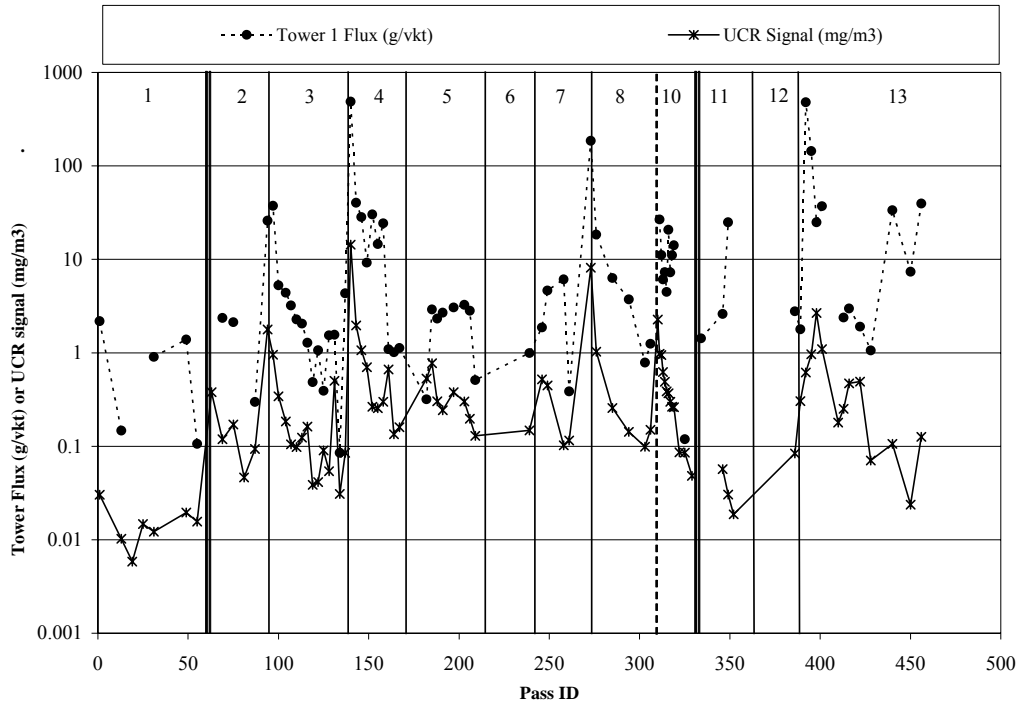
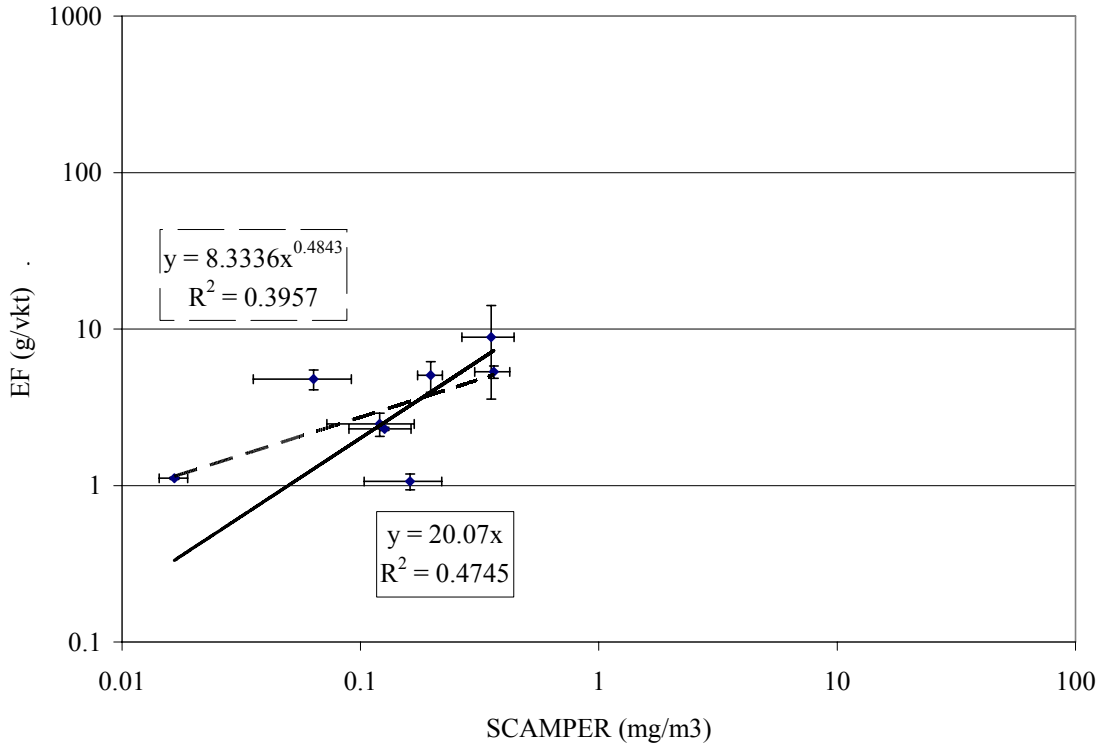


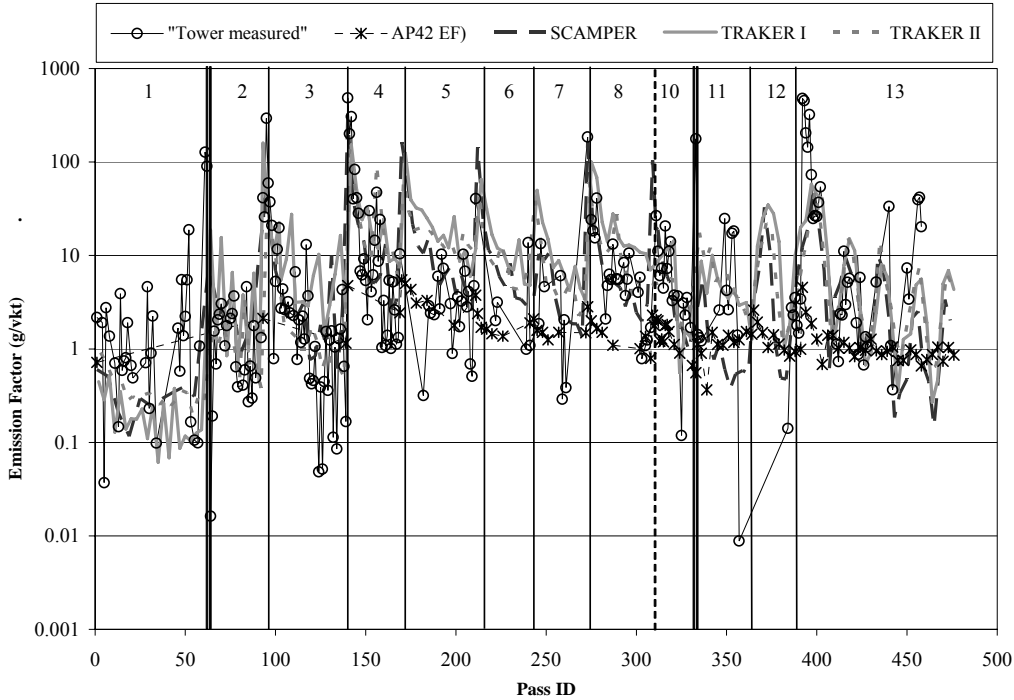
Figure 6-13. PM₁₀ emission factors versus SCAMPER average signal. Solid squares represent emission factors that are averages of valid tower measurements for sets 1, 2, 3, 4, 5, 8, 10, and 11. SCAMPER data shown are averages of SCAMPER passes during the respective set. Averages include only passes after the ninth pass following silt application for sets when silt was applied to the test road. The solid line in the Figure represents a least-squares linear fit to the data with a zero intercept while the dashed line represents a power law fit.



6.4 Comparison of Calibrated Mobile Technologies Emission Factors to EPA Method AP-42 Emission Factors to measured PM₁₀ Horizontal Flux Tower Values

Figure 6-14 shows a time series comparison of pass-averaged emission factors using the five different methods. The Figure shows direct PM₁₀ horizontal flux measurements with the tower system, emission factors estimated from silt measurements and use of AP-42 equations, and calibrated emission factors from the three mobile systems, TRAKER I, TRAKER II, and SCMAPER. The mobile system emission factors are calculated by multiplying the respective pass-averaged signals (in mg/m³) by the appropriate calibration factors discussed in Section 6.3 (Equations 1 – 3). The Figure illustrates how well the mobile systems track one another and to a lesser extent, the horizontal flux tower measurements. It also shows that the silt-based AP-42 method tends to underestimate the measured emission factors and does not respond to changes in emission factors that appear to be related to vehicle speed (see for example the speed test cycles in Set 13 measurements).

Figure 6-14. Emission factors (g/vkt) for all valid passes. Tower data are direct measurements, AP-42 data are based on silt measurements and use of AP-42 equations, SCAMPER, TRAKER I, and TRAKER II data are based on the regression between those mobile systems and measured PM₁₀ tower fluxes (using Equations 1-3 in Section 6.).



The current approved AP-42 PM₁₀ emission factor equation does not include speed as a factor in estimating PM₁₀ emissions. The equation assumes an equilibrium silt loading, SL, that is determined by rates of removal by mechanical and aerodynamic shear that are opposed by rates of creation and deposition from road, brake and tire wear, and atmospheric and hydrologic transport and vehicle track-out. Equilibrium silt loadings are known to be lower on roadways with higher average daily traffic (ADT), and higher ADT's are usually accompanied by higher average speeds.

In this experiment, freshly applied silt on the road surface was not in equilibrium, and was progressively depleted by successive vehicular passes. Rapid depletion was observed in both the first 9 passes of the mobile technologies data and in the “quickie strip” AP-42 silt sampling.

Additionally, effects of varying vehicular speed can be clearly observed in sets 12 and 13 (from Pass_ID 360 onwards) in **Figure 6-14**, where mobile technologies vehicle speeds were increase from 25 mph to 45 mph and then decreased back to 25 mph over several cycles. All three mobile technologies emissions factors consistently increased with increasing vehicle speed, and decreased with decreasing speed.

It is illustrative to examine the estimates of emission factors from the different mobile systems, tower measurements, and AP-42 silt based method on a set-averaged basis. As was done previously, during sets when silt was applied to the road surface, we include in the set average only data from passes after the ninth pass following silt application. **Figure 6-15** shows the estimated emission factors using the calibrated mobile systems (SCAMPER, TRAKER I, TRAKER II) and AP-42 equations that utilize on-site silt measurements. Overall, 1) mobile methods measured higher emission factors when higher silt loadings were applied, and 2) the mobile methods track each other quite well. The silt-based AP-42 emission factor method captures some of the variability exhibited by the mobile systems, but agreement of AP-42 with mobile systems is not as good as agreement among mobile systems. The same information is shown as scatter plots of TRAKER I, II, and silt based EF versus SCAMPER EF in **Figure 6-16** and TRAKER II, SCAMPER, and silt-based EF in **Figure 6-17**.

Figure 6-15. Comparison of set-averaged emission factors (g/vkt). Figure shows averages over sets with valid data for mobile systems calibrated against PM₁₀ tower flux measurements as described in Equations 1-3 of Section 6.2 and silt-based emission factors using AP-42 equations. Averages include only passes after the ninth pass following silt application for sets when silt was applied to the test road. AP-42 emission factors are calculated using measured silt loadings at the end of a measurement set.

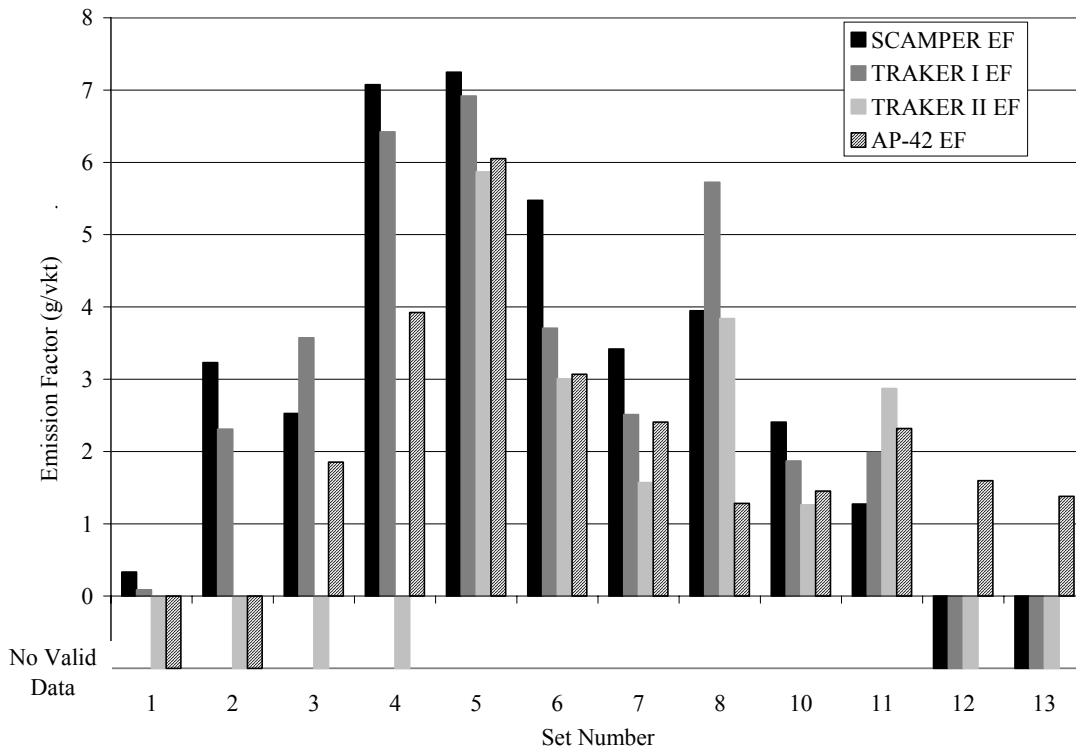


Figure 6-16. Set averaged TRAKER I EF, TRAKER II EF, and AP-42 silt-based EF plotted against SCAMPER EF.

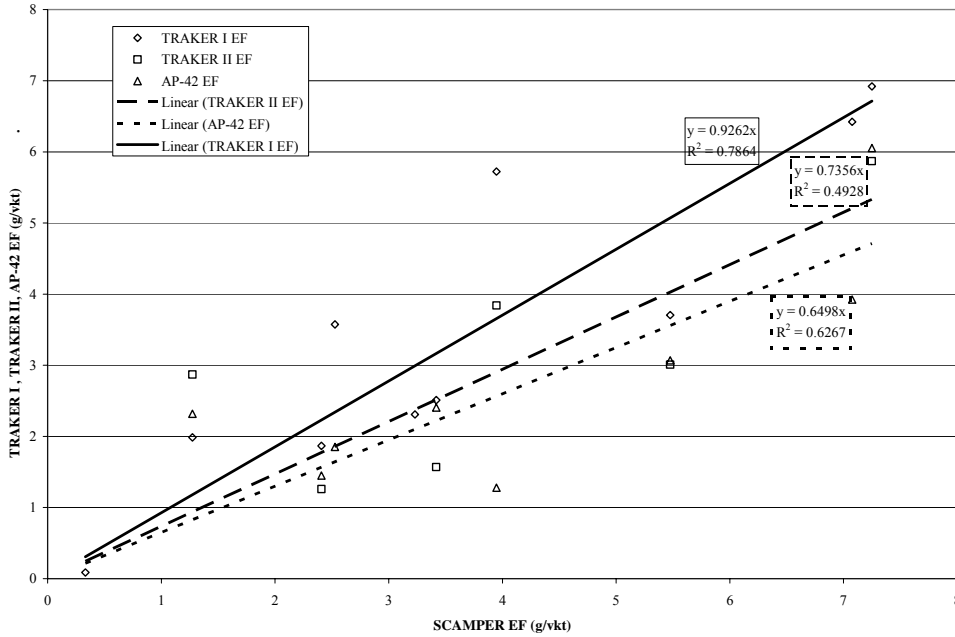
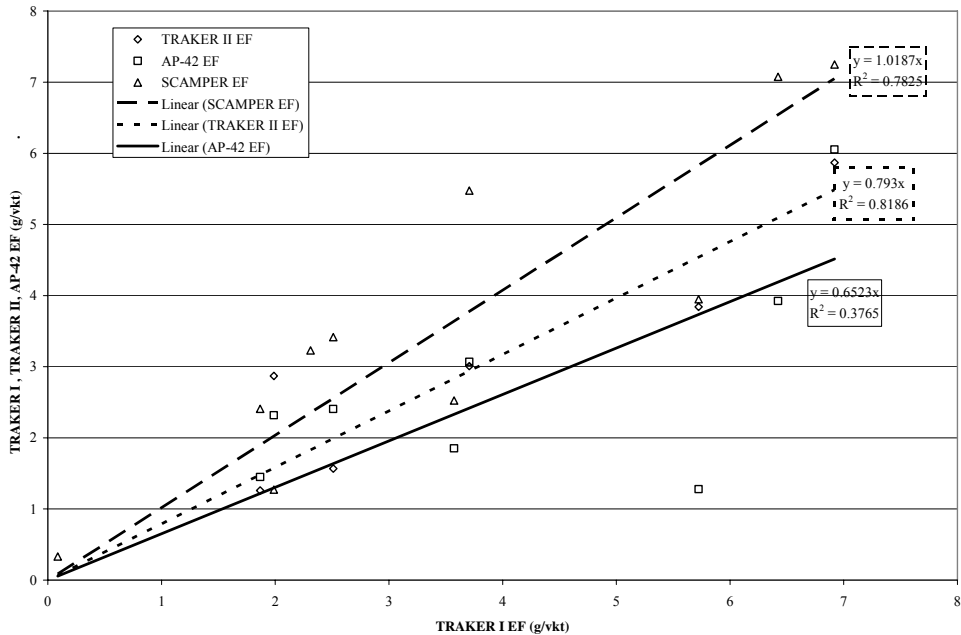


Figure 6-17. Set averaged TRAKER II EF, SCAMPER EF, and AP-42 silt-based EF plotted against TRAKER I EF.



7.0 DISCUSSION

7.1 Real World Precision and Reproducibility

7.1.1 UCR Paved Road Phases II & III for DAQEM

In the DAQEM's Phase II (need reference to Phase II report) evaluation of mobile emissions from paved roads the SCAMPER system was used to characterize PM₁₀ emission rates on a single 120 mile long test route in Las Vegas, NV. Tests were conducted February 14-17, 2005, with one traverse of the route per day. Emission rates for speeds less than 10 mph were excluded, as we would not expect a well-developed plume behind the SCAMPER vehicle. The results showed that PM₁₀ emission rates were generally near zero except when occasional "hot spots" were encountered, which is consistent with previous measurements. The daily average PM₁₀ emission rates for the routes were 0.086, 0.105, 0.040 and 0.012 g/VKT (0.14, 0.17, 0.064, and 0.019 g/VMT) for February 14th, 15th, 16th, and 17th, respectively. Due to likely enforcement activities after the second measurement day, the precision of the measurement approach could not be quantified. The two initial days suggest that the precision is approximately 10%. The emission rates for the first two days were approximately a factor of two lower than those measured in the summer of 2004 during phase I. The test route, however, was different than the summers and there are likely to also be seasonal differences that affect emission rates.

In the DAQEM's Phase III evaluation of mobile emissions from paved roads (need reference to Phase III report) the SCAMPER system was used to characterize PM₁₀ emission rates from road loops in the Las Vegas area. One of the primary objectives of this study was to determine measurement uncertainty. This was done by making consecutive measurements over a loop of roads. One loop was short with high emission potential roads in an industrial area so that a large number of traverses could be made. Two longer loops were chosen to be more representative of emission potential of roads in the area. High PM₁₀ emission rates were expected from one of the longer loops, while low rates were expected from the other. The measurements were also used to compare the SCAMPER results with AP-42 silt sampling, and evaluate diurnal variations of the emission factors.

The results showed that PM₁₀ emission rates met the loop expectations and were generally low except when "hot spots" were encountered, which is consistent with previous measurements. We concluded that the measurement uncertainty, based on the coefficient of variation for each loop, was approximately 25%. The PM₁₀ emission rates did not change significantly during the course of the day, but on the high emission longer loop the rates dropped by a factor of two over the weekend. The comparison with AP-42 silt sampling showed good correlation ($R^2 = 0.86$) with the SCAMPER segment results, which were three times lower. The SCAMPER data, however were not calibrated to actual mass measurement. The calibration factor, based on a limited (8) number of filter samples was approximately 2, which compares well with the value of 2.4 reported here. Applying this factor, the SCAMPER and AP-42 silt PM₁₀ emission rates were equivalent

well within experimental uncertainty. Since SCAMPER directly measures PM emission rates, it is likely to be a more direct and accurate measure of PM emissions from roads..

7.1.2 DRI Studies- Clark County Phase II, Lake Tahoe and Idaho

The study reported here is the latest in a series of TRAKER studies that started in 1999 when a passenger vehicle was outfitted with sample tubes behind the front tire. That earlier study in Las Vegas, Nevada, reported by Kuhns et al. (2001), was the “proof of concept” for the TRAKER idea. Since then a number of research efforts have been completed using the TRAKER in the Treasure Valley in Idaho (Etyemezian et al., 2003a, 2003b; Kuhns et al, 2003), near El Paso, Texas (Kuhns et al., 2005; Gillies et al., 2005), in the vicinity of Lake Tahoe on both the California and Nevada sides (Gertler et al., 2006), and again in Las Vegas, Nevada (Etyemezian et al., 2006).

The study near El Paso, Texas, involved the use of upwind/downwind flux towers to directly measure the PM₁₀ emissions from an unpaved road and correlate those measurements with the TRAKER signal. Three important findings came out of that study. First, it was found that the PM₁₀ emission factor for a vehicle traveling on an unpaved road was directly proportional to the speed of the vehicle as well as its weight (Etyemezian et al., 2003a; Gillies et al., 2005). This was tested for speeds ranging from 5 to 45 mph and vehicle sizes ranging from a small passenger vehicle (Dodge Neon) to a 22-wheeled tractor-trailer. Second, it was found that for the same paved road, the TRAKER signal increased with speed. Specifically, the TRAKER signal was proportional to a constant multiplied by the TRAKER travel speed raised to the third power. Third, it was found that for unpaved roads, the PM₁₀ emission factor scaled with the cube root of the raw TRAKER signal. In summary, it was found that the TRAKER signal could be related to PM₁₀ road dust emissions from unpaved roads using the Equation:

$$EF = kT^{1/3} \qquad \text{Equation 7.1}$$

where EF is the emission factor (g/vkt), k is the constant that relates emissions to the TRAKER signal and is approximately 0.33 ($\sigma_g=1.5$), and T is the TRAKER signal as defined in Equation 5.3 in Section 5.3.2. This provided the fit shown in **Figure 7-1** for the solid circles.

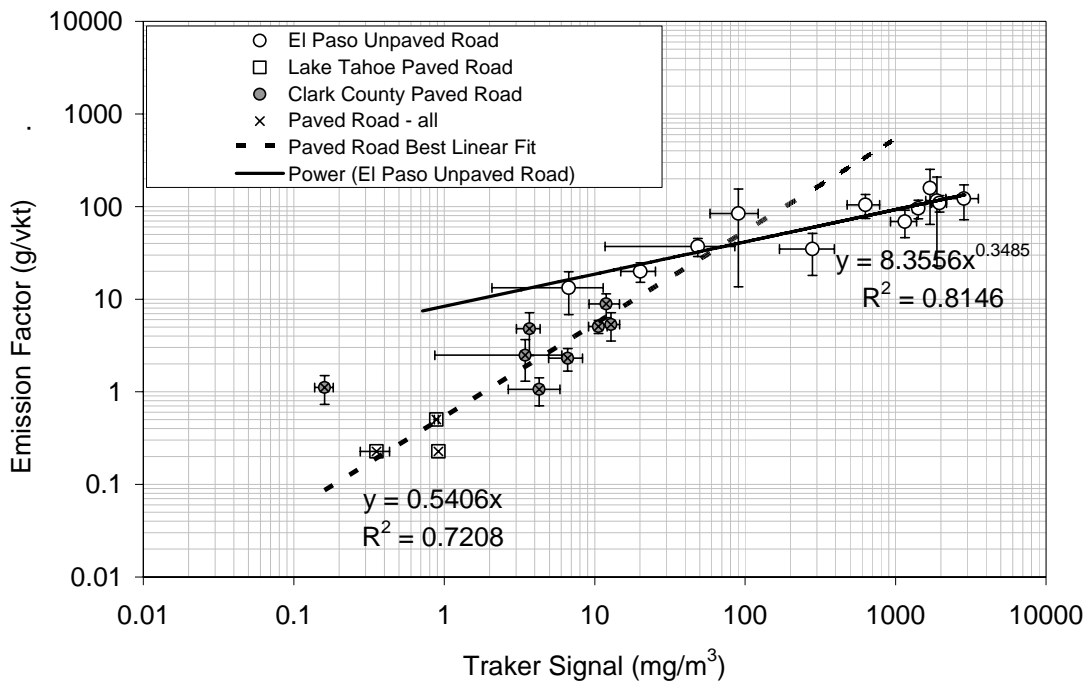
For the Treasure Valley Road Dust Study, Etyemezian et al., (2003b) used TRAKER I data collected over 150 miles of roads near Boise, Idaho over two seasons to assemble a PM₁₀ paved and unpaved road dust emission inventory. At the time of that study, the TRAKER I had not been calibrated against an independent measure (such as horizontal flux towers) on a paved road. Therefore, those authors extrapolated the unpaved road calibration to obtain preliminary estimates of emissions from Treasure Valley Roads. It was clear from the relative magnitude of road dust emissions in the emissions inventory that the unpaved road calibration was providing unreasonably high values for PM₁₀ emission factors. This was reinforced during the Lake Tahoe Study (Gertler et al., 2006), when TRAKER I was operated on a paved road segment that was also outfitted with a horizontal tower flux emission measurement system. This resulted in three data points

(shown as open squares in **Figure 7-1**) that were clearly not in line with the unpaved road calibration used in the Treasure Valley Study.

It is worth noting that up until the present study, emission factors reported for TRAKER I measurements were based on calibration of the TRAKER I primarily on unpaved roads. In the absence of a paved road calibration, those earlier calibrations from an unpaved road were extrapolated to measurements on paved roads. The present study provides a direct paved road calibration for the TRAKER I (and TRAKER II).

In the present research effort, TRAKER I – along with SCAMPER and TRAKER II – was extensively operated on a paved road in conjunction with horizontal tower flux measurements. The results of this study, shown in **Figure 7-1** as gray circles, along with the Lake Tahoe measurements (open squares), indicate that the relationship between the TRAKER signal and PM_{10} emission factors on paved roads is quite different from unpaved roads. This shows that earlier emissions estimates obtained with the TRAKER I (using unpaved road calibration extrapolated to paved roads) were substantially higher than emissions that would have results from using a paved road calibration (See **Figure 7-1**).

Figure 7-1. TRAKER I calibrations. White circles show data collected from unpaved road calibration near El Paso, Texas (Etyemezian et al., 2003a). Open squares show later data collected on a paved road near Lake Tahoe in California (Gertler et al., 2006). Gray circles are data collected on paved road from the present study. Dashed line is best linear fit to data from current study and Lake Tahoe study.



As part of an earlier phase (Phase II) of the Clark County research effort, the TRAKER I was used to measure road dust emission potential over a road circuit (~100 miles) on four consecutive days in February, 2005. Researchers from UNLV were also collecting silt samples for AP-42 based emissions estimation from points along the road circuit over the same period. Two important findings resulted from the Phase II study that is relevant to the present effort. First, Etyemezian et al. (2006), reported that over the 645 separate road segments that constituted the road circuit, the precision of the TRAKER I measurement system was better than 20% for 62% of the road segments and the precision was better than 50% for 96% of the road segments.

Second, the data collected as part of Phase II were re-processed using the relationship between the TRAKER signal and paved roads that has resulted from the present study (namely, Equation 1 in Section 6.3). Where data were available from both the TRAKER I measurement and silt samples collected from UNLV, the emission factors measured by TRAKER I were compared to the emission factors estimated from silt measurements and application of the AP-42 equations. Emission factors using these two methods are shown side by side in **Figure 7-2**. For the majority of the streets where both measurements were completed, the TRAKER I emission factors using the paved road calibration obtained from the present study are substantially lower than the silt based emission factors

calculated using the AP-42 equations. Two exceptions are Sapphire Light and Hardin, both of which were heavily loaded with soil. Combined with the information provided in **Figure 6-15** in Section 6.4, these data point to a preliminary trend. It appears that for heavily loaded roads, mobile measurement systems such as TRAKER I provide higher emission factor estimates than silt-based methods. This seems to be true for most of the Phase IV measurements (with mobile system emission factors in the range of 2 – 7 g /vkt) as well as the Sapphire Light and Hardin roads measured in Phase II of the Clark County Study (with mobile emission factors around 10 g/vkt). In contrast, for lightly loaded roads (Emission factors less than 1 g/vkt), the mobile systems appear to provide a lower estimate of emission factors than silt based methods.

Figure 7-3 shows the same information in scatter plot format. The regression between AP-42 silt based emission factor estimates and TRAKER I emission factor estimates exhibits a poor correlation ($R^2 \sim 0$). This is in contrast to the regression of silt-based methods against TRAKER I from the Phase IV study, where the relationship is not one to one, but does exhibit at least a weak correlation ($R^2 = 0.37$, See **Figure 6-17**, Section 6.4). There are two possible reasons for this difference between the Phase IV study and the real-World conditions of the Phase II study. In the Phase IV study, the same parent road material was used for silt application for all tests and silt was applied to the entire roadway test section more or less homogeneously. In contrast, in the real World, the road material that can result in road dust may be of quite variable composition (in terms of size distribution at least). Furthermore, there are likely to be rather large differences in road dirt loading over several kilometers of the same street. These differences cannot be captured by what is essentially a single point silt sample.

Figure 7-2. Emission factors (g/vkt) from Phase II Clark County study. Data are shown for streets where both TRAKER I and silt-based measurements were conducted. TRAKER I emission factors were calculated using the paved road calibration resulting from the present study (See Equation 1 Section 6.2).

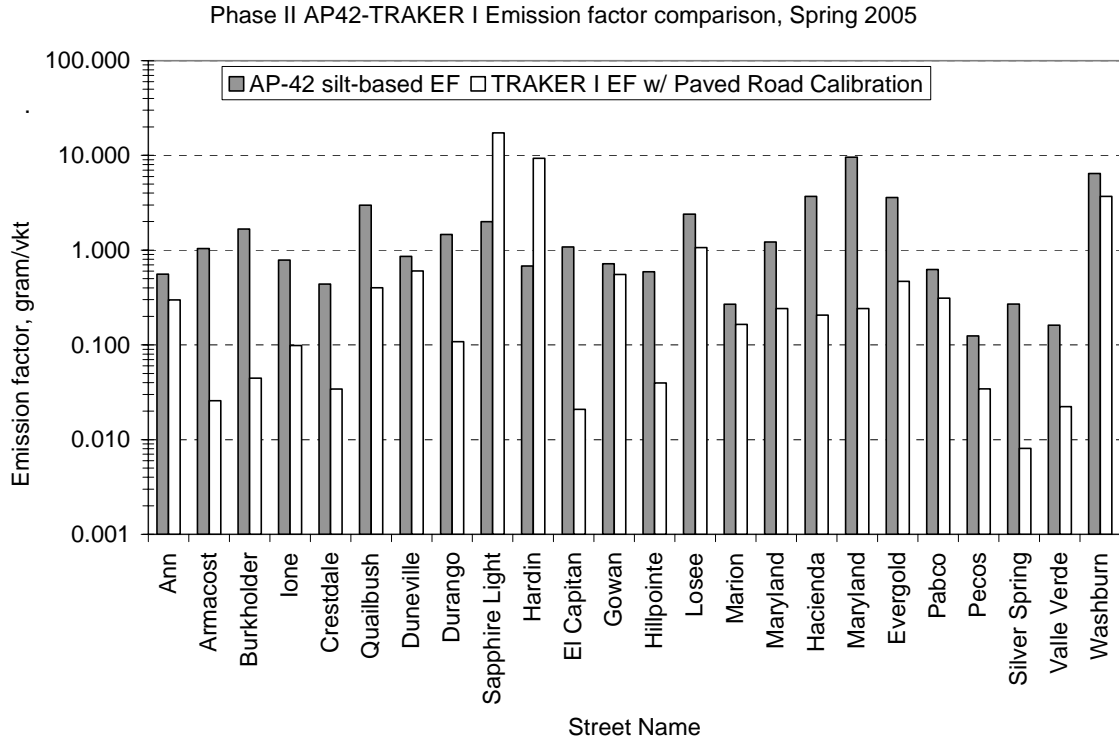
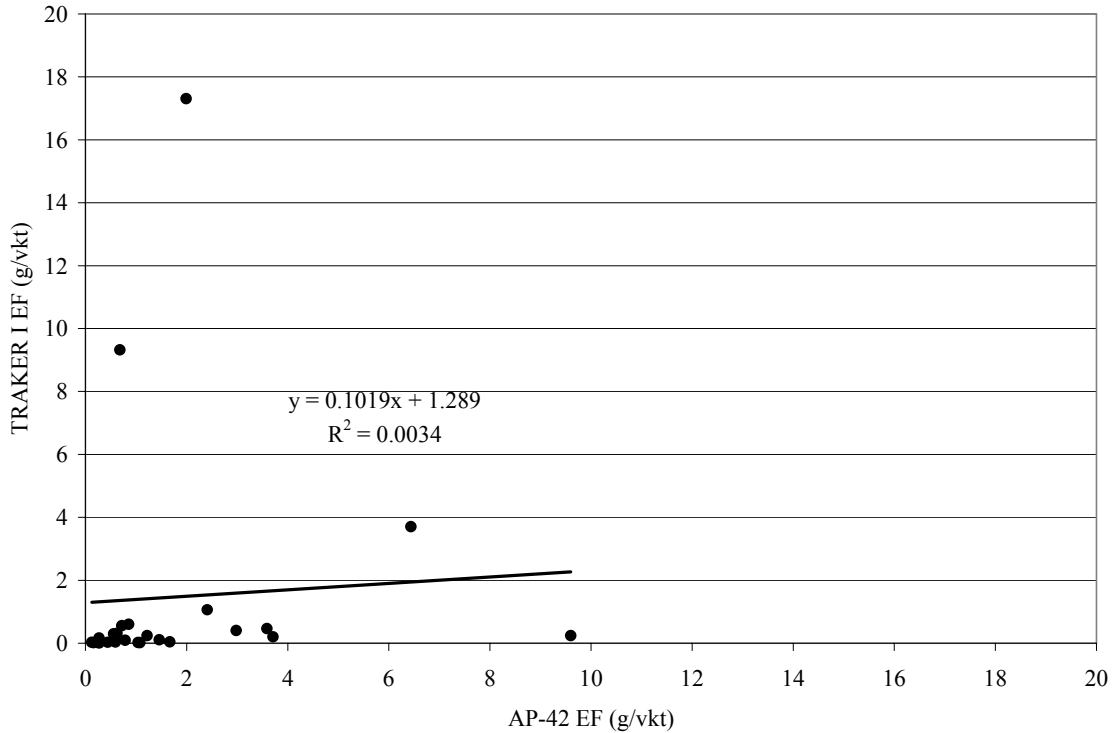


Figure 7-3. Scatter plot of TRAKER I EF (g/vkt) versus AP-42 silt based EF (g/vkt).



7.2 Applying Phase IV Results in Real World Conditions- Explanation of Higher EF's in Phase IV

We propose a working hypothesis about the cause of the shift in the relationship between AP-42 emission factors and mobile technologies emission factors, which we call the “differential silt mobilization hypothesis”, or DSMH, for short. We will attempt to use DSMH to explain why, in Phase II, AP-42 EF's were higher than mobile EF's compared Phase IV, where AP-42 EF's were lower than mobile EF's. We believe that these observations are caused by both different availabilities of silt for resuspension in Phase II and Phase IV, and by the higher amount of shear applied to mobilize silt in the AP-42 method compared to mobile technologies methods.

- a) The Phase IV experiment was conducted on a road surface in excellent condition with very low physical roughness. In comparison, the roadways sampled during Phase II exhibited a variety of roughness, but are thought to have generally higher physical roughness, and have more highly worn pavements than the Phase IV site.
- b) Silt deposited from natural processes on well-traveled road surfaces tends to be swept into the pits of the road surface, between the protrusions caused by aggregate embedded in the asphalt binder.
- c) Measurements by Rodriguez-Bettancourt (2006) showed that aerodynamic shear applied by a conventional vacuum cleaner head during AP-42 silt

recovery is likely to be one to three orders of magnitude higher than the shear applied by vehicles.

The combined result of a), b) and c) makes it more difficult to mobilize silt into the air when it is embedded in the pits of a normally-traveled, medium-rough road surface during conditions of moderate shear applied by vehicle tires and aerodynamic wakes compared to the greater degree of mobilization resulting from conditions of higher shear applied by a vacuum cleaner head during AP-42 sampling. As a result, on natural, rougher road surfaces, a higher mobilization of the silt fraction by a vacuum cleaner would lead to a higher AP-42 emission factor, for the same amount of silt loading, than the emission factors observed by mobile technologies vehicles.

In contrast, during the Phase IV experiment, freshly applied road silt was more evenly distributed between the smaller “protrusions” and “pits” on a smoother, well-sealed road surface, and was therefore easier to mobilize in conditions of moderate applied vehicle shear than a similar loading on a normally traveled paved road. As a result, observed mobile EF’s would be higher, for the same silt loading, on the Phase IV experimental road surface, than they were on the normally traveled paved roads that were measured in Phase II. AP-42 vacuumed EF’s would be similar, since four vacuum passes have been shown to recover greater than 99% of applied road silt on both smooth and rough road surfaces, and the vacuum exerts a very high level of aerodynamic shear. The result is that mobile technologies EF’s are hypothesized to have increased relative to AP-42 EF’s on the Phase IV surface compared to the Phase II surface.

This hypothesis would also explain why, in conditions of heavy soil loading, such as Hardin and Sapphire Light in Phase II, as well as for the Veterans Memorial Boulevard loadings in Phase IV, mobile technologies emissions factors were higher than for AP-42, because, under these conditions, there is a large amount of silt on top of the protrusions that can be easily suspended

7.3 Advantages of Mobile Technologies

Real-time vehicle mounted sampling systems provide a number of very significant improvements over the current AP-42 paved road dust emissions estimating equation. The mobile sampling systems are not subject to many of the assumptions and limitations applicable to the AP-42 equation, including the requirement for free flowing traffic, speed ranges between 10 and 55 mph, the need to block lanes of traffic for silt sampling, the ability to sample on all road functional classes, and the ability to collect a large number of measurements over a short time period.

Mobile sampling systems can effectively sample on congested urban streets where traffic is not free flowing, whereas the AP-42 emissions equation is predicated on free flowing traffic. Applying AP-42 emissions estimating methodology to roadways with heavily congestion results in unknown but potentially significant errors. The GPS linked data collection system utilized in the mobile sampling systems allow the operator to easily exclude data points collected below a specified *de minimus* threshold speed, typically set at 10 mph.

Mobile sampling systems are speed independent and can accurately measure emissions at all non-*de minimus* (>10 mph) speed ranges, including speeds above 55 mph. By comparison, the AP-42 emissions equation is not validated for vehicle speeds above 55 mph.

Mobile sampling systems provide a safer method of measuring paved road dust emissions. The mobile sampling systems can operate without the need for lane closures and the associated public safety risk and increased traffic congestion.

Mobile sampling systems can accumulate paved road emissions data much faster and more economically than the AP-42 emissions equation methodology. The mobile sampling systems provide a means of sampling significant percentages of the entire road network in an airshed or nonattainment area. The abundance of data developed with the mobile sampling systems approach allows for the development of specific emission factors for many criteria known to affect the paved road dust emission rate. These include, in addition to road functional classification, road infrastructure development and land use type and development. Impacts of specific silt deposition sources may also be evaluated. These detailed breakdowns will allow SIP developers to prepare more complete and representative emissions inventories for the paved road dust source category. The benefits of more robust emission factor information would be even more profound for air regulatory agencies and MPOs developing future emissions projections for this source category. The mobile sampling systems ability to provide much larger data sets will allow SIP planners and MPOs to develop far more detailed and realistic projected emissions estimates for future year paved road dust emissions.

8.0 CONCLUSIONS

8.1 Conclusions

In this study, controlled measurements of PM₁₀ road dust emissions were completed on a test road in Boulder City, Nevada. Well-characterized parent soil was spread onto the test road surface at the beginning of most measurement sets. Silt samples were procured at the beginning and end of each measurement set as well as during the measurement set in some cases. Simultaneously, three mobile road dust measurement systems were used to traverse the test road: SCAMPER, TRAKER I, and TRAKER II. These mobile systems were used both to measure the potential for road dust emissions and to serve as road dust sources. Horizontal flux of PM₁₀ was measured using an instrumented tower system to obtain an independent measure of the PM₁₀ emission factors from travel on the test road section. The tower measurements were considered as the standard for comparing the other four measurement methods (three mobile methods and silt method).

It was clear from examining the data from both the horizontal flux towers and the mobile systems that after the application of soil to the test road, the first nine or so vehicle passes resulted in PM₁₀ emissions that were

- a. much higher than subsequent passes and
- b. apparently caused by a different mechanism than subsequent passes.

In comparisons of mobile and silt systems to horizontal tower measurements, the first nine vehicle passes were omitted as they likely represented a very short-lived mechanism for road dust emissions that would not be prevalent on a well traveled real road.

Averages of PM₁₀ emission factors measured with the tower system were calculated on a measurement set basis along with comparable averages for mobile systems. A simple linear fit appeared to be adequate for describing the relationship between the mobile systems' raw signal and the emission factors measured by the tower system. The raw signals for all three mobile units were calculated as the PM₁₀ concentration at a location that is influenced by the road dust generated by the vehicle minus the background PM₁₀ concentration. All three mobile systems correlated reasonably well with the tower measurements (with R² values ranging from 0.47 to 0.75). To obtain PM₁₀ emission factors, it was found that the TRAKER I, TRAKER II, and SCAMPER raw signals required multiplication by 0.54, 0.92, and 20, respectively.

Silt measurements were used to calculate emission factors following the equations provided in AP-42. Those emission factors were then compared to the tower data as well as to emission factors obtained with the calibrated mobile systems. The mobile systems agreed well with one another – not surprising since they were all calibrated against the same tower data – and showed reasonable correlation with silt-based emission factors.

In general, silt based measurements resulted in slightly lower emission factors than those measured by the tower and mobile systems. In contrast, when the same tower based calibration was applied to TRAKER I data acquired on a wide range of Clark County roads as part of an earlier phase of this research effort, and compared to AP-42 emissions factors derived from silt measurements obtained from those same roads over the same sampling period, the TRAKER I measurements generally provided much lower emission factors than emission factors calculated from the silt measurements.

As described in Section 7.2, we believe that this shift in the relationship between mobile technologies EF's and AP-42 EF's is caused by differential silt mobilization, which occurred as a result of a greater proportion of the applied silt loading being distributed on the tops of the embedded road surface aggregates, and hence being more easily entrained by vehicle mechanical and aerodynamic shear from the Phase IV experimental road surface, compared to the less easily entrained silt more likely to be embedded between the road surface aggregates on the Phase II road surfaces.

8.1 Recommendations

At the time of report preparation, the DAQEM had concluded that real-time based vehicle mounted sampling systems provided a superior and more flexible approach for developing SIP emissions inventories for emissions from paved road dust sources. These systems also provide similar advantages for inventorying emissions from stabilized unpaved haul roads and other public and private unpaved roads. In addition SIP emissions inventory development, these systems provide a superior method for measuring road dust emissions at major stationary sources for permitting purposes.

DAQEM has discussed approval of real-time based vehicle mounted sampling systems for SIP emissions inventory development with EPA Region IX and EPA OAQPS. Both agencies have indicated the need for a peer review process prior to a regional or OAQPS approval. In addition, the OAQPS will need endorsements from a significant number of state and local air regulatory agencies or from associations such as WRAP and NACAA before entertaining approval under the AP-42 procedures. Clark County has informally contacted a number of state and local air regulatory agencies, many of which have expressed support for this alternative method of emission inventory development. This alternative method was also discussed with certain Metropolitan Planning Organizations (MPOs), all of who were very interested.

Following presentation of this paper at the 16th Annual International Emissions Inventory Conference, Clark County will initiate a formal peer review process in collaboration with EPA OAQPS and EPA Region IX. A number of air regulatory agency staff and research scientist have agreed to participate in the peer review. Certain MPO have agreed to participate. As the peer review is nearing completion, the DAQEM will begin to formally solicit endorsements and letters of support for consideration of approval under AP-42. Following completion of the peer review process, Clark County will initiate a formal request for EPA Region IX approval of real-time vehicle-mounted sampling systems as a locally approved method and EPA OAQPS for approval as an alternative AP-42 method.

9.0 References

U.S. Environmental Protection Agency, Emission Factor Documentation for AP-42, EPA Contract No. 68-D0-0123, MRI Project No. 9712-44 dated March 8, 1993.

Geotechnical and Environmental Services, Inc., *Presentation of Final Versions of Deliverables for Re-Evaluating and Updating the Particulate Emission Potential Map and Soil Classification for Dust Mitigation Best Management Practices Manual for Clark County*, dated September 26, 2003.

Etyemezian V., H. Kuhns, J. Gillies, M. Green, M. Pitchford, and J. Watson (2003). Vehicle based road dust emissions measurements (I): Methods and Calibration. *Atmospheric Environment* 37: 4559-4571.

Etyemezian V., H. Kuhns, J. Gillies, J. Chow, K. Hendrickson, M. McGown, and M. Pitchford (2003b). Vehicle based road dust emissions measurements (III): Effect of speed, traffic volume, location, and season on PM₁₀ road dust emissions. *Atmospheric Environment* 37: 4583-4593.

Etyemezian, V., H. Kuhns, and G. Nikolich (2006). Precision and repeatability of the TRAKER vehicle-based paved road dust emission measurement. *Atmospheric Environment* 40: 2953-2958.

Gertler A, H. Kuhns, M. Abu-Allaban, C. Damm, J. Gillies, V. Etyemezian, R. Clayton, D. Profitt (2006). A Case Study of the Impact of Winter Road Sand/Salt and Street Sweeping on Road Dust Re-entrainment. *Atmospheric Environment* 40 (31): 5976-5985.

Gillies, J.A.; V. Etyemezian, H. Kuhns, D. Nikolic, and D.A. Gillette (2005). Effect of vehicle characteristics on unpaved road dust emissions; *Atmospheric Environment* 39, 2341–2347.

Kuhns, H., Etyemezian, V., Landwehr, D., MacDougall, C., Pitchford, M., and M. Green. (2001). Testing Re-entrained Aerosol Kinetic Emissions from Roads (TRAKER): A New Approach to Infer Silt Loading on Roadways. *Atmospheric Environment* 35: 2815-2825.

Kuhns H., V. Etyemezian, M. Green, Karin Hendrickson, Michael McGown, Kevin Barton, Marc Pitchford (2003) Vehicle-based road dust emissions measurement (II): Effect of precipitation, winter time road sanding, and street sweepers on PM₁₀ fugitive dust emissions from paved and unpaved roads. *Atmospheric Environment* 35: 4572-4583

Kuhns, H., M.-C. O. Chang, J.C. Chow, V. Etyemezian, L.-W. A. Chen, N. Nussbaum, S.K.K. Nathagoundenpalayam, D. Trimble, S. Kohl, M. MacLaren, M. Abu-Allaban, J. Gillies, A. Gertler, C. Damm, C. Denney, C. Gallery, and J. Skotnik (2004). DRI Lake Tahoe Source Characterization Study: Final Report. Prepared for California Air Resources Board, 1001 I Street, Sacramento, CA 95812, Oct. 2004.

Kuhns, H., V. Etyemezian, J. Gillies, D. DuBois, S. Ahonen, and D. Nikolic (2005). Spatial Variability of Unpaved Road Dust PM₁₀ Emission Factors near El Paso, Texas. *Journal of the Air and Waste Management Association*.55: 3-12.

- Etyemezian, V., H. Kuhns, J. Gillies, M. Green, M. Pitchford and J. Watson (2003). "Vehicle-based road dust emission measurement: I - methods and calibration." *Atmospheric Environment* 37(32): 4559-4571.
- Kuhns, H., V. Etyemezian, D. Landwehr, C. MacDougall, M. Pitchford and M. Green (2001). "Testing Re-entrained Aerosol Kinetic Emissions from Roads (TRAKER): a new approach to infer silt loading on roadways." *Atmospheric Environment* 35(16): 2815-2825.
- Countess, R. (2001). Methodology for Estimating Fugitive Windblown and Mechanically Resuspended Road Dust Emissions Applicable for Regional Scale Air Quality Modeling. Prepared for the Western Governors Association by Countess Environmental, Westlake Village, CA, April, 2001
- Cowherd, C. (1984). Paved Road Particulate Emissions: Source Category Report. Report No. EPA-600/7-84-077. Prepared by U.S. Environmental Protection Agency, Research Triangle Park, NC, USA.
- Cowherd, C. (1999). Profiling Data for Open Fugitive Dust Sources. Prepared for U.S. Environmental Protection Agency, Emission Factors and Inventory Group, Office of Air Quality Planning and Standards, Research Triangle Park, NC, by Midwest Research Institute, Kansas City, MO.
- Cowherd, C., and T. Pace (2002). Potential role of vegetative ground cover in the removal of airborne fugitive dust. Presented at the Annual meeting of the Air and Waste Management Association, Baltimore, MD, June 2002.
- Etyemezian V., Kuhns, H., Chow, J., Gillies, J., Green, S. Kohl, and M. Pitchford (2001). The Treasure Valley Road Dust Study: Final Report. Prepared for the Idaho Department of Environmental Quality, Boise, Idaho by the Desert Research Institute, Las Vegas, NV. February, 2002.
- Etyemezian V., Kuhns, H., Chow, J., Gillies, J., Green, M., Hendrickson, K., McGown, M., and M. Pithford (2003a). Vehicle Based Road Dust Emissions Measurement (I): Methods and Calibration. Manuscript submitted as companion paper to *Atmospheric Environment*.
- Etyemezian, V., Gillies, J., Kuhns, H., Nikolic, D., Watson, J., Veranth, J., Laban, R., Seshadri, G., and D. Gillette (2003b). Report prepared for the WESTAR Council, Lake Oswego, OR, USA by DRI, Las Vegas, NV, USA, January 2003.
- Etyemezian, V., H. Kuhns, G. Nikolich, and K. Graham (2004). The Las Vegas Road Dust Emissions Technology Assessment: Final Report. Prepared by the Desert Research Institute, Las Vegas NV for the Clark County Department of Air Quality and Environmental Management, Las Vegas, NV, July, 2005.

Gillette, D. (2002). The Long-distance “Transportable Fraction” of the Vertical Flux of wind-transported dust. *Proceedings of ICAR5/GCTE-SEN Joint Conference*, Jeffrey A. Lee and Ted M. Zobeck editors, Lubbock, Texas, USA Publication 02-2 p. 34.

Gillies, J.A.; Watson, J.G.; Rogers, C.F.; Dubois, D.; Chow, J.C.; Langston, R.; and Sweet, J. (1999). Long Term Efficiencies of Dust Suppressants to Reduce PM₁₀ Emissions from Unpaved Roads. *JAWMA*, 49:3-16.

Kuhns, H., Etyemezian, V., Landwehr, D., MacDougall, C., Pitchford, M., Green, M. (2001). Testing Re-entrained Aerosol Kinetic Emissions from Roads (TRAKER): A New Approach to Infer Silt Loading on Roadways. *Atmospheric Environment Vol 35*: 2815-2825.

Kuhns, H., Etyemezian, V., Gillies, J., Green, M., Hendrickson, K., McGown, M., and M. Pitchford (2003). Vehicle Based Road Dust Emissions Measurement (II): Effect of Precipitation, Wintertime Road Sanding, and Street Sweepers on PM₁₀ Fugitive Dust Emissions from Paved and Unpaved Roads. Manuscript submitted as companion paper to *Atmospheric Environment*.

Moosmuller, H., Gillies, J.A., Rogers, C.F., Dubois, D.W., Chow, J.C., Watson, J.G., and R. Langston (1998). Particulate Emission Rates for Unpaved Shoulders along a Paved Road. *J. Air & Waste Manage. Assoc.*, Vol 48: 398-407.

Raupach, M.R., and F.L. Leys (1999). The Efficacy of Vegetation in Limiting Spray Drift and Dust Movement. Report Prepared for the Department of Land and Water Conservation, Gunnedah, Australia by CSIRO, Canberra, Australia.

Sehmel, G.A. (1973). Particle Resuspension from an Asphalt Road Caused by Car and Truck Traffic. *Atmospheric Environment*, Vol 7: 291-309.

U.S. EPA (1995). Compilation of Air Pollutant Emission Factors. Report No. AP-42. Prepared by the U.S. Environmental Protection Agency, Research Triangle Park, NC, USA.

U.S.EPA (1998). National air pollutant emission trends, procedures document, 1900-1996. Report No. EPA-454/R-98-008. Prepared by U.S. Environmental Protection Agency, Research Triangle Park, NC, USA.

U.S.EPA (1999). Compilation of air pollutant emission factors - Vol. I, Stationary point and area sources. Report No. AP-42, 5th ed. Prepared by U.S. Environmental Protection Agency, Research Triangle Park, NC, USA.

U.S.EPA (2002). User’s Guide to MOBILE6.0 Mobile Source Emission Factor Model. Report No. EPA-420/R-02-001. Prepared by U.S. Environmental Protection Agency, USA.

Venkatram, A. (2000). A Critique of Empirical Emission Factor Models: A Case Study of the AP-42 Model for Estimating PM₁₀ Emissions from Paved Roads. *Atmospheric Environment*, Vol 34: 1-11.

Venkatram, A. (2001). Response to Comments by Nicholson. A Critique of Empirical Emission Factor Models: A Case Study of the AP-42 Model For Estimating PM₁₀ Emissions from Paved Roads. *Atmospheric Environment* Vol 35: 187.

Watson, J.G., and J. Chow (2000). Reconciling Urban Fugitive Dust Emission Inventory and Ambient Source Contribution Estimates: Summary of Current Knowledge and Needed Research. DRI Document No. 6110.4F. Prepared for the U.S. Environmental Protection Agency, by Desert Research Institute, Reno, NV. May, 2000.

Watson, J.G., Chow, J.C., Pace, T.G. (2000). Fugitive dust emissions. *Air Pollution Engineering Manual*, Davis, W.T., Ed. Van Nostrand Reinhold, New York, NY, pp. 117-134.

Watson, J.G., and J. Chow (2000). Reconciling Urban Fugitive Dust Emissions Inventory and Ambient Source Contribution Estimates: Summary of Current Knowledge and Needed Research. DRI Document No. 6110.4F. Prepared for the U.S. Environmental Protection Agency, by Desert Research Institute, Reno, NV. May, 2000.

Countess, R. (2001). Methodology for Estimating Fugitive Windblown and Mechanically Resuspended Road Dust Emissions Applicable for Regional Scale Air Quality Modeling. Prepared for the Western Governors Association by Countess Environmental, Westlake Village, CA, April, 2001.

Veranth, J. M., G. Seshadri and E. Pardyjak (2003). Vehicle-generated fugitive dust transport: Analytic models and field study. *Atmos Env* 37(16): 2295-2303.

Raupach, M.R., N. Woods, G. Dorr, J.F. Leys, and H.A. Cleugh (2001). The Entrapment of Particles by Windbreaks. *Atmos. Env.* 35: 3373-3383.

Lamb, R.G., and D.R. Duran (1977). Eddy Diffusivities Derived from a Numerical Model of the Convective Boundary Layer. *Nuovo Cimento*, 1c: 1-17.

Shir, C.C. (1973). A preliminary Numerical Study of Atmospheric Turbulent Flows in the Idealized Planetary Boundary Layer. *J. Atmos Sci.*, 30: 1327-1339.

Venkatram, A. (1993). The Parametrization of the Vertical Dispersion of A Scalar in the Atmospheric Boundary Layer. *Atmos Env.*, 27A: 1963-1966.

U.S. EPA, (1995). User's Guide for the Industrial Source Complex (ISC3) Dispersion Models Volume II: Description of Model Algorithms. US Environmental Protection Agency, Office of Air Quality Planning and Standards: Emissions, Monitoring, and Analysis Division, RTP, NC.

Seinfeld, J.H., and S.N. Pandis (1997). *Atmospheric Chemistry and Physics: From Air Pollution to Climate Change*. Wiley Interscience. New York, USA.

- Willeke, K., and M. Xu (1992). Impaction and rebound of particles from surfaces. *J. Aerosol Sci.* 23, Supplement: S15-S18.
- Gillies, J.A., J.G. Watson, C.F. Rogers, D. Dubois, J.C. Chow, R. Langston, and J. Sweet. (1999). Long term efficiencies of dust suppressants to reduce PM₁₀ emissions from unpaved roads. *J. Air Waste Manage. Assoc.* 49:3-16.
- Cowherd, C. (1999). Profiling data for open fugitive dust sources. Prepared for U.S. Environmental Protection Agency, Emissions Factor and Inventory Group, Office of Air Quality Planning and Standards, RTP, NC, by Midwest Research Institute, Kansas City, MO.
- Niu, J., B.M.K. Lu, and T.C.W. Tung (2002). Instrumentation Issue in Indoor Air Quality Measurements: The Case with Respirable Suspended Particulates. *Indoor Built Environment* 11: 162-170.
- Moosmüller, H., W.P. Arnott, C.F. Rogers, J.L. Bowen, J.A. Gillies, W.R. Pierson, J.F. Collins, T.D. Durbin, and J.M. Norbeck (2001). Time resolved characterization of diesel particulate emissions. 1. Instruments for particle mass measurement. *Environ. Sci. Technol.* 35: 781-787.
- Chung, A., D.P.Y. Chang, M.J. Kleeman, K.D. Perry, T.A. Cahill, D. Dutcher, E.M. McDougall, and K. Stroud (2001). Comparison of real-time instruments used to monitor airborne particulate matter. *J. Air & Waste Manage. Assoc.* 51: 109 – 120.
- Etyemezian, V., J. Gillies, H. Kuhns, D. Nikolic, J. Watson, J. Veranth, R. Labban, G. Seshadri, and D. Gillette (2003). Field Testing and Evaluation of Dust Deposition and Removal Mechanisms: Final Report. Report Prepared for WESTAR Council, Lake Oswego, OR, by DRI, Las Vegas, NV. January 2003.
- Etyemezian, V., D. Gillette, J. Gillies, H. Kuhns, D. Nikolic, J. Veranth, and J. Watson (2003). PM₁₀ Emissions Factors for Unpaved Roads: Correction for Near-Field Deposition. PM AAAR 2003: Atmospheric Sciences, Exposure, Health and Welfare Effects, Policy. Poster. American Association for Aerosol Research, Pittsburgh, PA, March 31 – April 4, 2003.
- Rodrigues, Geisa Bettancourt, 2006. Improved Techniques for estimation of PM₁₀ emissions. Master's thesis, University of Nevada, Las Vegas, NV. 171 pp.
- US EPA 2006. AP42 Emissions Factors. Miscellaneous Sources, Section 13.2.1. Paved Roads. US Environmental Protection Agency, Research Triangle Park, NC, November, 2006. 15 pp.
- US EPA 1993a. AP42 Emissions Factors. Miscellaneous Sources, Section 13.2.1. Paved Roads. Appendix C.1. Procedures for Sampling Surface/Bulk Dust Loading. US Environmental Protection Agency, Research Triangle Park, NC, November, 2006 13 pp.
- US EPA 1993b. AP42 Emissions Factors. Miscellaneous Sources, Section 13.2.1. Paved Roads. Appendix C.2. Procedures for Laboratory Analysis of Surface/Bulk Dust Loading

Samples. US Environmental Protection Agency, Research Triangle Park, NC, November, 2006 9 pp.

10.0 Key Words

Aerodynamic Entrainment

AP-42

Emission Inventory

Fugitive Dust

Geospatial Analysis

Paved Road Emissions

PM₁₀ Emissions

SCAMPER

TRAKER

11.0 Acknowledgments

The authors gratefully acknowledge the field and technical assistance provided by Sebastian Uppapalli and George Nikolich. We would also like to thank James King, Robert Powell, Ilias Kavouras, and Alex Nikolich for logistical support during the field study. Also, Kurt Bumiller for operating the SCAMPER and preparing the data for that portion of the report.